Volume 2

TABLES AND FIGURES

BRITISH LIBRARY

IMAGING SERVICES NORTH

Boston Spa, Wetherby
West Yorkshire, LS23 7BQ
www.bl.uk

BEST COPY AVAILABLE.

VARIABLE PRINT QUALITY

BRITISH LIBRARY

IMAGING SERVICES NORTH
Boston Spa, Wetherby
West Yorkshire, LS23 7BQ
www.bl.uk

TEXT CUT OFF IN THE ORIGINAL

TABLES

TABLE 1

Concentration (%)

Element	SAE 4042	API 5LX X65
C	0.45	0.052
S	0.012	0.005
P	0.015	<0.002
Mo	<0.02	<0.02
Ni	<0.02	0.04
B	0.001	<0.001
Si	<0.22	0.36
W	<0.02	<0.02
V	<0.02	0.07
Cr	<0.02	0.29
Mn	0.87	1.39
Nb	<0.02	0.06
Ti	<0.02	<0.02
Co	<0.02	<0.02
Al	0.037	<0.071
Cu	<0.02	0.29

TABLE 2

Grain Size Measurements

Material	Mean Linear Intercept (mm)		Volume Fraction (%)		Grain Shape
	α	β	α	β	
S10BM	0.003703	0.012010	24.3	75.7	Equiaxed
S12BM	0.000027	0.000013*	63.7	26.3	Equiaxed
CR68	0.000935#$\$_1$	0.000061#$\$_2$	72.3	27.7	Elongated in rolling direction.
CR80	0.000716#$£_1$	0.000284#$£_2$	61.0	39.0	Elongated in rolling direction.
R80AN	0.000612	<0.00001	>99.5	<0.5	Equiaxed

α = ferrite β = pearlite *β = carbide in this case.

\# = measured parallel to rolling direction

A = Grain aspect ratio = longitudinal grain size/transverse grain size.

$\$_1$ A = 1.16

$\$_2$ A = 0.21

$£_1$ A = 1.58

$£_2$ A = 0.53

TABLE 3

Mechanical Property Predictions

Material	Angle to R.D.	Yield Stress	r-value	Elastic Modulus (GPa) Reuss	Voigt	Hill
S10BM	0	3.058	0.805	193.6	226.7	210.2
	45	3.052	0.878	191.8	224.9	208.4
	90	3.072	0.835	194.3	227.4	210.9
S12BM	0	3.077	0.973	194.2	227.2	210.7
	45	3.074	0.944	194.2	227.3	210.7
	90	3.078	0.938	193.8	226.9	210.4
CR68	0	3.222	0.829	212.9	243.6	228.3
	45	3.012	1.790	183.5	216.2	199.9
	90	3.186	0.745	211.9	242.8	227.3
CR80	0	3.042	0.140	197.4	230.4	213.9
	45	2.975	0.922	176.1	207.6	191.8
	90	3.189	0.522	212.6	243.4	228.0
R80AN	0	3.008	0.575	184.3	217.1	200.7
	45	3.046	0.747	193.3	226.4	209.8
	90	3.078	1.113	195.8	228.8	202.3

TABLE 4

Young's Modulus, E, Determined by Resonance Method

Material	Angle to R.D.	Specimen Dimensions t(m)	l(m)	Density (kg/m^3)	Resonant Frequencies			Young's Modulus E (G Pa)			Mean E (G Pa)
	0	2.08E-3	1.12E-1	9357.46	806,	2216,	4313	209.2,	208.3,	205.6	207.7
S10BM	45	2.08E-3	1.00E-1	9357.46	1000,	2780,	5368	204.9,	208.3,	202.4	205.2
	90	2.08E-3	1.08E-1	9357.46	872,	2372,	4649	211.7,	206.4,	206.5	208.2
	0	2.08E-3	1.12E-1	9418.40	792,	2219,	4341	203.3,	210.2,	209.6	207.7
S12BM	45	2.08E-3	1.00E-1	9418.40	1003,	2781,	5408	207.3,	209.7,	206.7	207.9
	90	2.08E-3	9.10E-2	9418.40	1208,	3367,	6525	206.4,	210.9,	206.4	207.9
	0	3.93E-3	9.54E-2	7793.21	2356,	6613,	12788	219.7,	227.7,	221.9	223.1
CR68	45	3.93E-3	9.54E-2	7793.21	2265,	6144,	11880	203.0,	196.5,	191.5	197.0
	90	3.93E-3	9.54E-2	7793.21	2354,	6504,	12952	219.4,	220.2,	227.6	222.4
	0	3.86E-3	9.13E-2	7811.54	2462,	6746,	13347	209.2,	206.5,	210.7	208.8
CR80	45	3.96E-3	9.14E-2	7811.54	2253,	6510	12761	191.1,	192.3,	192.6	192.0
	90	4.39E-3	9.20E-2	7811.54	2845,	7718,	15092	233.2,	285.8,	225.0	228.0
	0	4.39E-3	9.20E-2	7831.63	2749,	7539,	14623	208.3,	206.1,	202.1	205.5
R80AN	45	4.39E-3	9.20E-2	7831.63	2783,	7703,	15086	213.5,	215.2,	215.1	214.6
	90	4.39E-3	9.16E-2	7831.63	2825,	7906,	15439	220.0,	226.7,	225.3	224.0

TABLE 5

Experimental r-values

Material	Angle to R.D.	Mean r-value
S10BM	0	0.83
	22.5	0.93
	45	0.98
	67.5	0.95
	90	0.86
S12BM	0	1.09
	22.5	2.00
	45	0.98
	67.5	1.22
	90	1.07
CR68	0	1.10
	22.5	1.30
	45	2.11
	67.5	1.70
	90	1.23
CR80	0	0.70
	22.5	1.15
	45	1.83
	67.5	1.49
	90	1.35
R80AN	0	0.90
	22.5	1.07
	45	1.11
	67.5	1.37
	90	1.55

TABLE 6

Mechanical Properties of S10BM0

Monotonic data

Elastic modulus = 212.6 GPa
Yield strength = 427.9 MPa
U.T.S. = 743.9 MPa

Cyclic data

Strain amplitude	Fatigue life (revs)	Stress amplitude (MPa)	Plastic strain amplitude	Elastic modulus (GPa)
0.00213	149680	302.0	0.00062	200.0
0.00292	96960	308.0	0.00100	160.4
0.00384	24540	369.5	0.00192	192.2
0.00155	15160600	251.6	0.00010	173.1
0.00216	318860	302.0	0.00057	189.3
0.00710	8548	417.7	0.00425	146.3
0.01025	2120	479.3	0.00720	157.0
0.00865	7876	422.4	0.00525	124.1
0.00198	461200	285.9	0.00050	192.6

TABLE 7

Mechanical Properties of S10BM45

Monotonic data

Elastic modulus = 216.2 GPa
Yield Strength = 432.3 MPa
U.T.S. = 729.0 MPa

Cyclic data

Strain amplitude	Fatigue life (revs)	Stress amplitude (MPa)	Plastic strain amplitude	Elastic modulus (GPa)
0.00620	5696	408.8	0.99375	166.9
0.00800	1804	467.6	0.00570	203.3
0.00267	65400	303.3	0.00100	181.6
0.00260	72600	311.4	0.00103	198.3
0.00320	71000	329.0	0.00134	176.9
0.00320	107700	322.0	0.00122	162.6
9.0042	24320	363.3	0.0022	181.7
0.00710	7730	396.5	0.00430	141.6

TABLE 8

Mechanical Properties of S10BM90

Monotonic data

Elastic modulus = 244.9 GPa
Yield strength = 490.0 MPa
U.T.S. = 837.0 MPa

Cyclic data

Strain amplitude	Fatigue life (revs)	Stress amplitude (MPa)	Plastic strain amplitude	Elastic modulus (GPa)
0.00213	737800	271.2	0.00052	168.4
0.00418	30180	365.3	0.00198	166.1
0.00315	86200	333.2	0.00124	174.5
0.00810	4098	415.4	0.00553	161.7
0.01010	970	435.0	0.00740	161.1
0.00910	4854	407.9	0.00550	113.3
0.00604	16000	394.0	0.00357	159.5

TABLE 9

Mechanical Properties of S12BM0

Monotonic data

Elastic modulus = 138.8 GPa
Yield strength = 277.6 MPa
U.T.S. = 446.0 MPa

Cyclic data

Strain amplitude	Fatigue life (revs)	Stress amplitued (MPa)	Plastic strain amplitude	Elastic modulus (GPa)
0.00612	14000	282.1	0.00367	115.1
0.00806	6920	312.4	0.00544	119.7
0.00907	5750	316.0	0.00615	108.2
0.00414	11800	247.0	0.00244	145.3
0.00220	103000	211.8	0.00077	148.6
0.00319	39800	220.5	0.00150	130.5
0.00412	27220	286.2	0.00228	155.6
0.00174	667600	204.5	0.00037	149.2

TABLE 10

Mechanical Properties of S12BM45

Monotonic data

Elastic modulus = 158.6 GPa
Yield strength = 317.2 MPa
U.T.S. = 482.0 MPa

Cyclic data

Strain amplitude	Fatigue life (revs)	Stress amplitude (MPa)	Plastic strain amplitude	Elastic modulus (GPa)
0.00218	179200	207.1	0.00070	139.9
0.00417	15120	246.6	0.00233	134.0
0.00813	3346	301.2	0.00582	130.4
0.00603	9840	251.8	0.00360	103.6
0.00170	251600	195.1	0.00045	156.1
0.00320	31200	243.9	0.00158	150.6
0.00920	4882	307.0	0.00665	120.4
0.00714	6360	296.0	0.00500	138.3
0.00172	128400	192.0	0.00054	162.7

TABLE 11

Mechanical Properties of S12BM90

Monotonic data

Elastic modulus = 178.0 GPa
Yield strength = 267.0 MPa
U.T.S. = 473.0 MPa

Cyclic data

Strain amplitude	Fatigue life (revs)	Stress amplitude (MPa)	Plastic strain amplitude	Elastic modulus (GPa)
0.00416	17780	262.7	0.00244	152.7
0.00613	1380	309.3	0.00422	161.9
0.00812	460	335.6	0.00608	164.5
0.01005	2165	312.3	0.00750	122.5
0.00217	95000	207.5	0.00066	137.9
0.00516	11160	281.5	0.00325	147.4
0.00717	5520	298.5	0.00490	131.5
0.00318	42600	251.5	0.00169	168.8
0.00167	279600	205.5	0.00045	168.4

TABLE 12

Mechanical Properties of CR680

Monotonic data

Elastic modulus = 148.7 GPa
Yield strength = 818.5 MPa
U.T.S. = 929.8 MPa

Cyclic data

Strain amplitude	Fatigue life (revs)	Stress amplitude (MPa)	Plastic strain amplitude	Elastic modulus (GPa)
0.00483	19240	607.9	0.00120	167.5
0.00300	103440	511.4	0.00023	184.6
0.00408	22766	585.2	0.00060	168.2
0.00347	55800	555.1	0.00038	179.7
0.00329	40800	550.8	0.00033	186.1
0.00328	49400	550.9	0.00034	187.4
0.00280	232200	471.6	0.00025	184.9
0.00260	581200	468.4	0.00015	191.2

TABLE 13

Mechanical Properties of CR6845

Monotonic data

Elastic modulus = 159.4 GPa
Yield strength = 880.9 MPa
U.T.S. = 932.8 MPa

Cyclic data

Strain amplitude	Fatigue life (revs)	Stress amplitude (MPa)	Plastic strain amplitude	Elastic modulus (GPa)
0.00312	135000	561.9	0.00014	188.6
0.00261	620000	453.9	0.00010	180.8
0.00404	21100	613.9	0.00062	179.5
0.00606	5380	645.0	0.00220	167.1
0.00246	2731600	450.9	0.00004	186.3
0.00509	13400	645.6	0.00123	167.3
0.00407	19200	626.7	0.00520	176.5

TABLE 14

Mechanical Properties of CR6890

Monotonic data

Elastic modulus = 171.3 GPa
Yield strength = 859.4 MPa
U.T.S. = 948.5 MPa

Cyclic data

Strain amplitude	Fatigue life (revs)	Stress amplitude (MPa)	Plastic strain amplitude	Elastic modulus (GPa)
0.00312	24200	609.4	0.00025	212.3
0.00410	30200	642.2	0.00099	206.5
0.00273	163600	566.2	0.00020	223.8
0.00505	2920	673.9	0.00172	202.4
0.00506	4580	671.5	0.00161	194.6
0.00251	1645000	498.9	0.00009	206.6
0.00312	146800	546.7	0.00028	192.5
0.00503	8600	656.3	0.00163	193.0
0.00708	1320	723.1	0.00331	191.6

TABLE 15

Mechanical Properties of CR800

Monotonic data

Elastic modulus = 163.7 GPa
Yield strength = 921.9 MPa
U.T.S. = 991.5 MPa

Cyclic data

Strain amplitude	Fatigue life (revs)	Stress amplitude (MPa)	Plastic strain amplitude	Elastic modulus (GPa)
0.00403	28000	599.2	0.00055	172.2
0.00500	7160	678.2	0.00138	187.3
0.00602	5180	706.8	0.00182	168.3
0.00261	354600	457.3	0.00009	181.5
0.00228	313600	451.4	0.00009	206.6
0.00242	469600	462.4	0.00005	195.5
0.00210	2041900	417.4	0.000003	199.1
0.00237	228000	488.9	0.00006	211.6
0.00226	2256200	447.5	0.000065	203.4
0.00305	106400	504.2	0.00017	175.1

TABLE 16

Mechanical Properties of CR8045

Monotonic data

Elastic modulus = 141.9 GPa
Yield strength = 945.9 MPa
U.T.S. = 991.3 MPa

Cyclic data

Strain amplitude	Fatigue life (revs)	Stress amplitude (MPa)	Plastic strain amplitude	Elastic modulus (GPa)
0.00310	766000	507.9	0.00008	168.2
0.00410	27800	643.6	0.00050	178.8
0.00310	231000	513.4	0.00013	172.8
0.00604	4920	716.3	0.00194	174.7
0.00503	8980	666.4	0.00088	160.6
0.00357	64400	602.3	0.00025	181.4
0.00800	1680	742.2	0.00400	185.6
0.00253	661200	474.8	0.00005	191.1
0.00285	171400	513.6	0.00010	186.8
0.00286	262400	503.2	0.00010	182.3
0.00245	689000	484.5	0.00004	200.6

TABLE 17

Mechanical Properties of CR8090

Monotonic data

Elastic modulus = 195.6 GPa
Yield strength = 988.5 MPa
U.T.S. = 1046.1 MPa

Cyclic data

Strain amplitude	Fatigue life (revs)	Stress amplitude (MPa)	Plastic strain amplitude	Elastic modulus (GPa)
0.00404	12200	679.0	0.00074	205.8
0.00718	1400	759.2	0.00260	165.8
0.00502	4240	737.1	0.00133	199.8
0.00455	8000	698.6	0.00107	200.7
0.00604	1600	779.9	0.00242	215.4
0.00304	25800	638.5	0.00035	237.4
0.00288	174600	556.4	0.00020	207.6
0.00358	13000	682.7	0.00047	219.5
0.00324	46200	604.8	0.00024	201.6
0.00277	157600	547.9	0.00010	205.2

TABLE 18

Mechanical Properties of R80AN0

Monotonic data

Elastic modulus = 162.8 GPa
Yeidl strength = 313.2 MPa
U.T.S. = 409.7 MPa

Cyclic data

Strain amplitude	Fatigue life (revs)	Stress amplitude (MPa)	Plastic strain amplitude	Elastic modulus (GPa)
0.00270	15480	251.6	0.00115	162.3
0.00216	75800	264.5	0.00080	194.5
0.00166	204200	255.7	0.00037	198.2
0.00150	20000000	233.2	0.00023	183.6
0.00145	10105000	250.7	0.00022	203.8
0.00140	445400	270.9	0.00015	216.7
0.00140	166600	240.0	0.00014	190.5
0.00127	21111400	244.8	0.00012	212.9

TABLE 19

Mechanical Properties of R80AN45

Monotonic data

Elastic modulus = 153.9 GPa
Yield strength = 386.8 MPa
U.T.S. = 464.0 MPa

Cyclic data

Strain amplitude	Fatigue life (revs)	Stress amplitude (MPa)	Plastic strain amplitude	Elastic modulus (GPa)
0.00410	430	347.5	0.00213	176.4
0.00186	58200	282.0	0.00047	202.9
0.00146	416000	291.9	0.00007	210.0
0.00303	8960	387.5	0.00116	206.6
0.00207	64600	367.6	0.00007	183.8
0.00256	12680	396.4	0.00067	209.7
0.00141	6956000	273.0	0.00002	197.5

TABLE 20

Mechanical Properties of R80AN90

Monotonic data

Elastic modulus = 199.0 GPa
Yield strength = 410.1 MPa
U.T.S. = 496.4 MPa

Cyclic data

Strain amplitude	Fatigue life (revs)	Stress amplitude (MPa)	Plastic strain amplitude	Elastic modulus (GPa)
0.00150	112400	278.3	0.00017	210.1
0.00316	4000	412.6	0.00115	205.3
0.00251	179000	382.2	0.00063	203.8
0.00215	14000	497.3	0.00030	220.1
0.00207	16400	360.5	0.00041	217.2
0.00158	146800	266.7	0.00025	200.2
0.00170	107000	356.2	0.00010	223.3
0.00203	14000	317.7	0.00055	213.9
0.00133	1714200	240.3	0.00012	198.6

Coffin exponent	=	-0.507
Fatigue ductility coefficient	=	0.124
Correlated coefficient	=	-0.981
Basquin exponent	=	-0.047
Fatigue strength coefficient	=	1006.5
Correlation coefficient	=	-0.997
Cyclic hardening exponent	=	0.092
Cyclic strength coefficient	=	1221.4
Correlation coefficient	=	0.972

Strain Amplitude	Fatigue Life (revs)	Stress Amplitude (MPa)	Plastic Strain Amplitude	Elastic Modulus (GPa)	Elastic Strain Amplitude	Corrected Strain Amplitude
0.00310	24200	609.4	0.00025	222.4	0.00274	0.00299
0.00410	30200	642.2	0.00099	222.4	0.00290	0.00389
0.00270	163600	566.2	0.00020	222.4	0.00250	0.00270
0.00505	2920	673.9	0.00170	222.4	0.00303	0.00473
0.00506	4580	671.5	0.00160	222.4	0.00302	0.00462
0.00250	1645000	498.9	0.00009	222.4	0.00220	0.00229
0.00310	146800	546.7	0.00028	222.4	0.00240	0.00268
0.00503	8600	656.3	0.00160	222.4	0.00290	0.00450
0.00708	1320	723.1	0.00330	222.4	0.00320	0.00650

TABLE 21: Fatigue Analysis for CR6890 Using the Sonic Modulus And The Stress Amplitude to Calculate the Elastic Strain Range

TABLE 22

Material Parameters

Material	Plastic ε'_f	Plastic -c	Elastic σ'_f	Elastic -b	Stress - strain n'	Stress - strain K' (MPa)	Stress - strain S' (MPa)	Strain - life n	Strain - life K (MPa)	Strain - life S (MPa)	Sonic Modulus (GPa)
S10BM0	0.438	0.506	812	0.077	0.153	954	369	0.152	911	354	208
S10BM45	0.181	0.453	978	0.099	0.216	1365	357	0.218	1422	504	205
S10BM90	0.182	0.430	755	0.072	0.168	1002	353	0.167	1003	355	208
S12BM0	1.033	0.608	542	0.075	0.169	733	256	0.123	539	251	208
S12BM45	0.047	0.629	726	0.107	0.171	716	247	0.170	1223	425	208
S12BM90	0.141	0.435	561	0.081	0.176	777	260	0.186	808	254	208
CR680	0.839	0.536	1301	0.079	0.136	1572	676	0.147	1335	535	223
CR6845	0.289	0.606	1201	0.068	0.103	1289	680	0.112	1380	688	197
CR6890	0.124	0.507	1006	0.047	0.092	1216	685	0.092	1221	689	222
CR800	1.69	0.795	1397	0.080	0.091	1163	662	0.100	1325	712	209
CR8045	0.661	0.703	1325	0.074	0.106	1388	715	0.105	1385	721	192
CR8090	0.244	0.629	1370	0.077	0.111	1514	761	0.122	1628	763	228
R80AN0	0.008	0.222	287	0.010	0.072	535	342	0.045	356	269	205
R80AN45	0.208	0.584	683	0.060	0.053	511	369	0.107	885	455	215
R80AN90	0.030	0.427	935	0.097	0.148	1092	435	0.227	2068	504	224

TABLE 23

Fatigue Crack Data - CR80

Specimen	Mode	m	C	$\Delta K_6 (MNM^{-\frac{3}{2}})$
0/1	Flat	2.81	1.47E-8	4.41
0/2	Flat	2.55	2.62E-8	4.17
0/3	Flat	2.68	1.91E-8	4.23
45/1	Inclined	2.53	3.00E-9	4.50
45/2	Inclined	2.62	5.04E-9	4.57
45/3	Inclined	2.77	1.76E-9	4.71
90/1	Flat	2.98	1.00E-8	4.00
90/2	Flat	2.50	3.03E-8	3.65
90/3	Flat	2.56	2.63E-8	3.61

TABLE 24

Fatigue Crack Data - R80AN

Specimen	Mode	m	C	$\Delta K_6 (MNM^{-\frac{3}{2}})$
0/1	Flat	2.14	9.14E-8	3.12
0/2	Flat	1.93	1.21E-7	3.10
0/3	Flat	1.68	1.62E-7	2.93
45/1	Inclined	1.50	1.24E-7	3.63
45/2	Inclined	2.20	3.57E-8	3.84
45/3	Inclined	1.98	6.75E-9	3.74
90/1	Flat	2.27	4.6E-8	3.23
90/2	Flat	2.01	4.54E-6	3.41
90/3	Flat	2.15	1.16E-5	3.71

TABLE 25

Material	Taylor Factor	K" (MPa)	n"	r
S10BM0	3.15	954	0.153	0.805
S10BM45	3.20	1365	0.216	0.878
S10BM90	3.19	1002	0.168	0.835
R80AN0	3.04	535	0.072	0.575
R80AN45	3.17	511	0.053	0.797
R80AN90	3.40	1092	0.148	1.113
CR680	3.32	1572	0.136	0.829
CR6845	3.26	1289	0.103	1.790
CR6890	3.26	1216	0.092	0.745
CR800	3.04	1163	0.091	0.140
CR8045	3.20	1388	0.106	0.922
CR8090	3.21	1514	0.111	0.522

TABLE 26

Material	Hardness (HV)
S10BM	192
S12BM	171
CR68	291
CR80	311
R80AN	156

FIGURES

FIGURE 1: The cyclic strain hardening and softening displayed by most materials. (Reference 5)

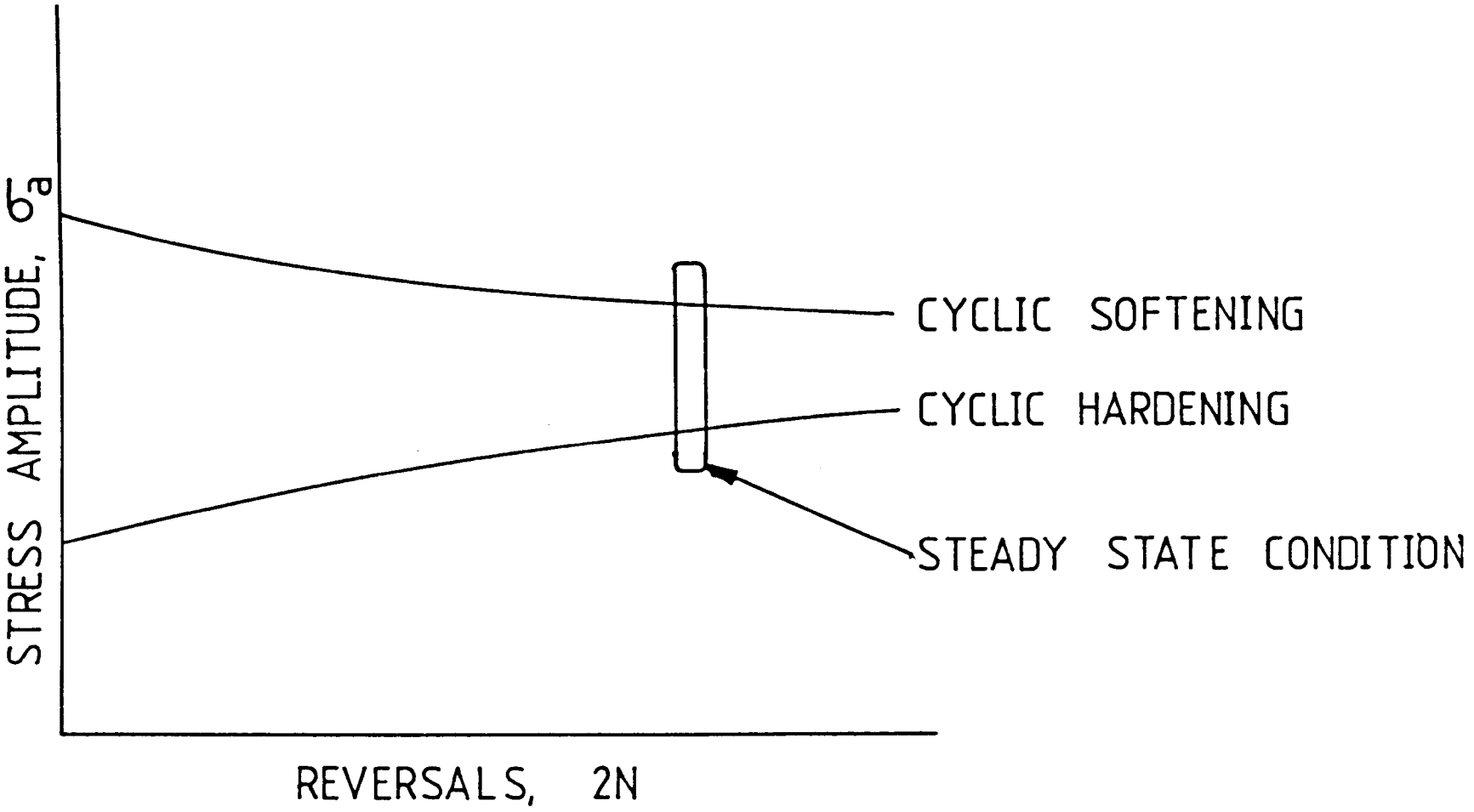

FIGURE 2: The idealized hysteresis loop. The curve shows the coincident stress and strain amplitudes during the saturation stage. (Reference 5)

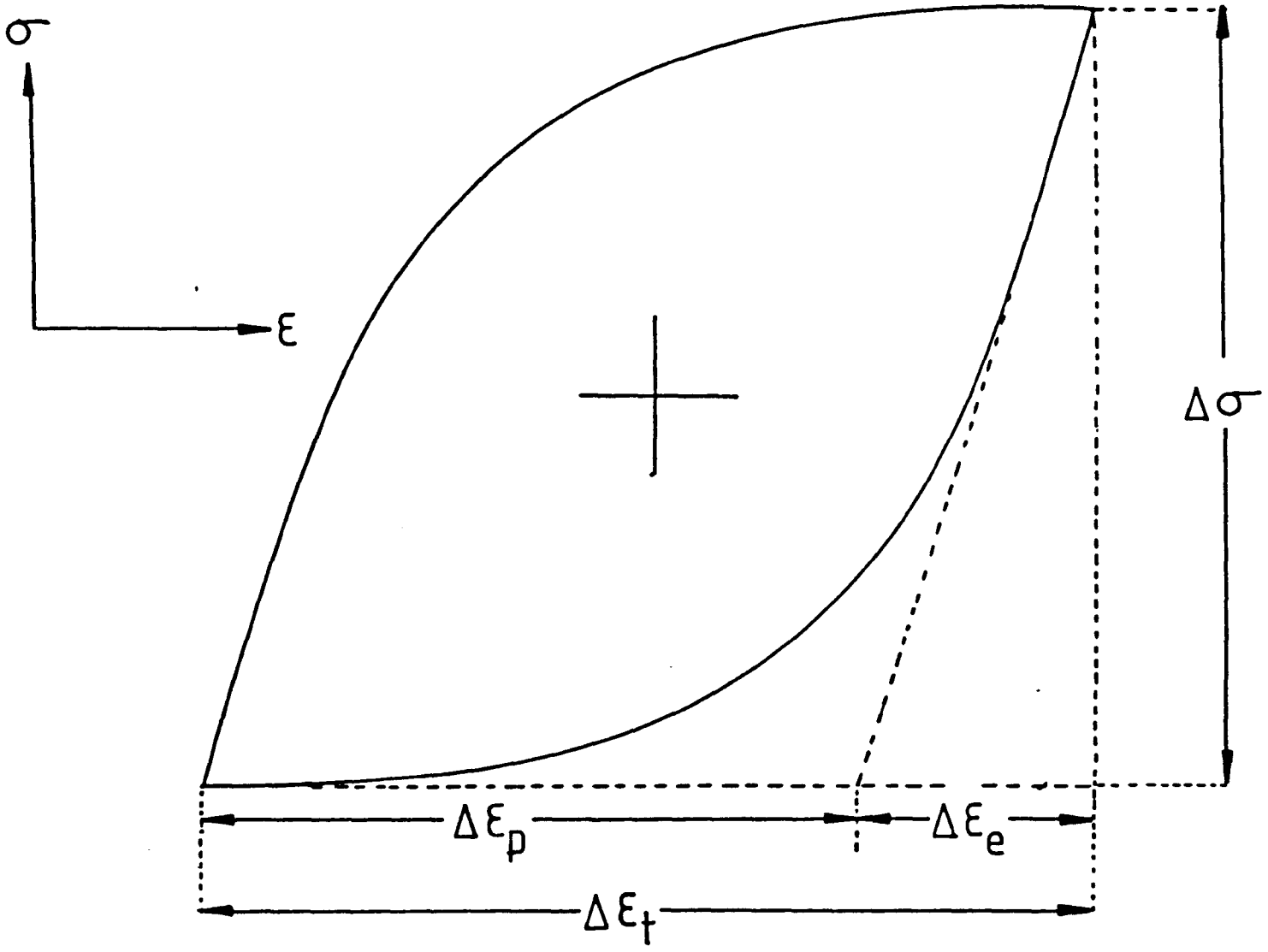

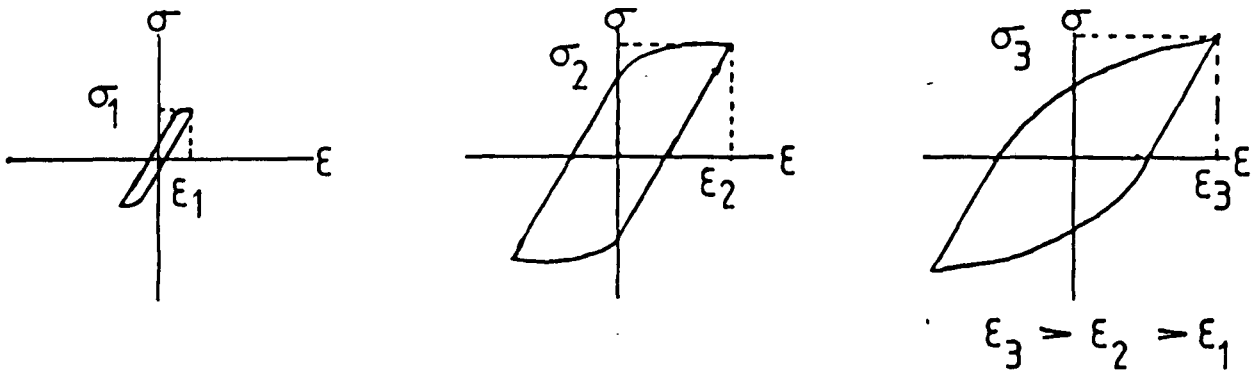

STEADY STATE HYSTERESIS LOOPS

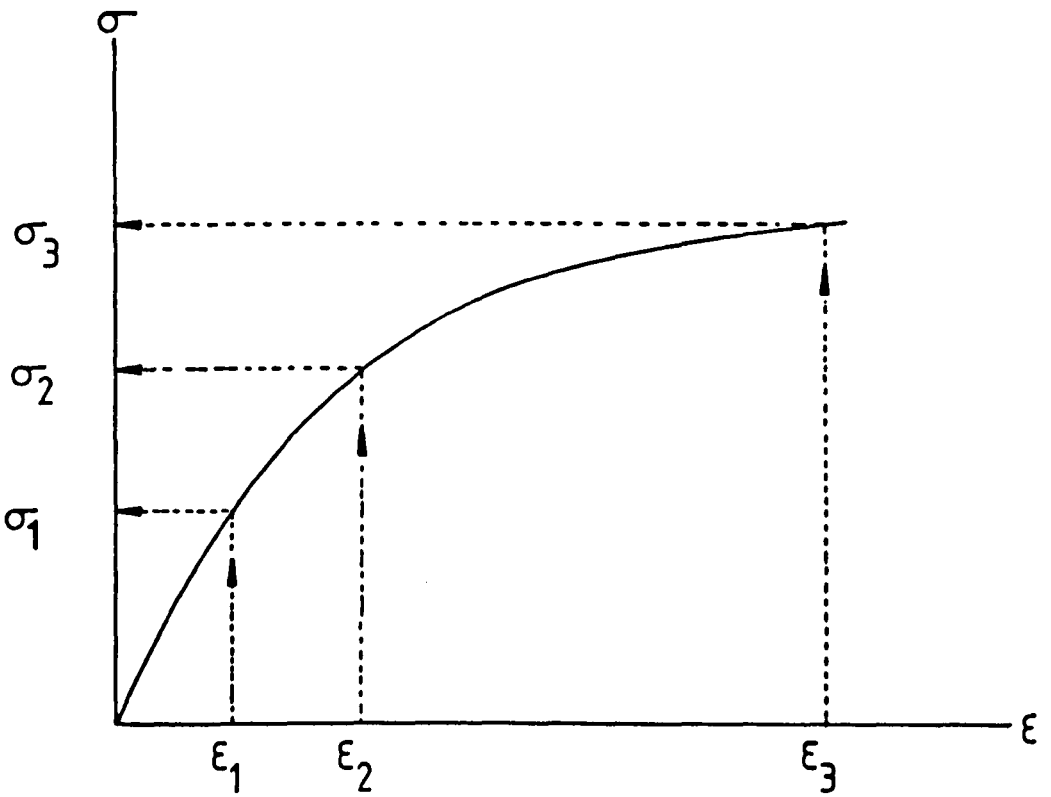

CYCLIC STRESS STRAIN CURVE

FIGURE 3: The cyclic stress-strain curve of a material, constructed from several idealized hysteresis loops from comparison specimen tests at various controlled strain amplitudes. (Reference 5)

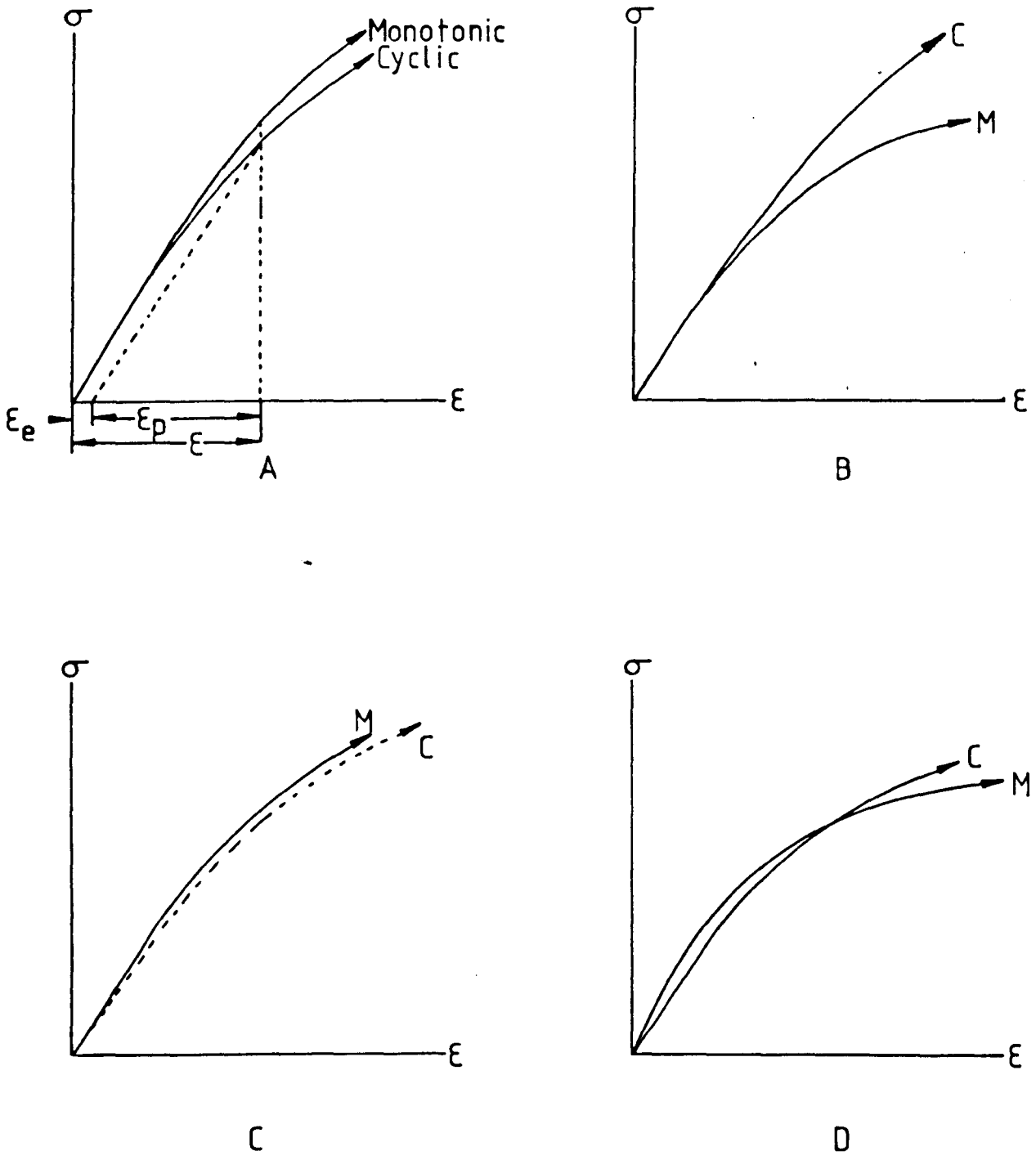

FIGURE 4: The various cyclically induced changes in mechanical behaviour. (Reference 5)

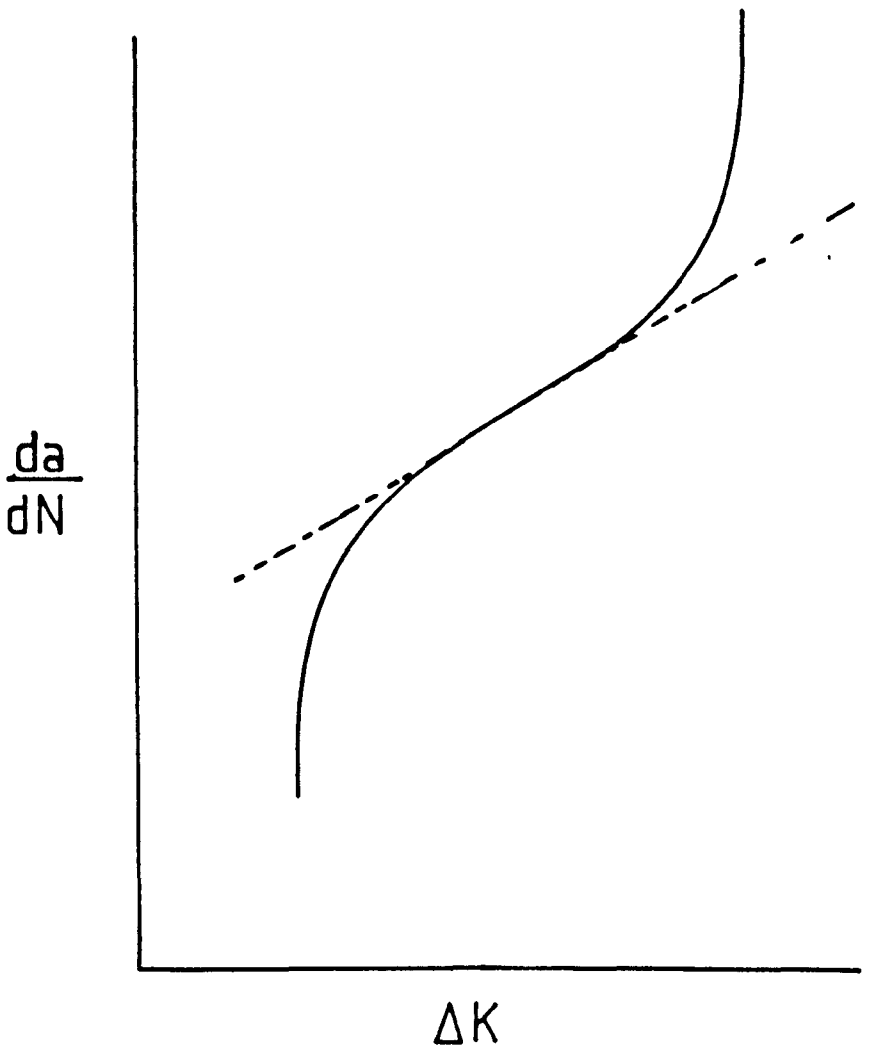

FIGURE 5: The general form of the dependence of the rate of fatigue crack growth propagation on the applied stress intensity. $da/dN = C(\Delta K)^m$ may be applied to the dotted region.

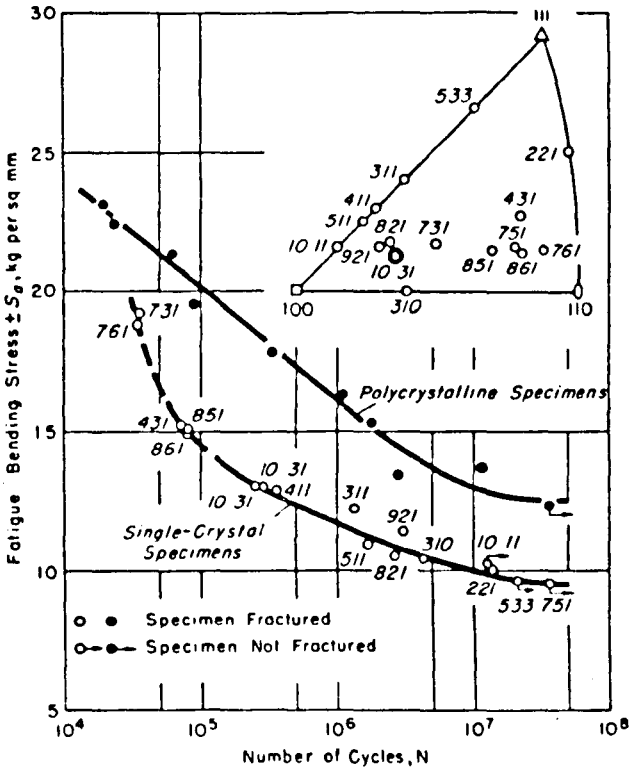

FIGURE 6: The S-N data of single crystal and polycrystalline ∝-iron, with the crystal orientations shown in inset. (Reference 22)

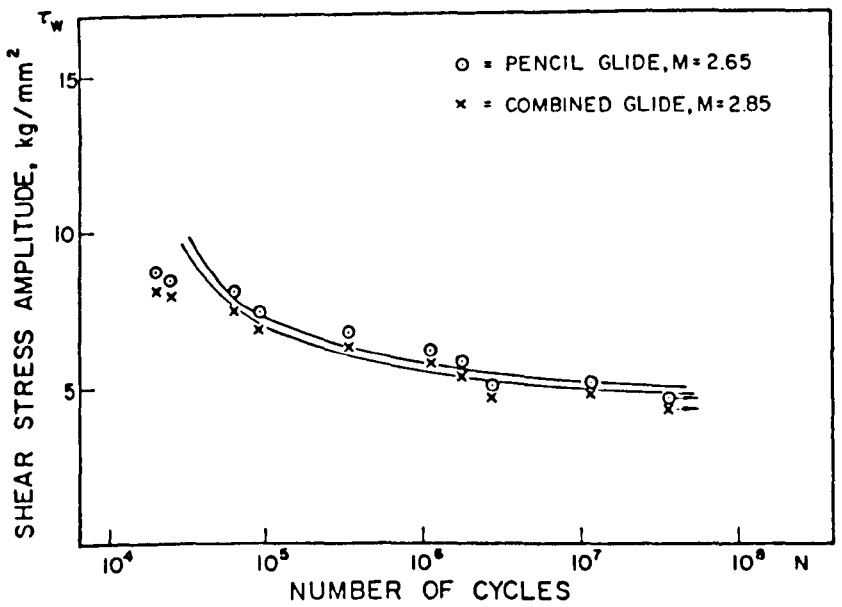

FIGURE 7: The data of Figure 6 as re-analysed by Kettunen[23].

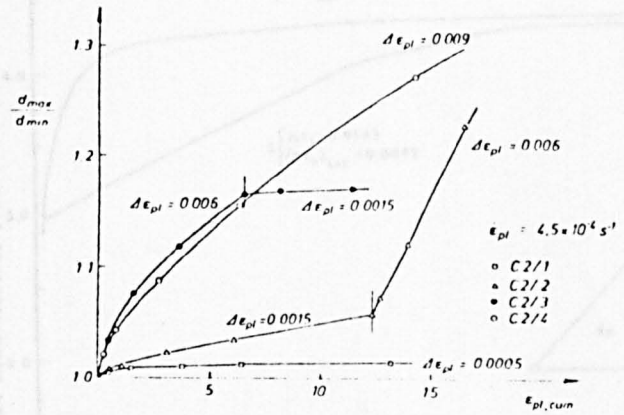

FIGURE 8: The development of shape changes of decarburized α-iron single crystals during cyclic deformation at different $\Delta\varepsilon_{pl}$. (Reference 32)

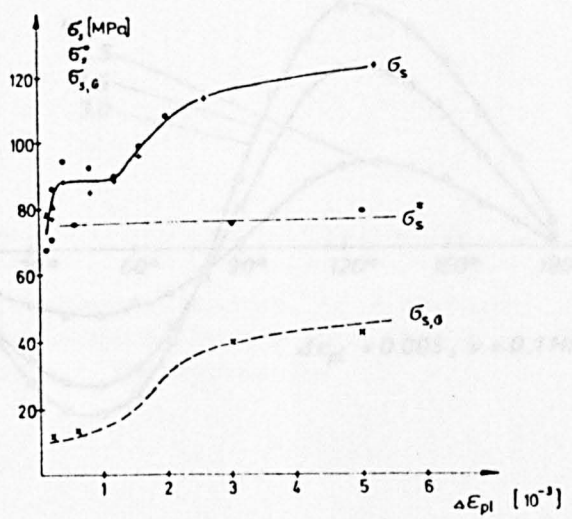

FIGURE 9: The cyclic σ-ε curve (σ_s) of decarburized α-iron single crystals. (Reference 32)

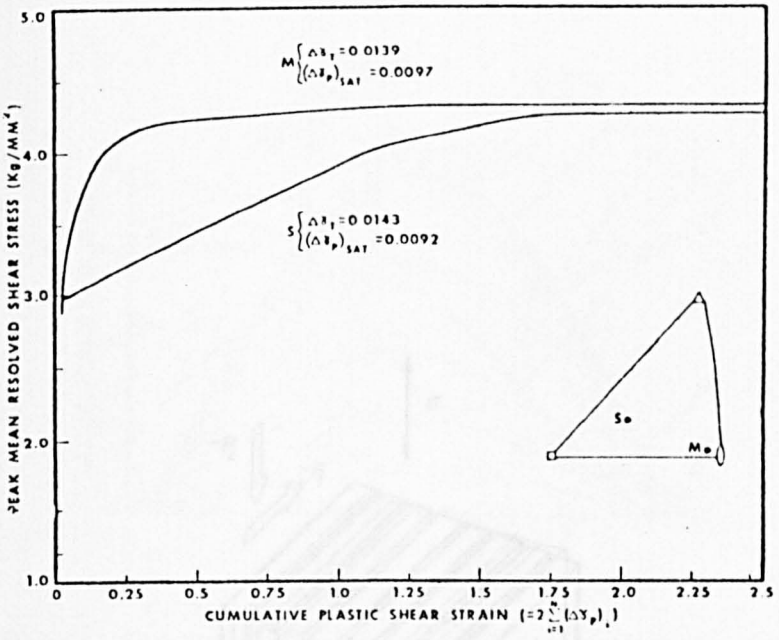

FIGURE 10: The fatigue hardening curves for single crystals of niobium as investigated by Doner et al[29]. Crystals were oriented for either single (S) or multiple (M) slip.

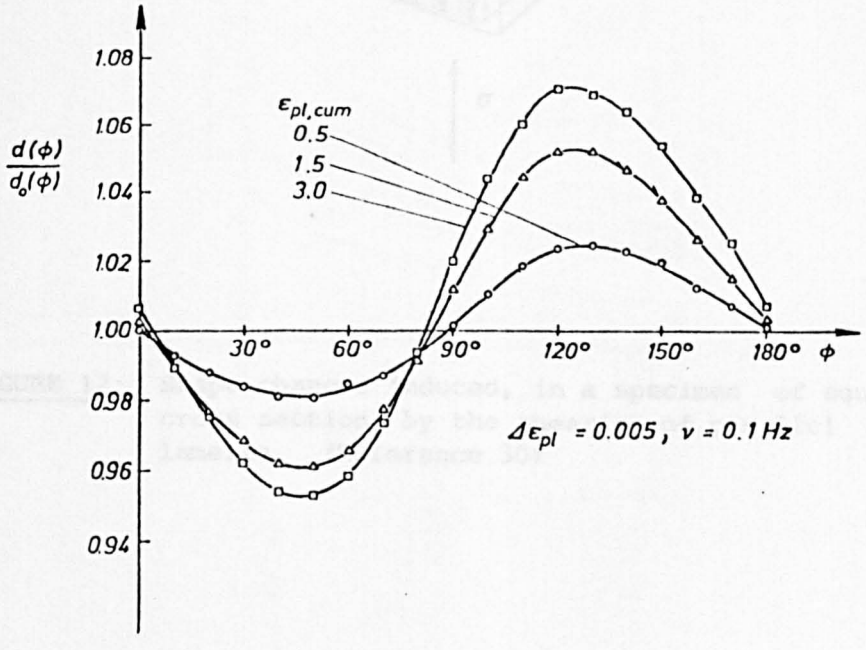

FIGURE 11: Changes of $d(\phi)/d_o(\phi)$ in single crystals of α-iron after different $\varepsilon_{pl,cum}$. (Reference 30)

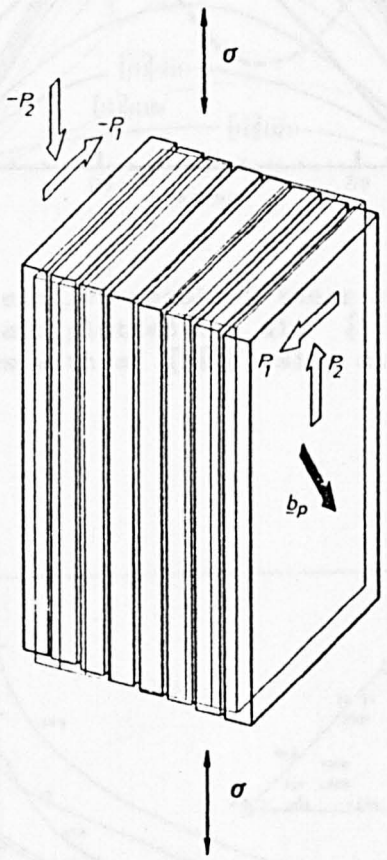

FIGURE 12: Shape changes induced, in a specimen of square cross section, by the shearing of parallel lamella. (Reference 30)

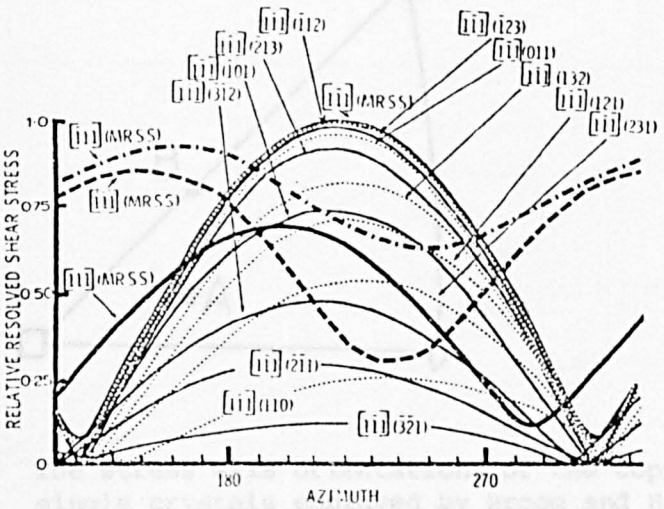

FIGURE 13: The relative resolved shear stress of iron single crystals plotted for all $\{110\}$, $\{112\}$ and $\{123\}$ planes with a $[1\bar{1}1]$ slip direction. (Reference 31)

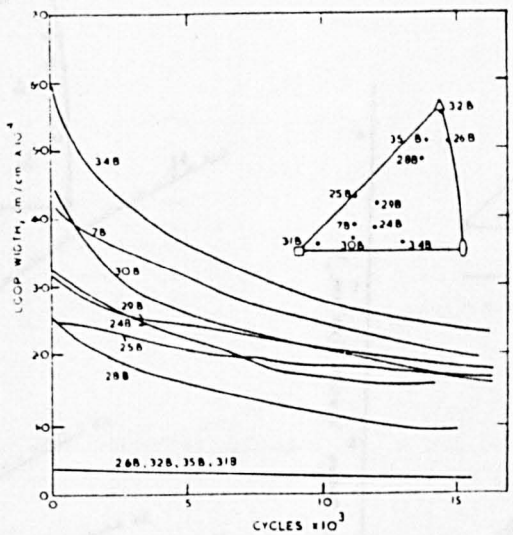

Crystal	Fatigue Shear Stress, g mm^{-2}	Cycles to Failure
34B	± 700	80,300
7B	± 680	426,000
30B	± 700	185,000
29B	"	114,000
24B	"	293,000
25B	"	647,000
28B	"	323,000
26B	"	$> 2 \times 10^6$
32B	"	"
35B	"	"
31B	"	"

FIGURE 14: The cyclic hardening response of A1 single crystals fatigued at a cyclic shear stress of ± 700 gm mm^{-2}. Differences in fatigue life are shown in the table. (Reference 49)

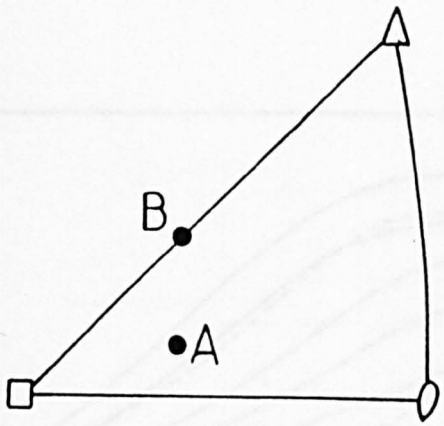

FIGURE 15: The stress axis orientations of the copper single crystals employed by Broom and Ham[50].

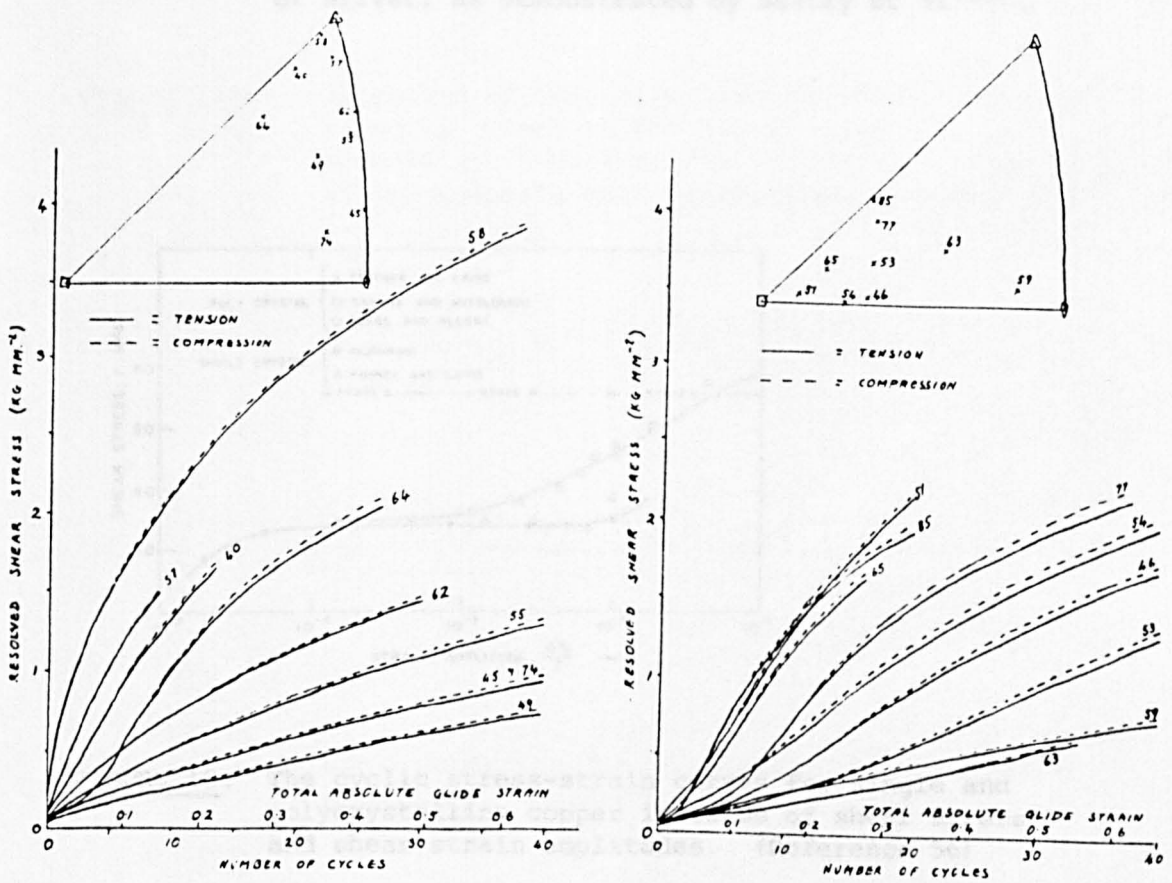

FIGURE 16: The strain hardening response of high purity copper single crystals, as demonstrated by Paterson[52].

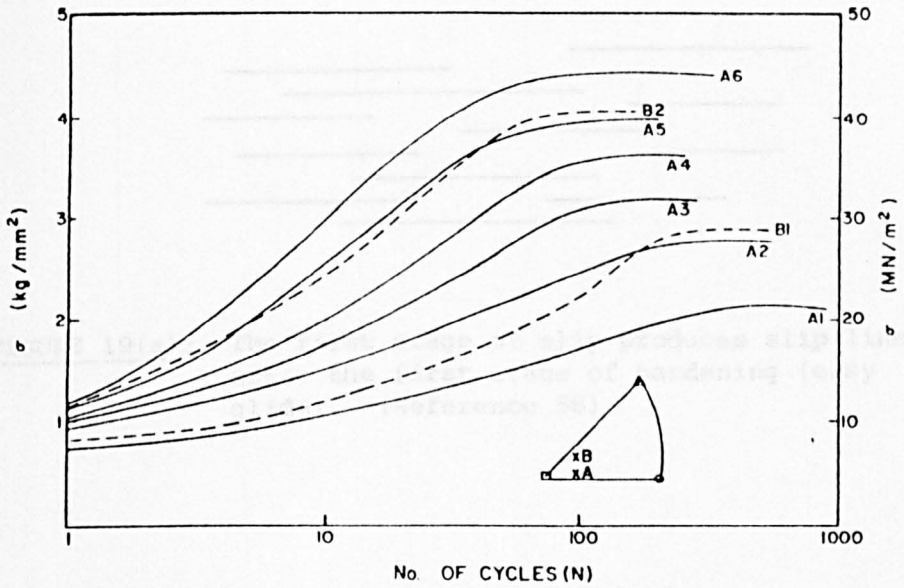

FIGURE 17: The orientation dependent cyclic hardening rates of silver, as demonstrated by Sastry et al(54).

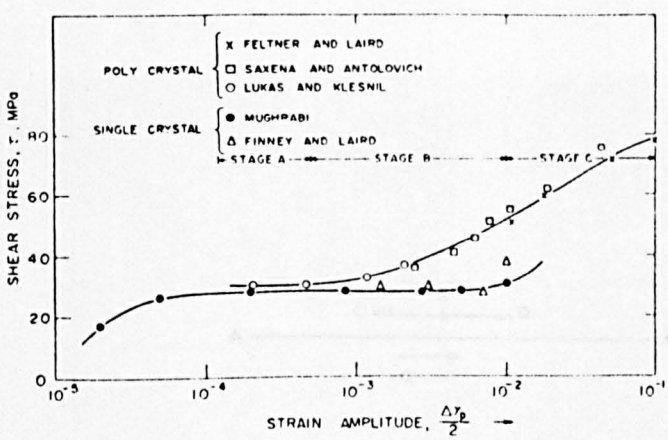

FIGURE 18: The cyclic stress-strain curves for single and polycrystalline copper in terms of shear stress and shear strain amplitudes. (Reference 56)

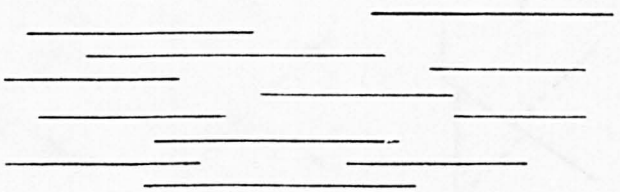

FIGURE 19(a): The first stage of slip produces slip lines, after the first stage of hardening (easy glide). (Reference 58)

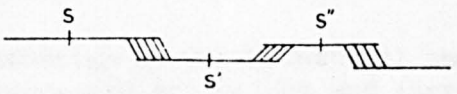

FIGURE 19(b): Formation of long slip lines by cross slip. Piled up groups at the end of lines are eliminated, therefore the sources S, S' and S" can generate more dislocations. (Reference 58)

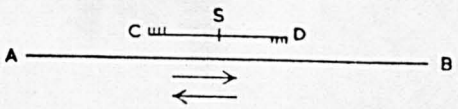

FIGURE 20: Local softening due to cross-slip during cyclic stressing. (Reference 58)

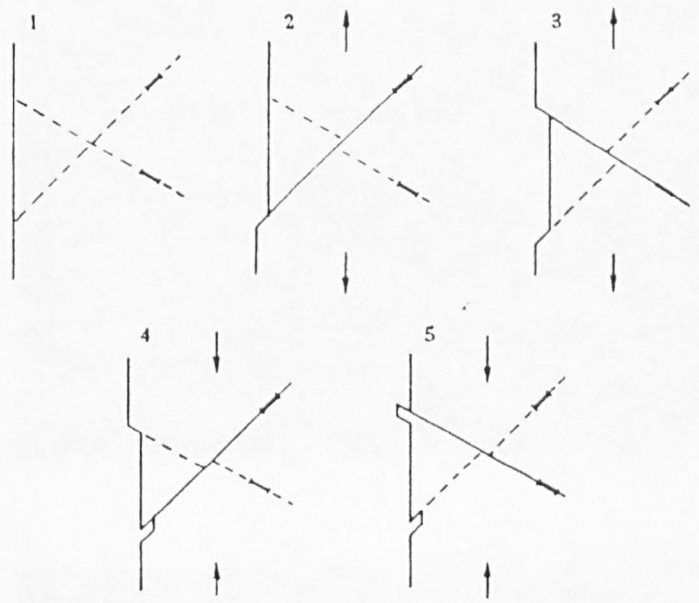

FIGURE 21: The mechanism by which Cottrell and Hull[66] have suggested extrusions and intrusions can occur.

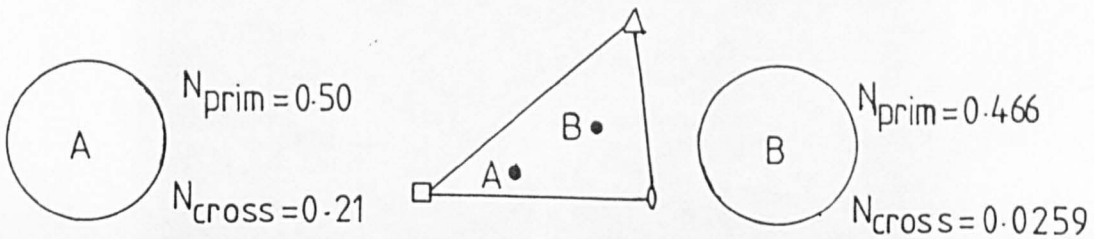

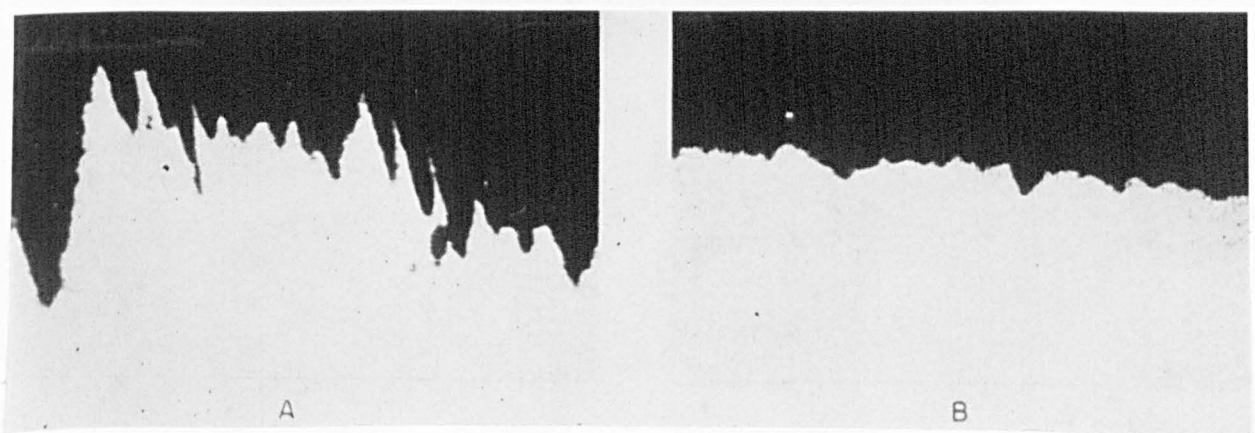

FIGURE 22: The difference in extrusion rate of copper single crystals as a function of the shear stress on the cross-slip system. (Reference 68)

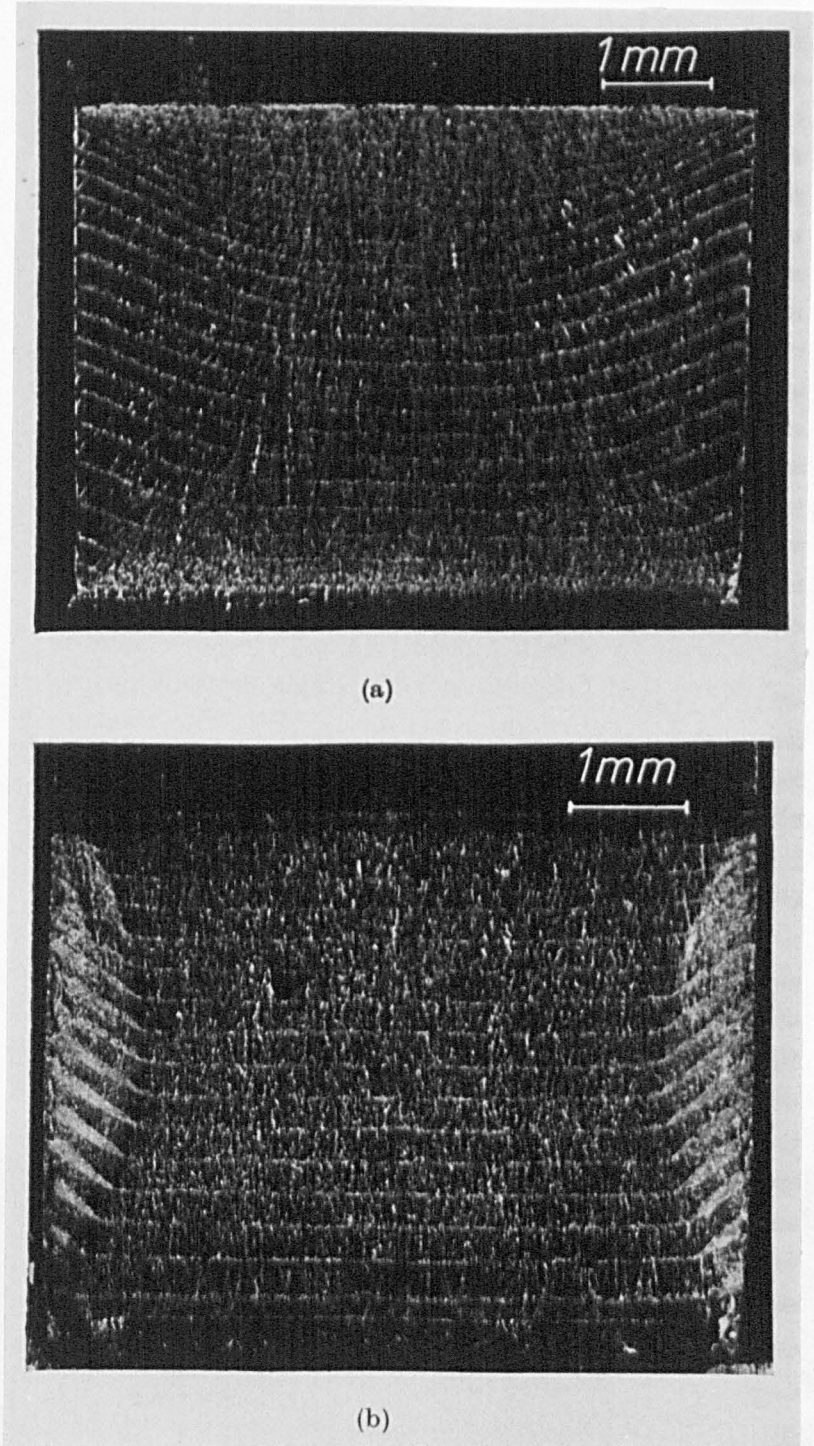

FIGURE 23: The straight crack front striations of the fatigue fracture surfaces of notched copper single crystals. Propagation is from top to bottom. The white rest lines indicate the position of the crack front every 400 cycles. Crystals (a) and (b) were at different oriations with respect to the stress axis. (Reference 45)

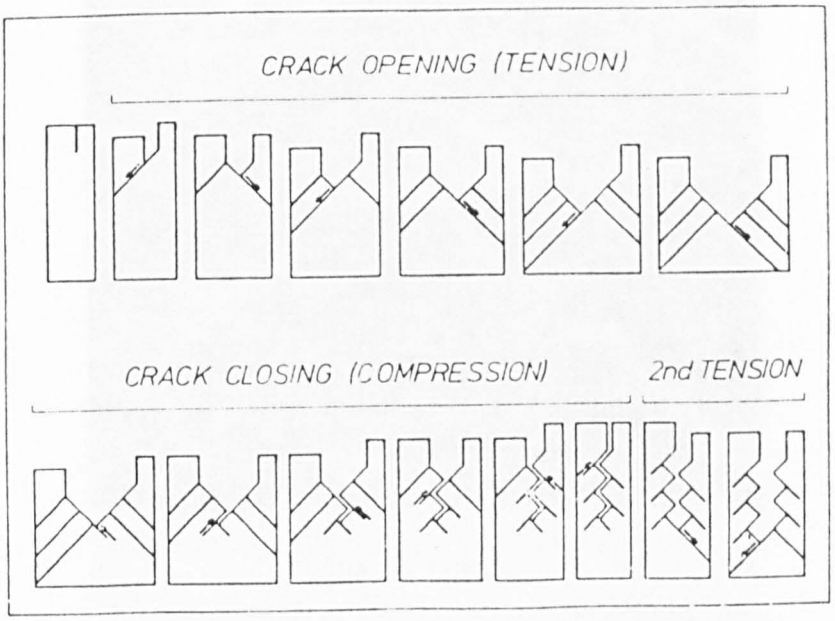

FIGURE 24: Slip processes during one loading cycle, according to the coarse slip fatigue model of Neumman[45].

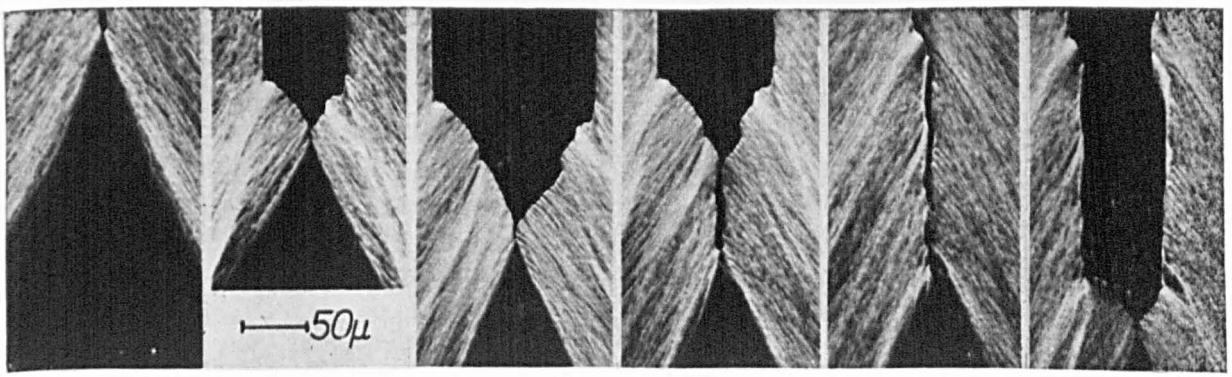

FIGURE 25: Successive shapes of the crack tip during one loading cycle. (Reference 45)

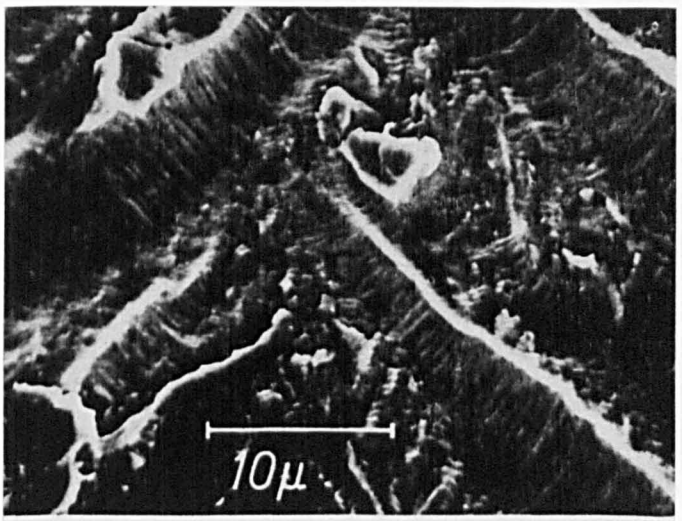

(a)

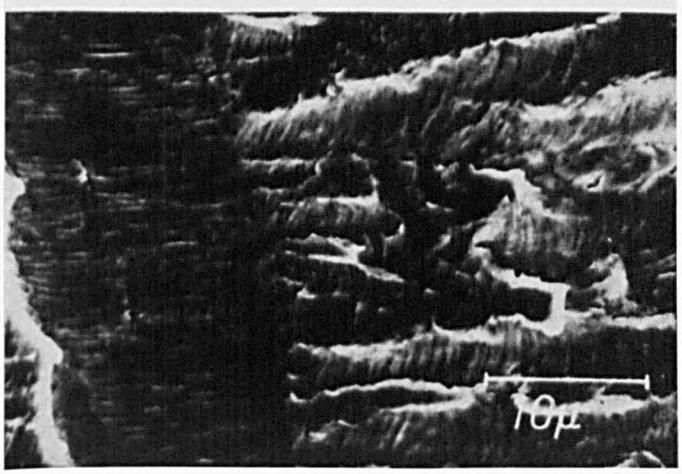

(b)

FIGURE 26: SEM micrographs of fatigue fracture surfaces of specimens (a) and (b) in Figure 23. The local direction of crack propagation is always perpendicular to <011>. (Reference 45)

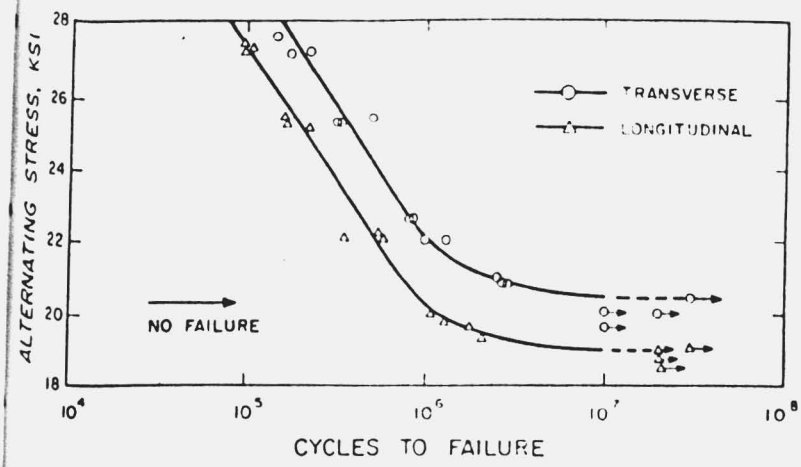

A

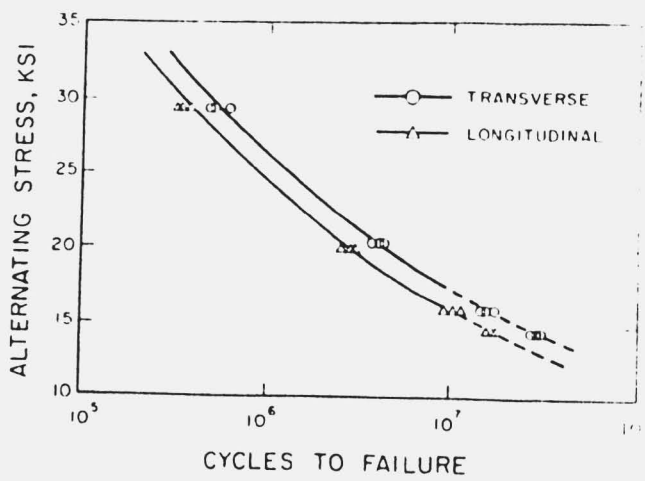

B

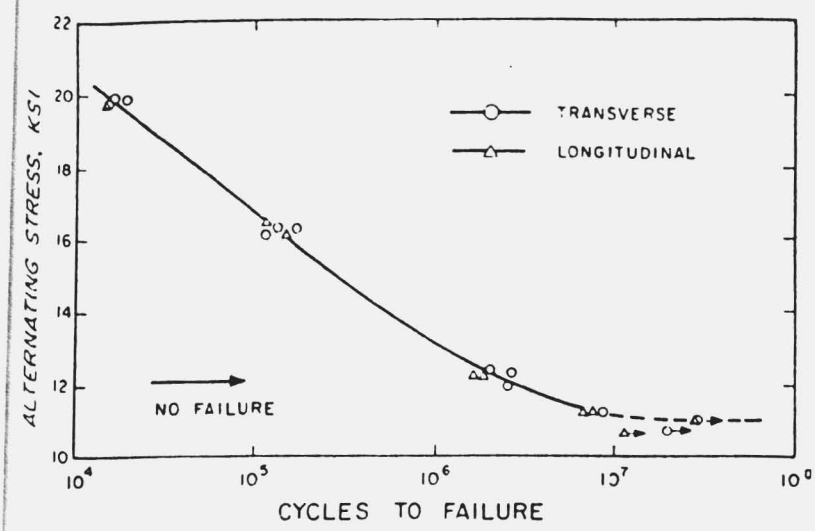

C

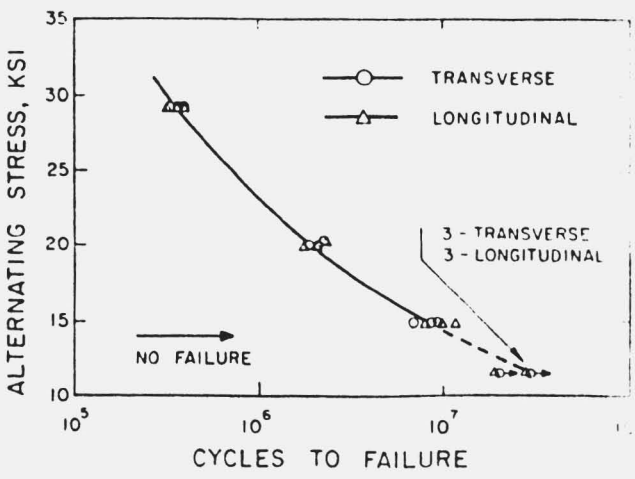

D

FIGURE 27: The S-N curves of some textured polycrystalline materials, taken, as shown, from the transverse or longitudinal directions of the plate.

(A) Cold rolled A1-Mg alloy,
(B) Cold rolled copper,
(C) Annealed A1-Mg alloy,
(D) Annealed copper.

(Reference 80)

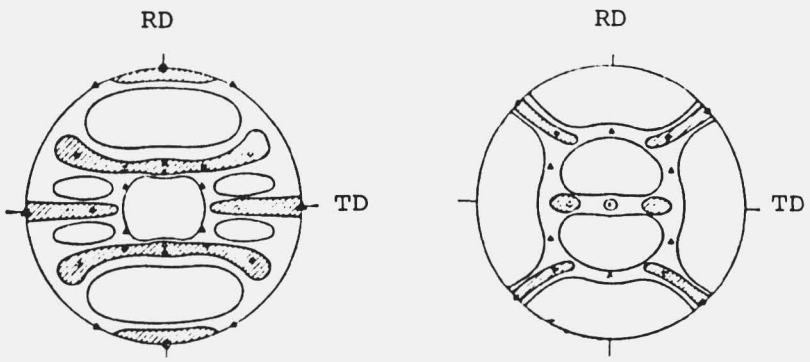

FIGURE 28: The 110 and 100 pole figures respectively of Fe cold-rolled 98.5%. RD is at the top.

= (100)[011]
= (112)[110]
= (111)[112]

(Reference 97)

FIGURE 29: Evidence of strain concentrations preceding crack linkage between voids of MnS inclusions[157].
(x 1200, 1200, 2000).

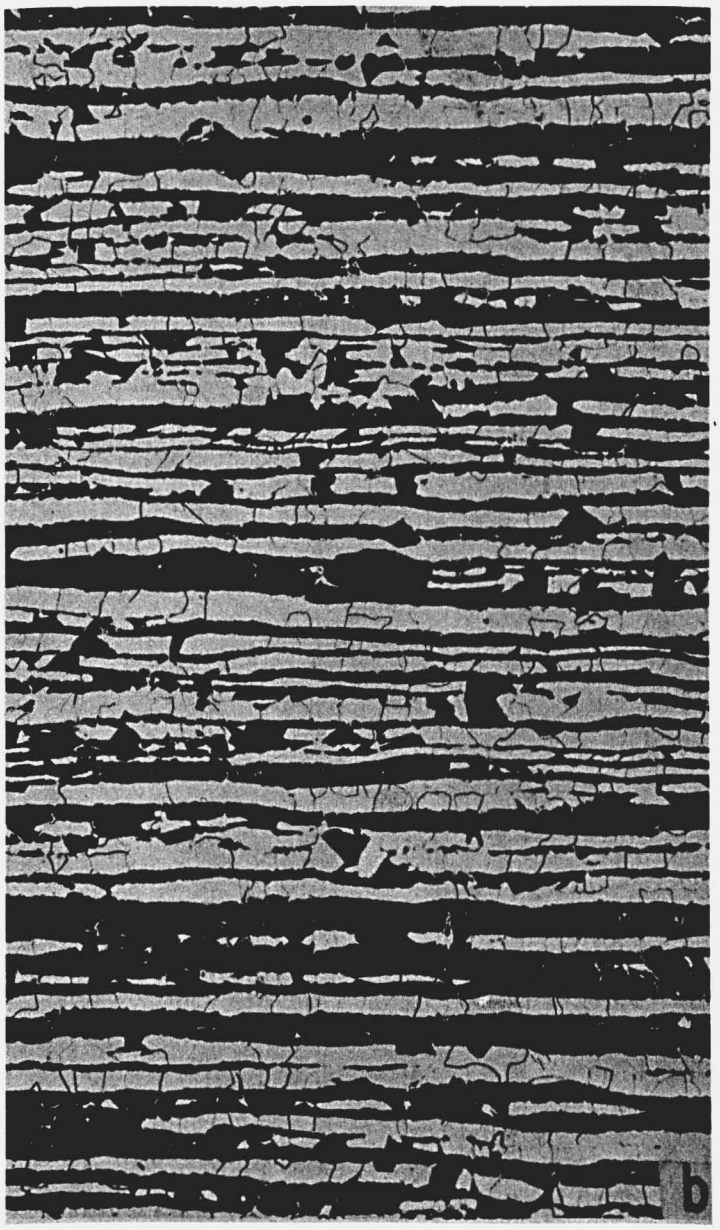

FIGURE 30: Microstructure of a steel showing pearlite banding[114].

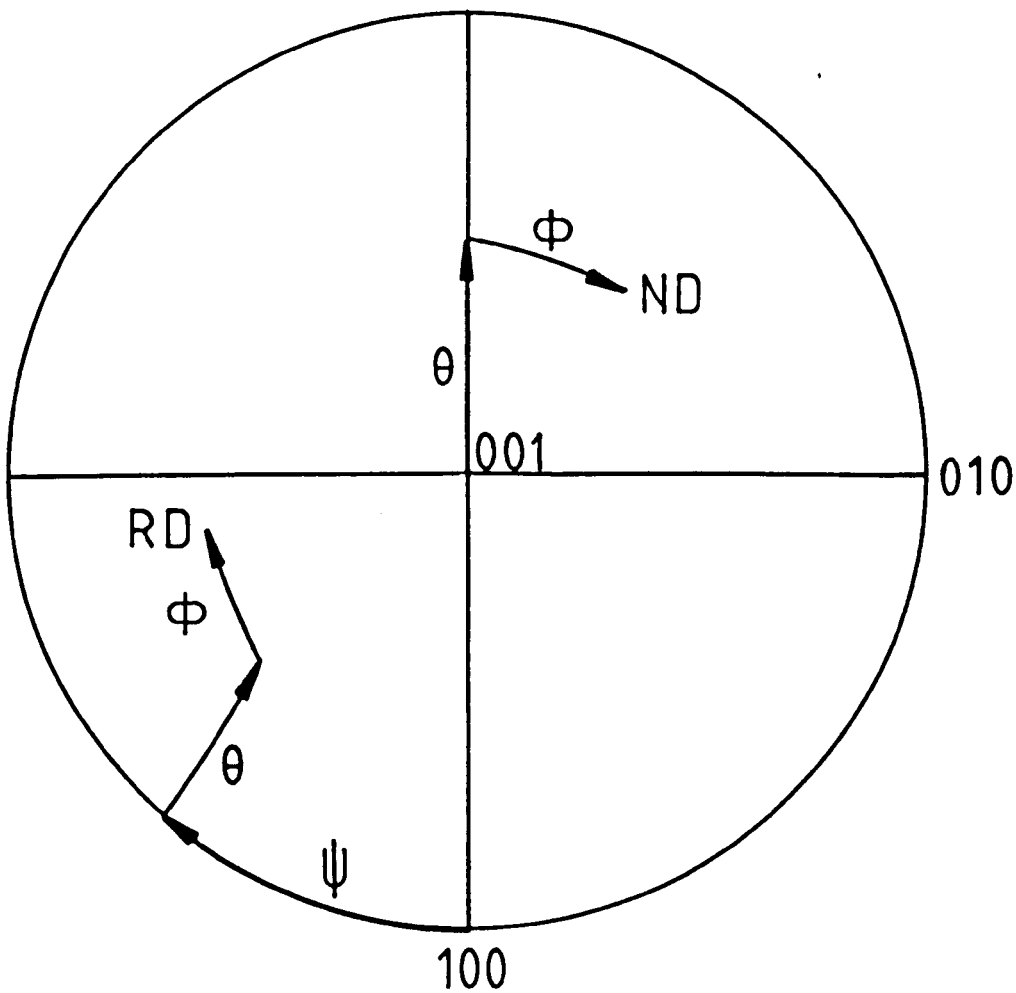

FIGURE 31: Stereographic projection illustrating the Euler angles relating the crystal axes with the specimen sheet normal direction as defined by Roe.

FIGURE 32: The Ψ , θ and ϕ Euler angles used to express the orientation of the crystal axes [100], [010] and [001] with respect to the specimen axes RD, TD and ND.

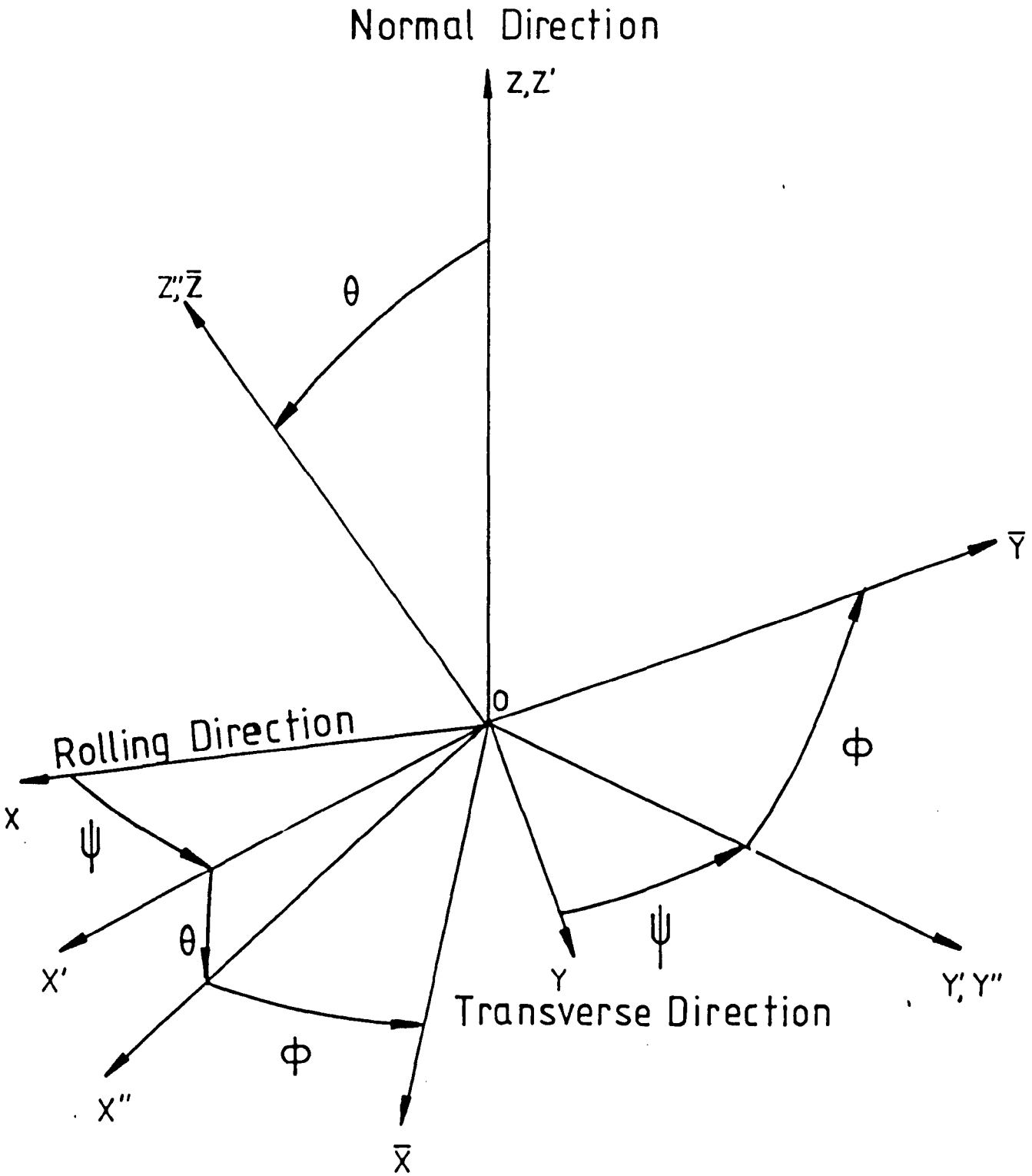

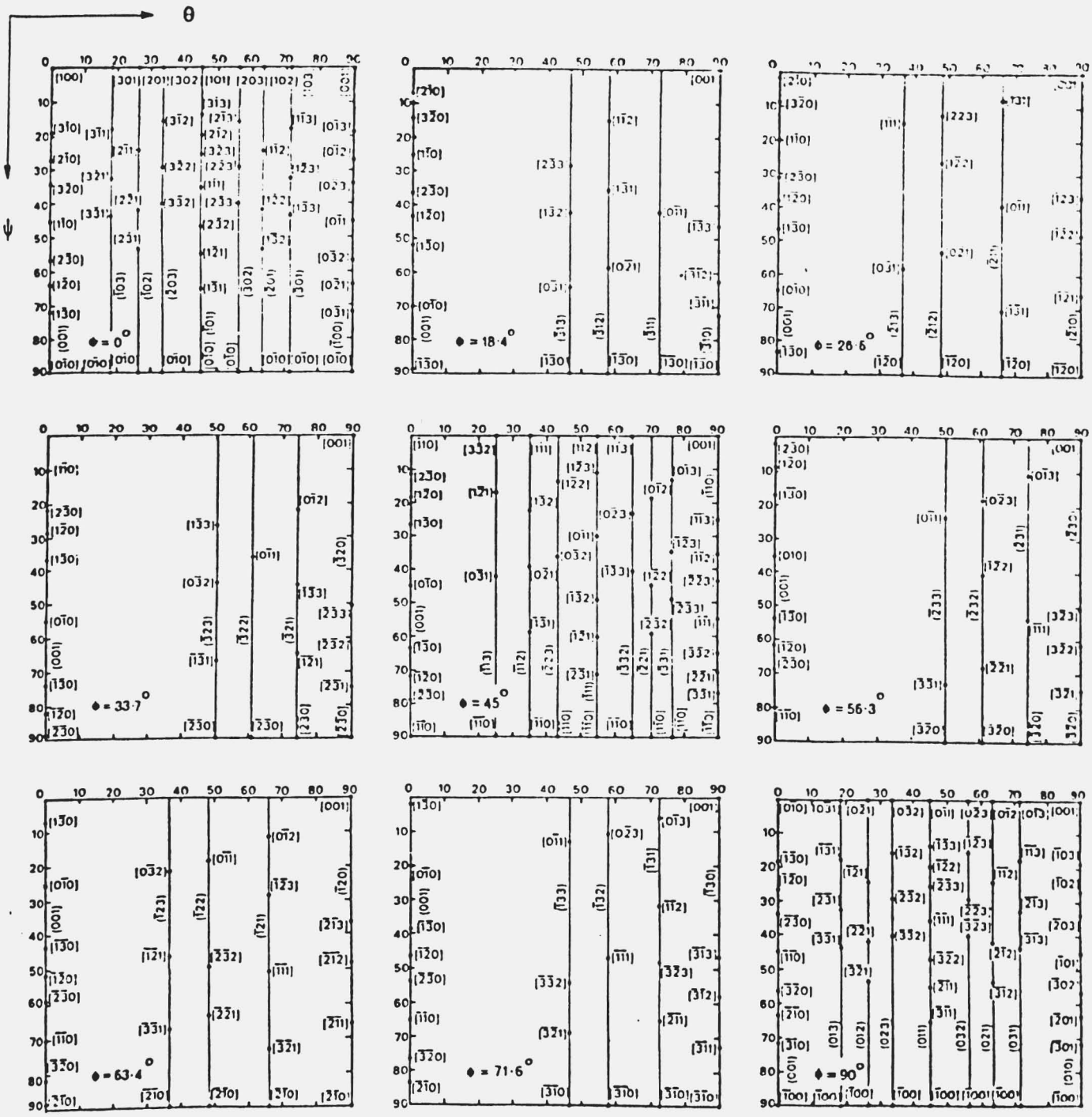

FIGURE 33: Indexing chart for CODF obtained by making constant sections through Euler space. Sections show low index ideal orientations (123).

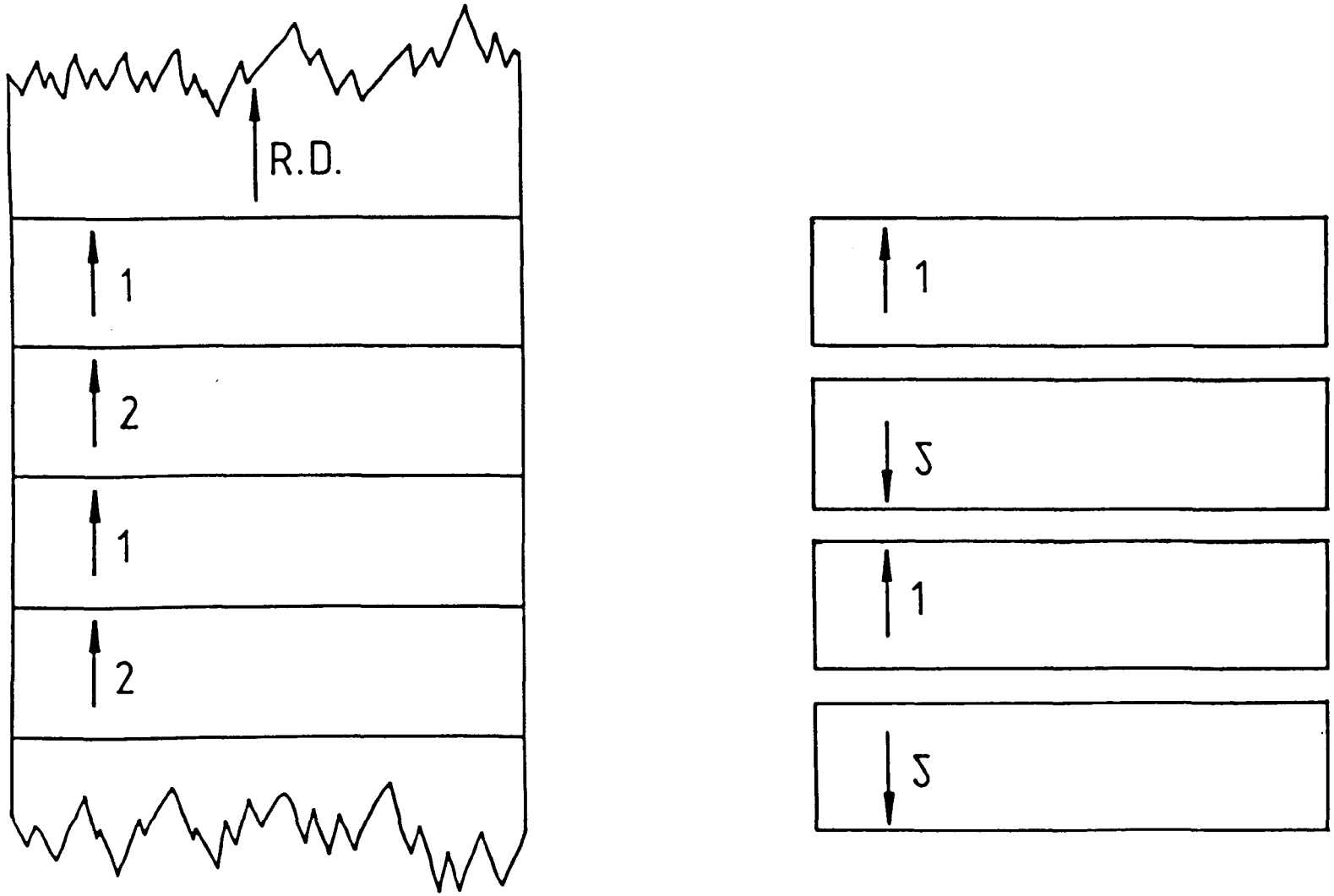

FIGURE 34: The stacking manner of the texture specimens.

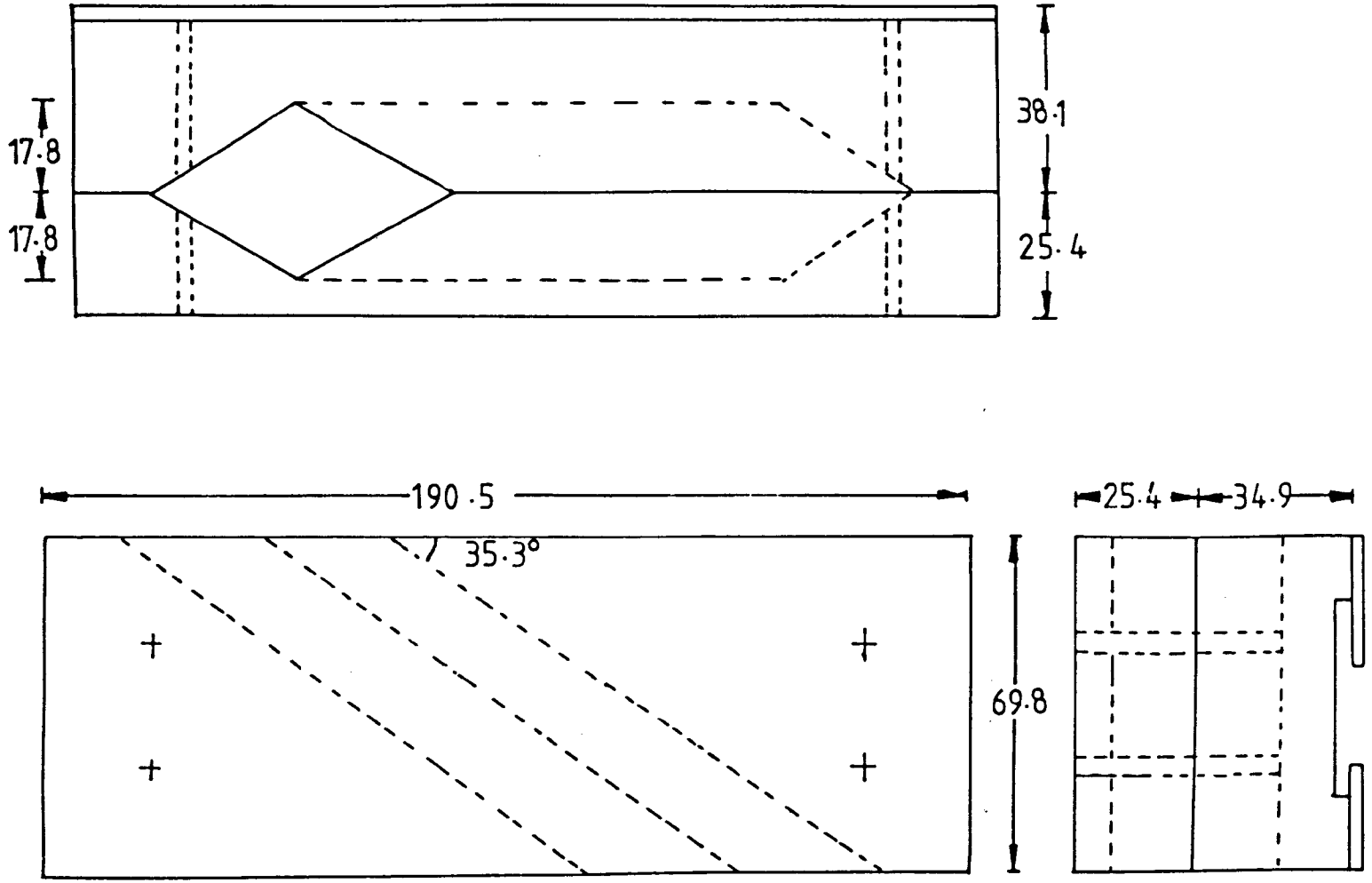

FIGURE 35: The jig used for cutting the texture specimens after being glued and stacked as in Figure 34.

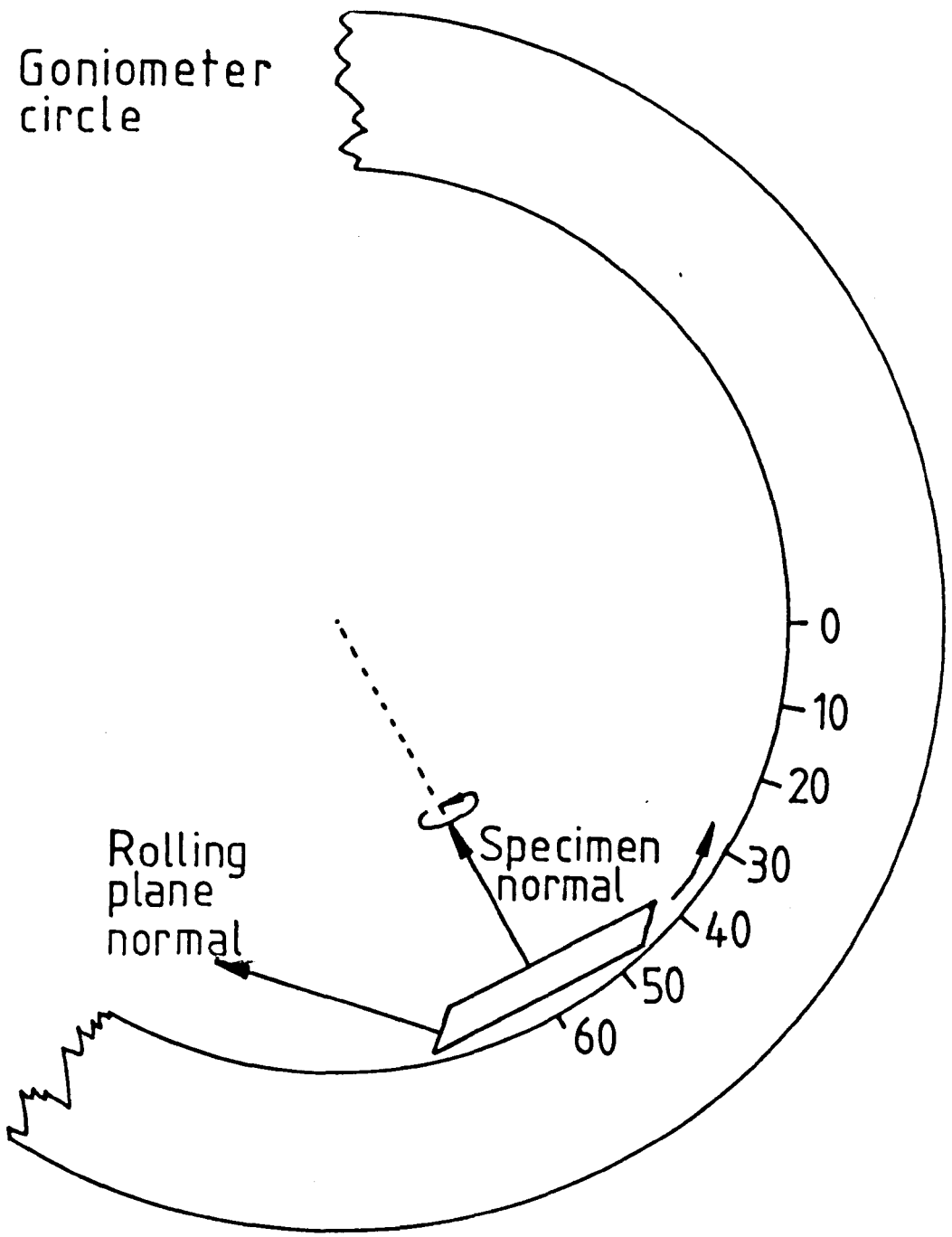

FIGURE 36: The starting position of the texture specimens on the goniometer circle.

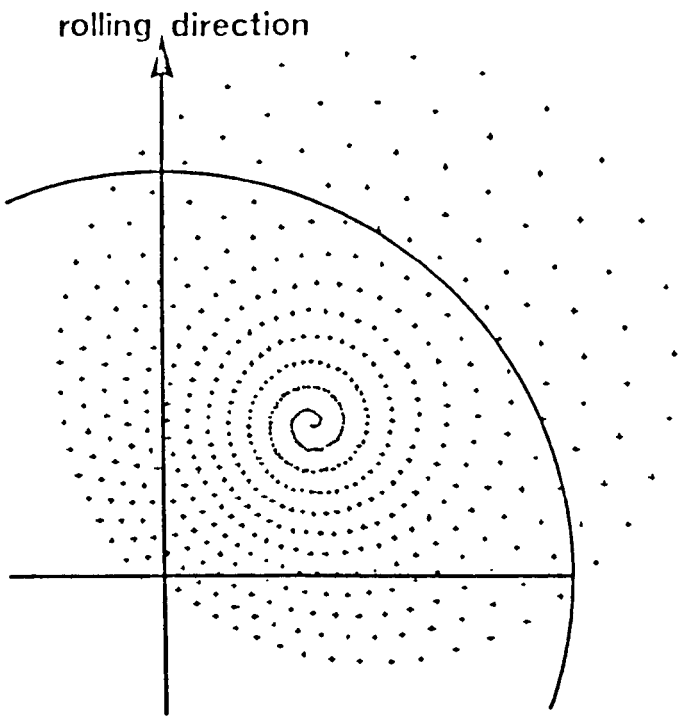

FIGURE 37: The spiral path traced by the diffracting plane normal during data acquisiton. The crosses indicate the data sampling points.

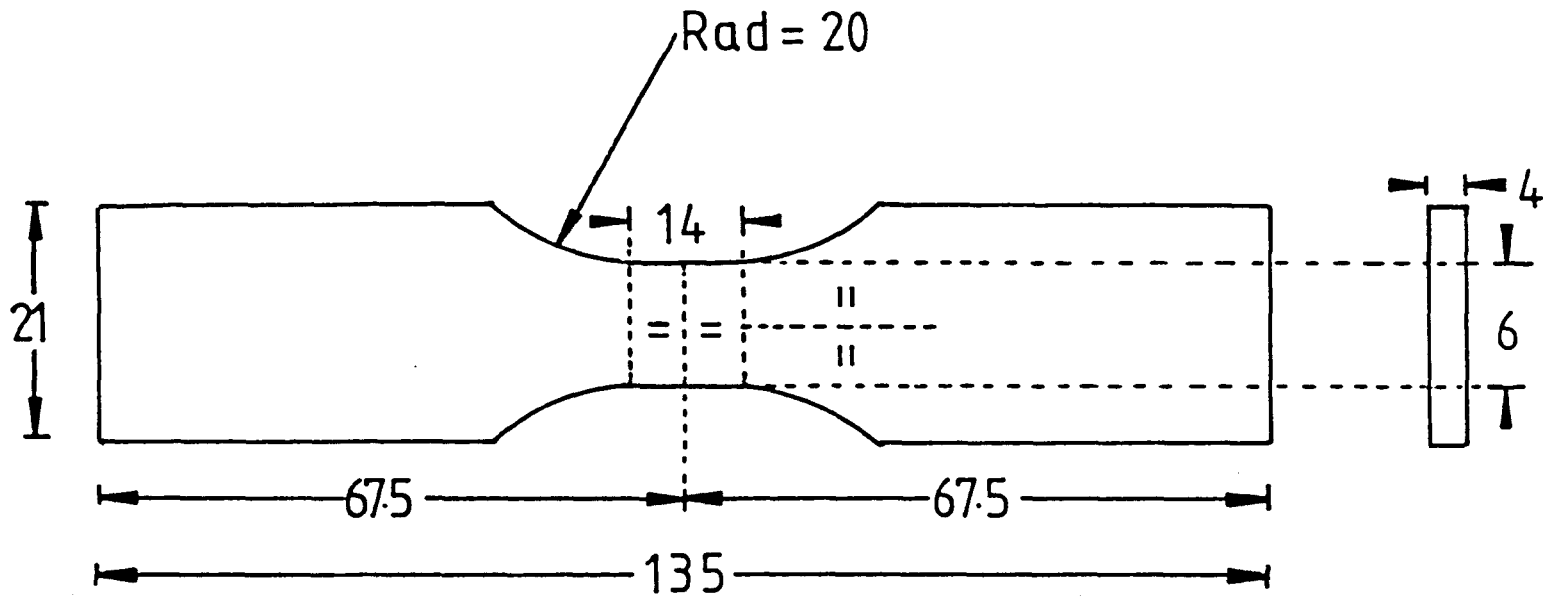

FIGURE 38: F.G.8 fatigue specimens. Dimensions in mm.

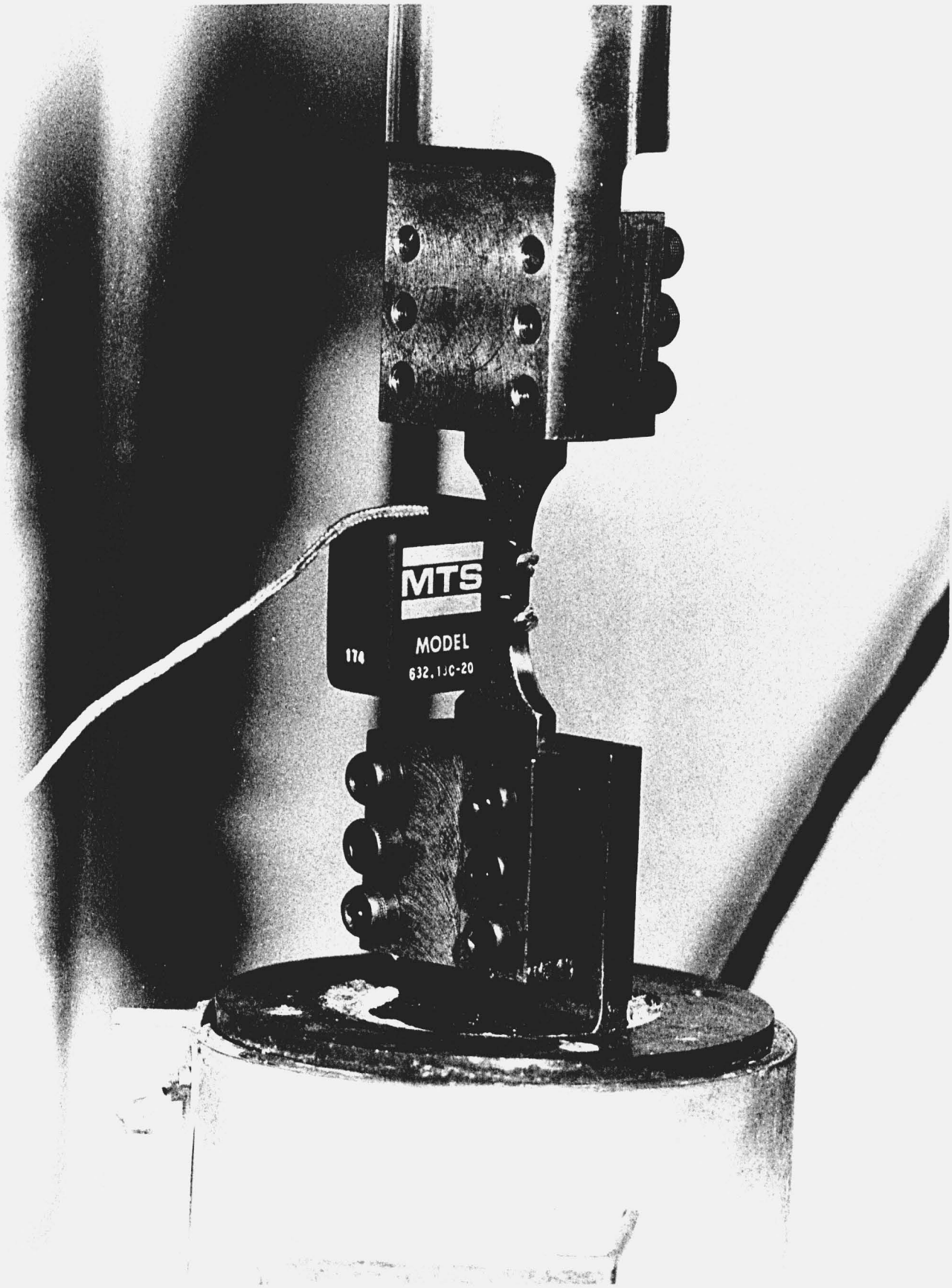

FIGURE 39: The MTS servo-hydraulic fatigue testing machine, with F.G.8 specimen (with strain gauge) in place.

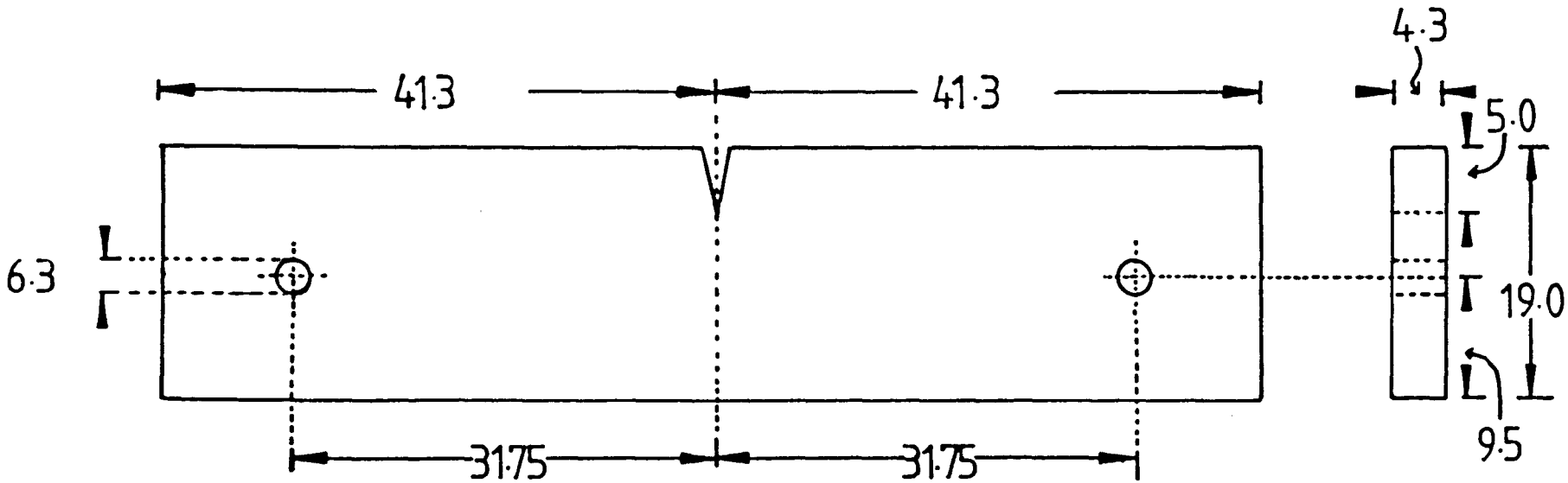

FIGURE 40: The dimensions of the single edge notched crack propagation specimens.

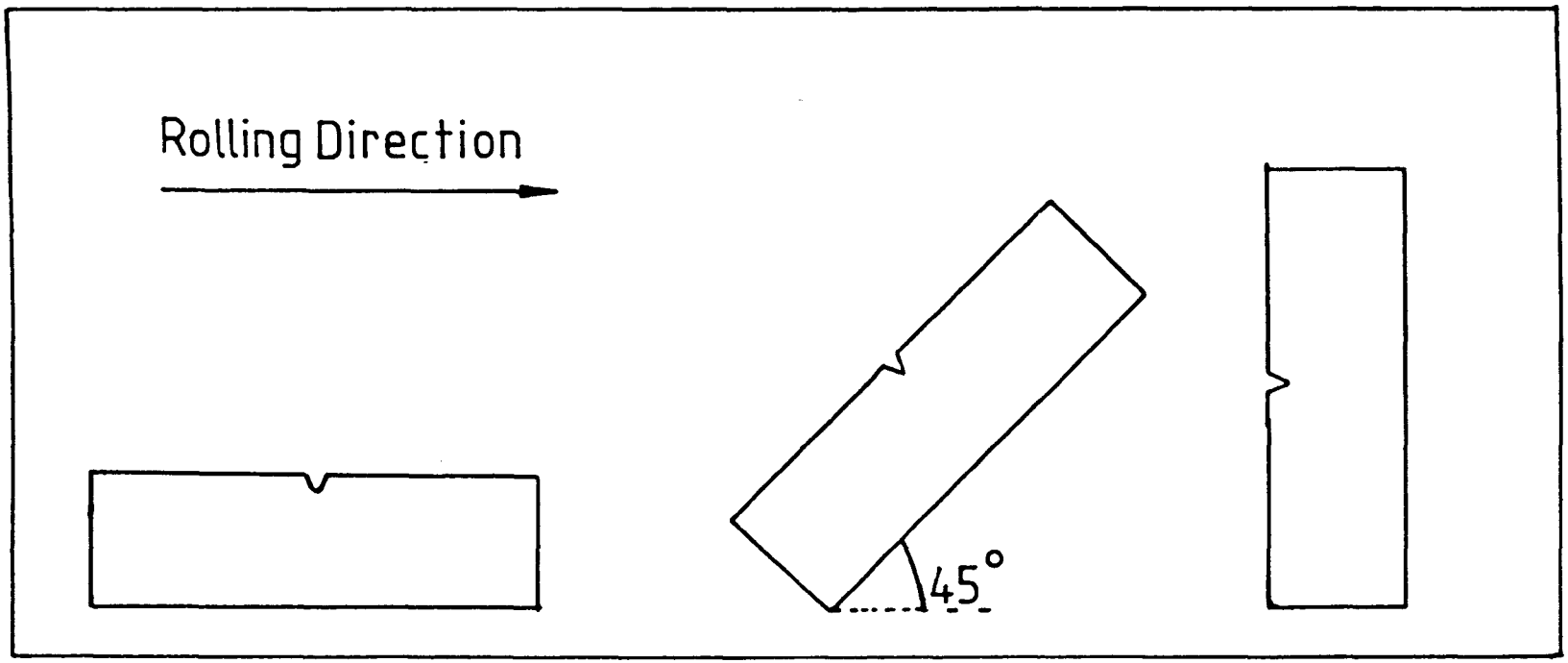

CR80 = (100)[011] + (111)[uvw] mfh = 12·8 tsp = 1·63

R80AN = (hkl)[110] + (111)[uvw] mfh = 4·7 tsp = 1·02

FIGURE 41: The orientation of the SEN specimens with respect to the sheet.

SHEFFIELD UNIVERSITY LIBRARY

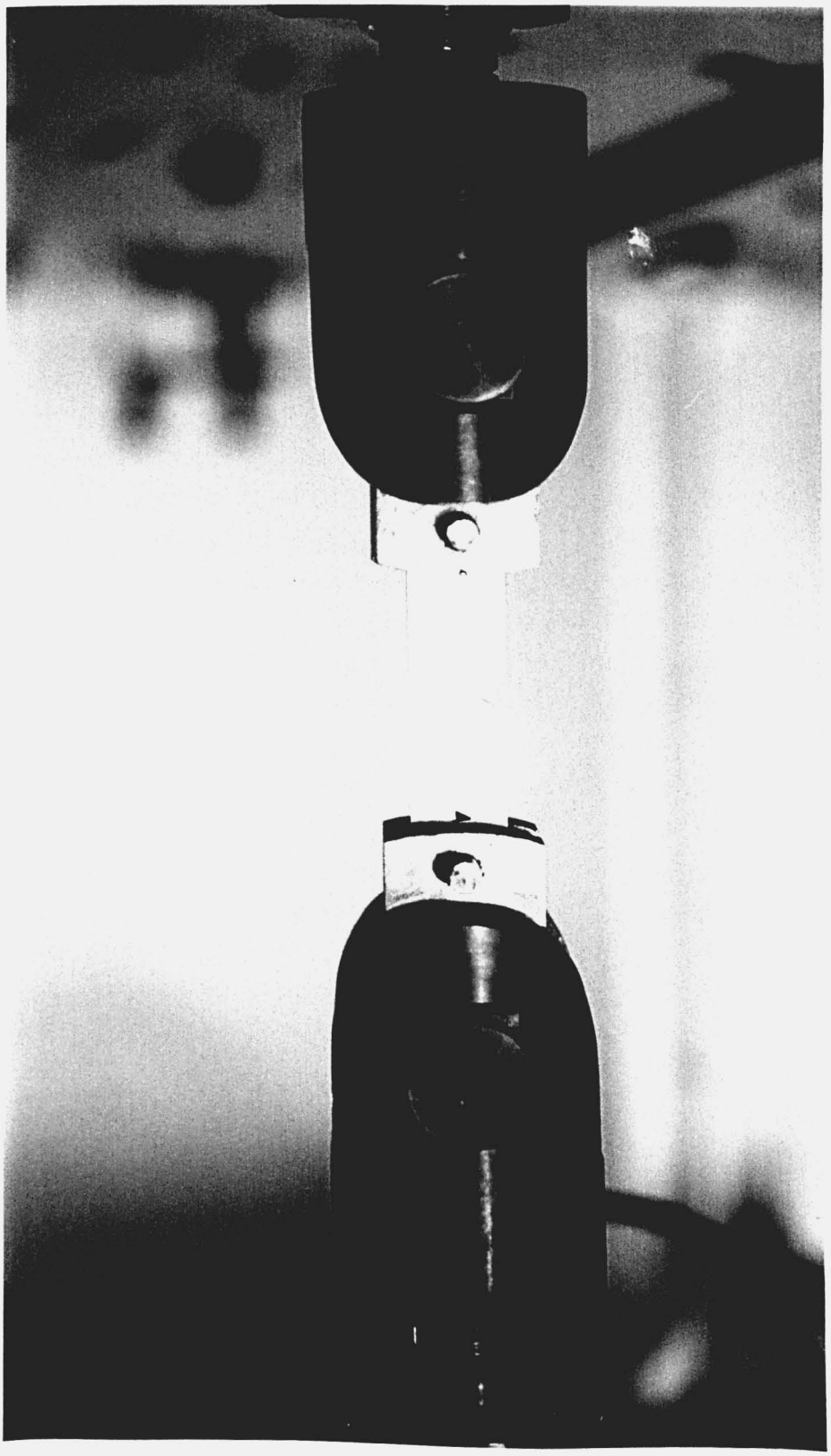

FIGURE 42: Amsler Vibraphore with SEN specimens in place.

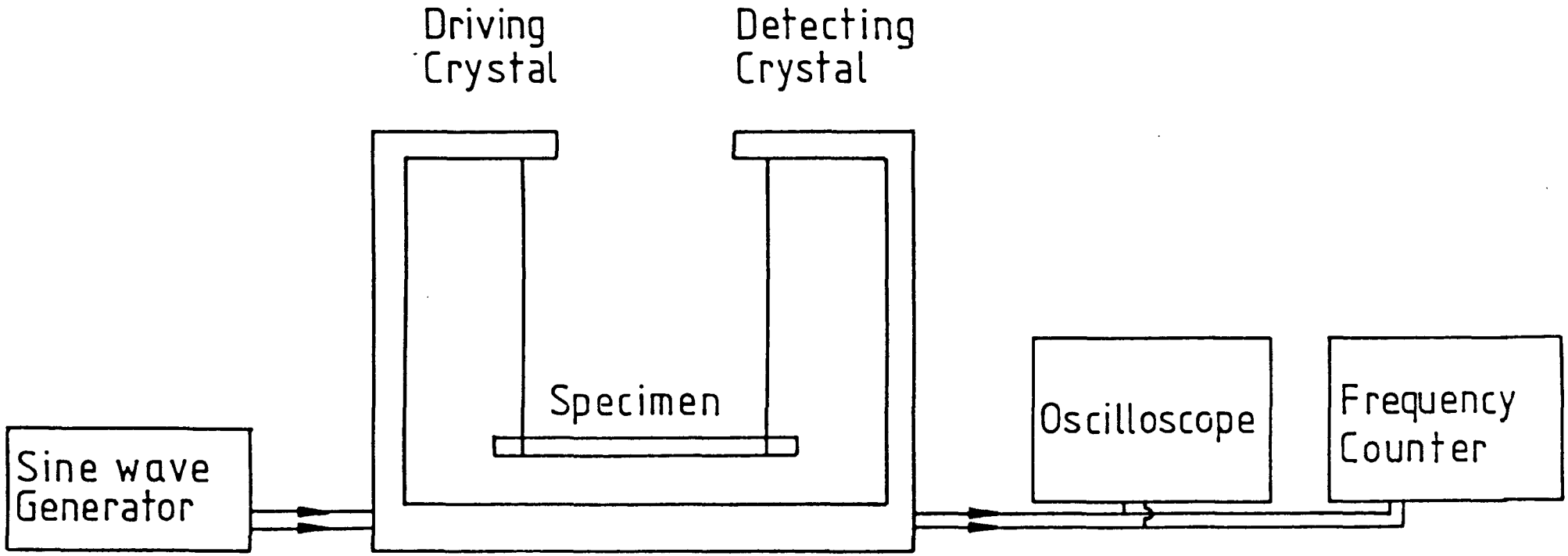

FIGURE 43: Schematic representation of the resonance method for finding Young's modulus, E.

FIGURE 44: The polar grid used for interpolation of the x-ray data.

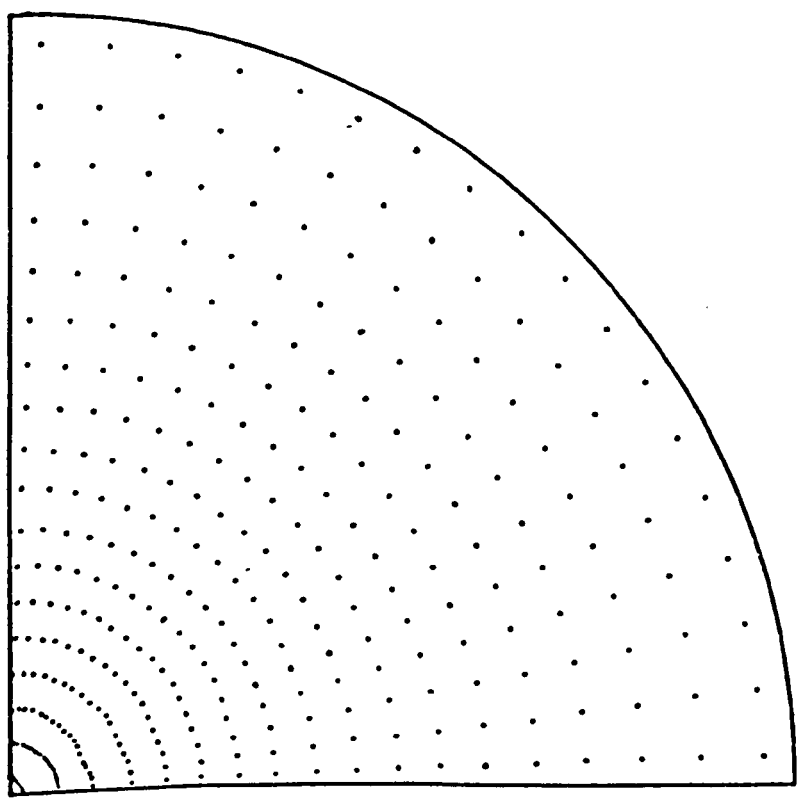

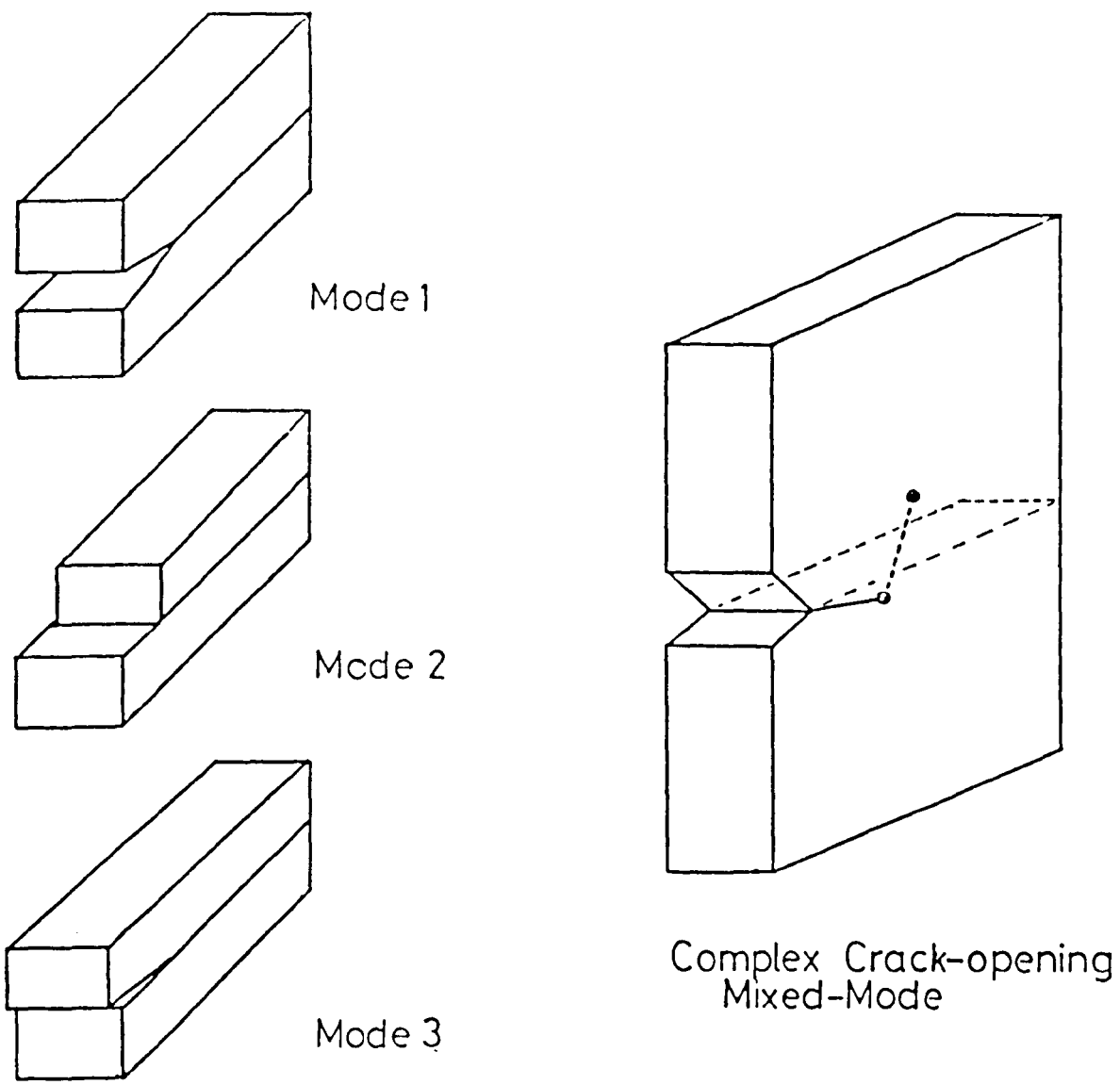

FIGURE 45: Schematic representation of modes I, II and III crack opening. Also a schematic diagram of the complex modes observed in some specimens.

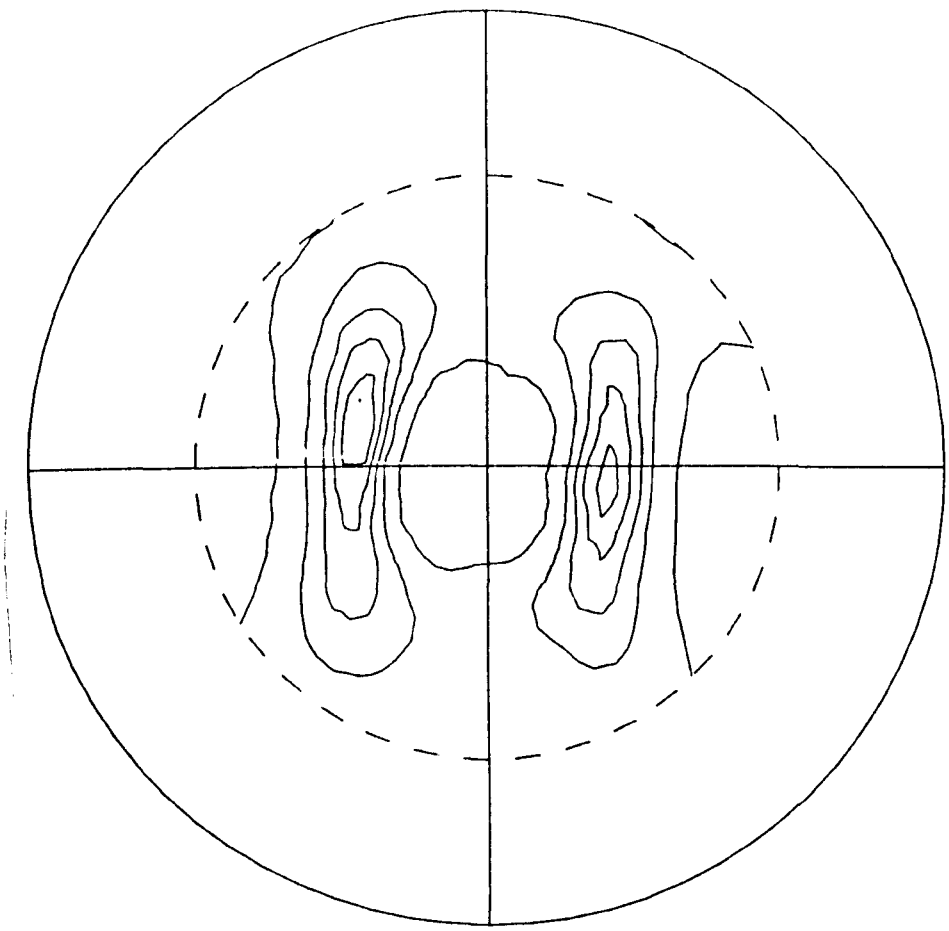

FIGURE 46: A typical direct pole figure (CR80110) displaying orthotropism in the plane of the sheet.

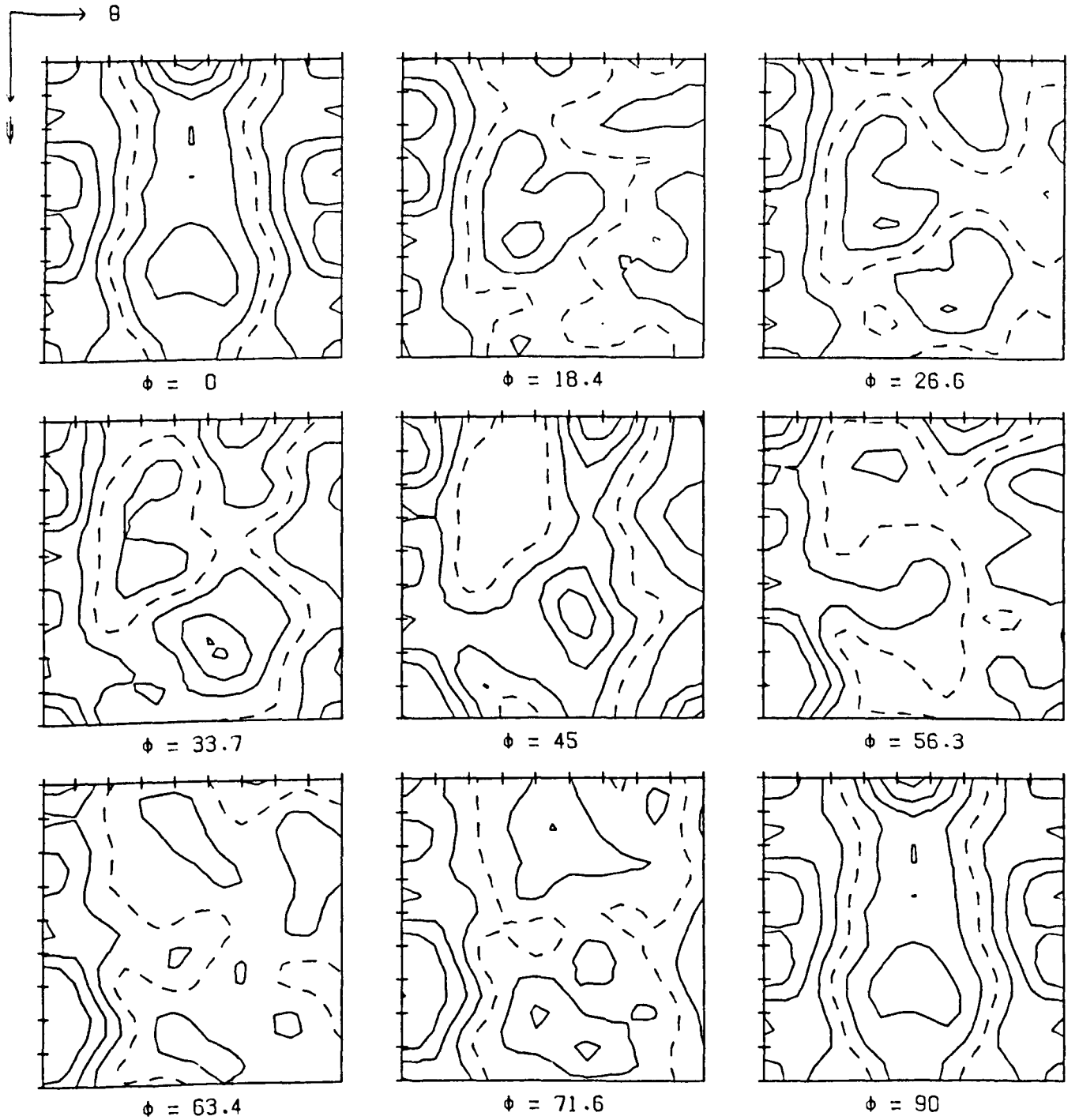

FIGURE 47: S10BM c.o.d.f. m.f.h. = 1.8 severity = 0.26

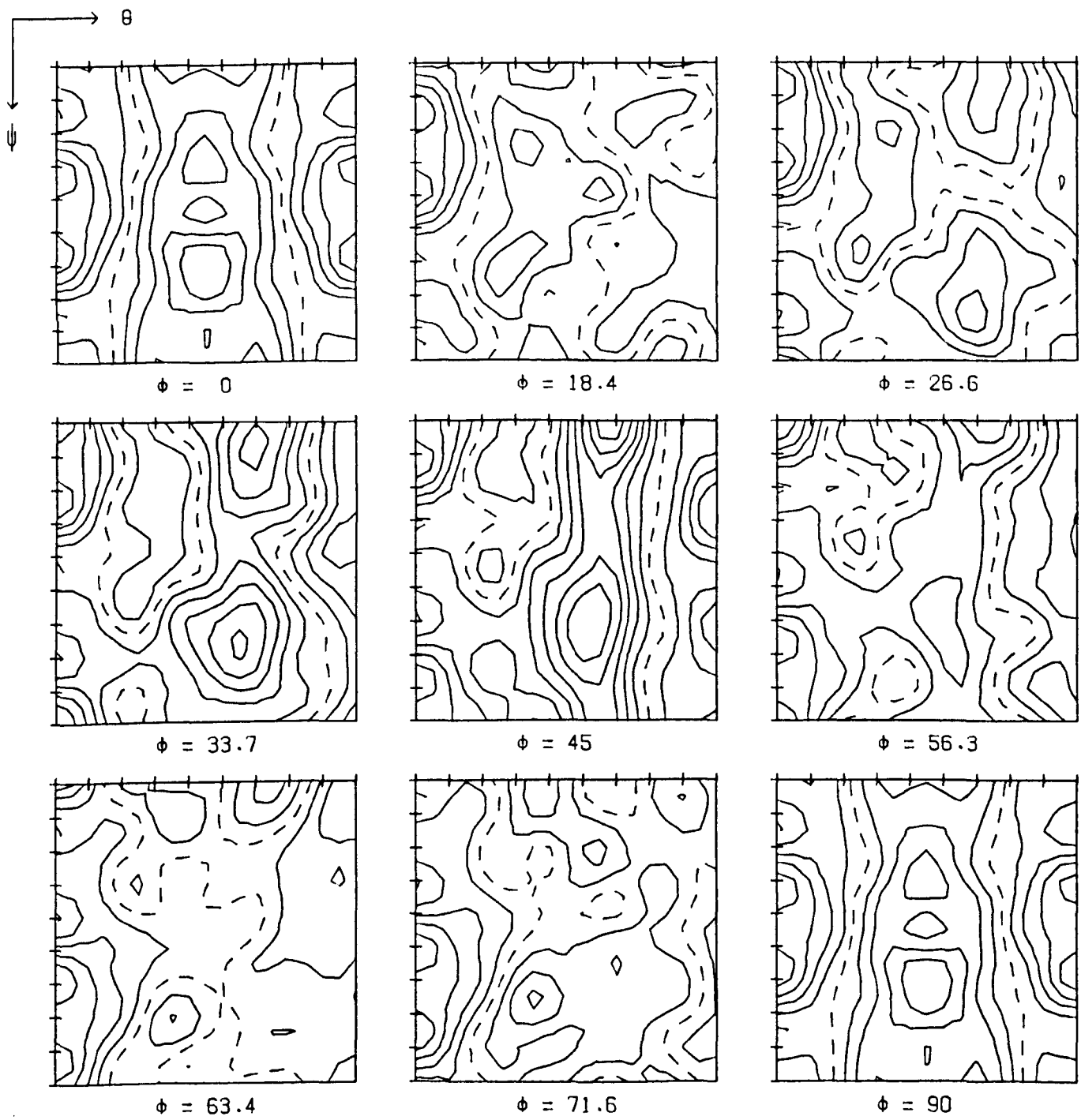

FIGURE 48: S12BM c.o.d.f. m.f.h. = 2.4 severity = 9.37

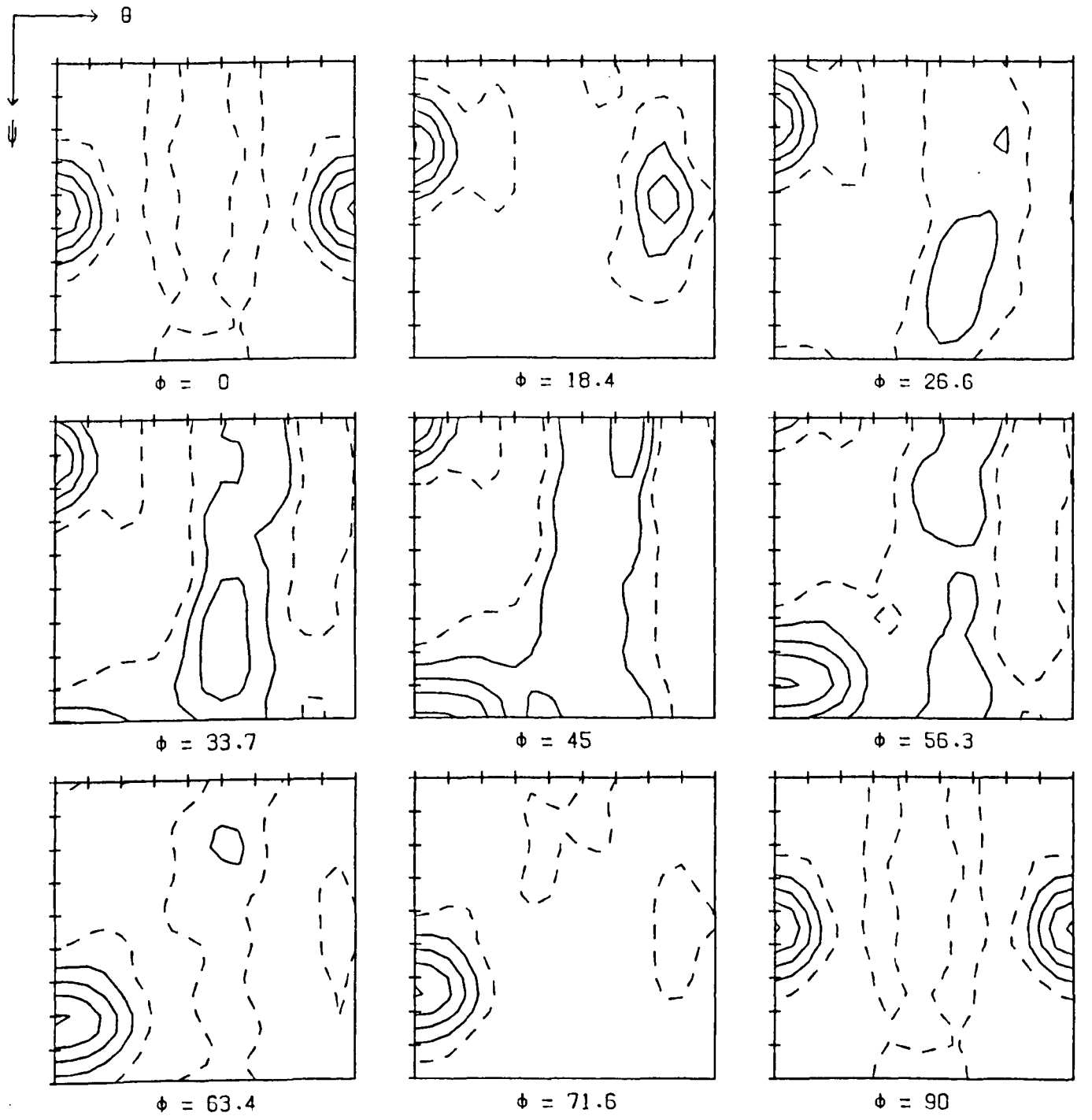

FIGURE 49: CR68 c.o.d.f. m.f.h. = 5.2 severity = 0.93

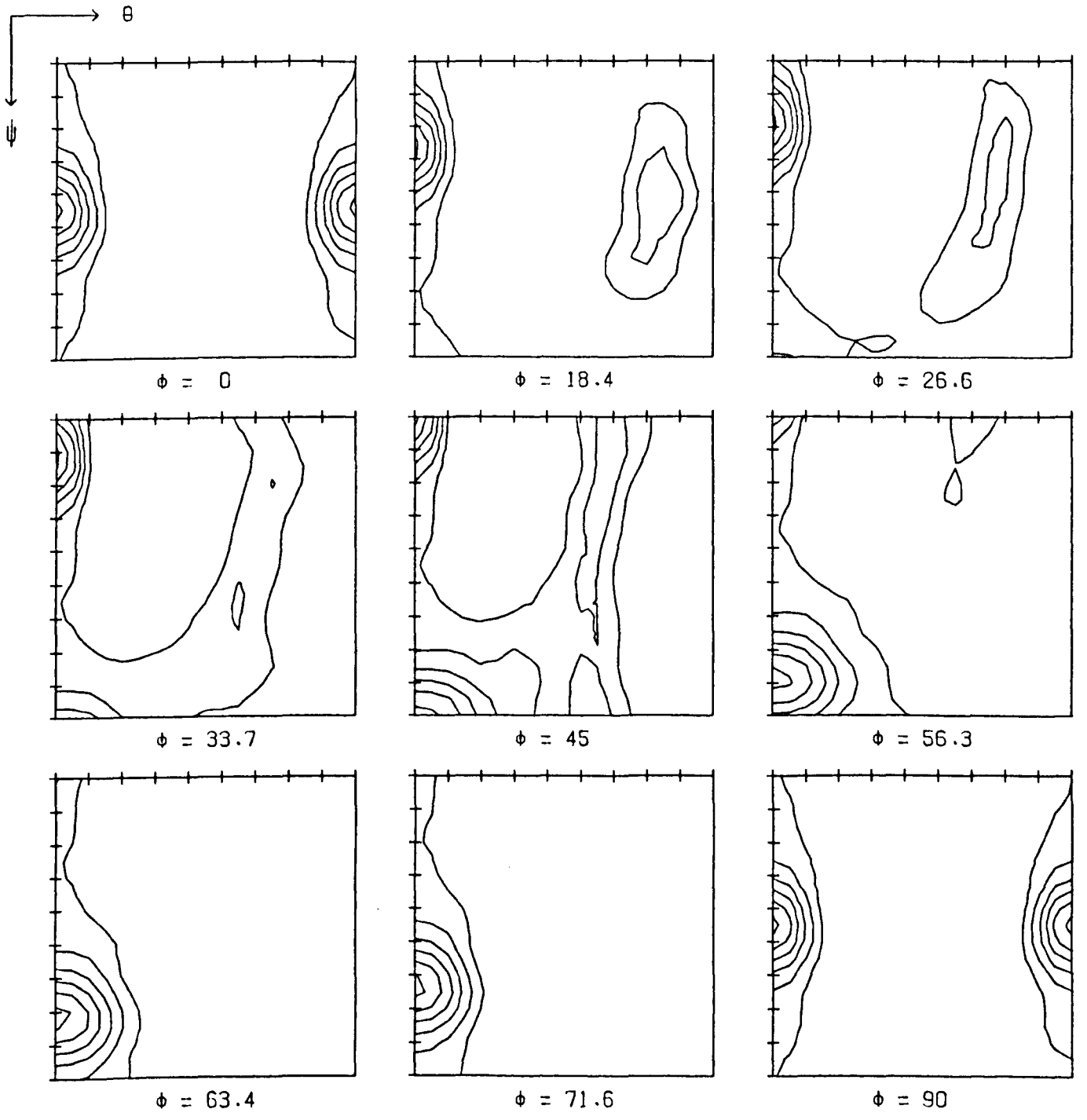

FIGURE 50: CR80 c.o.d.f. m.f.h. = 12.8 severity = 1.63

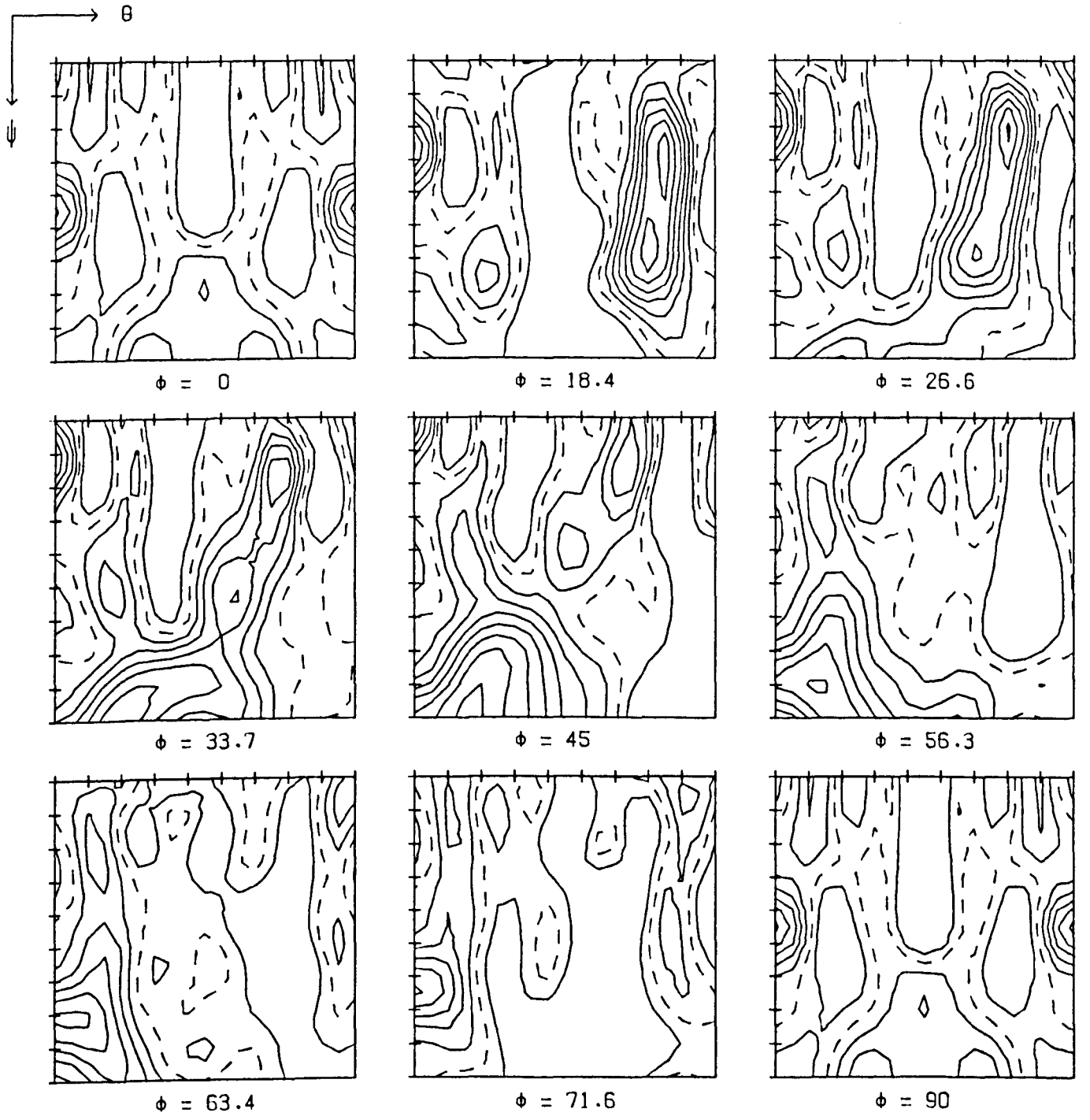

FIGURE 51: R80AN c.o.d.f. m.f.h. = 4.7 severity = 1.02

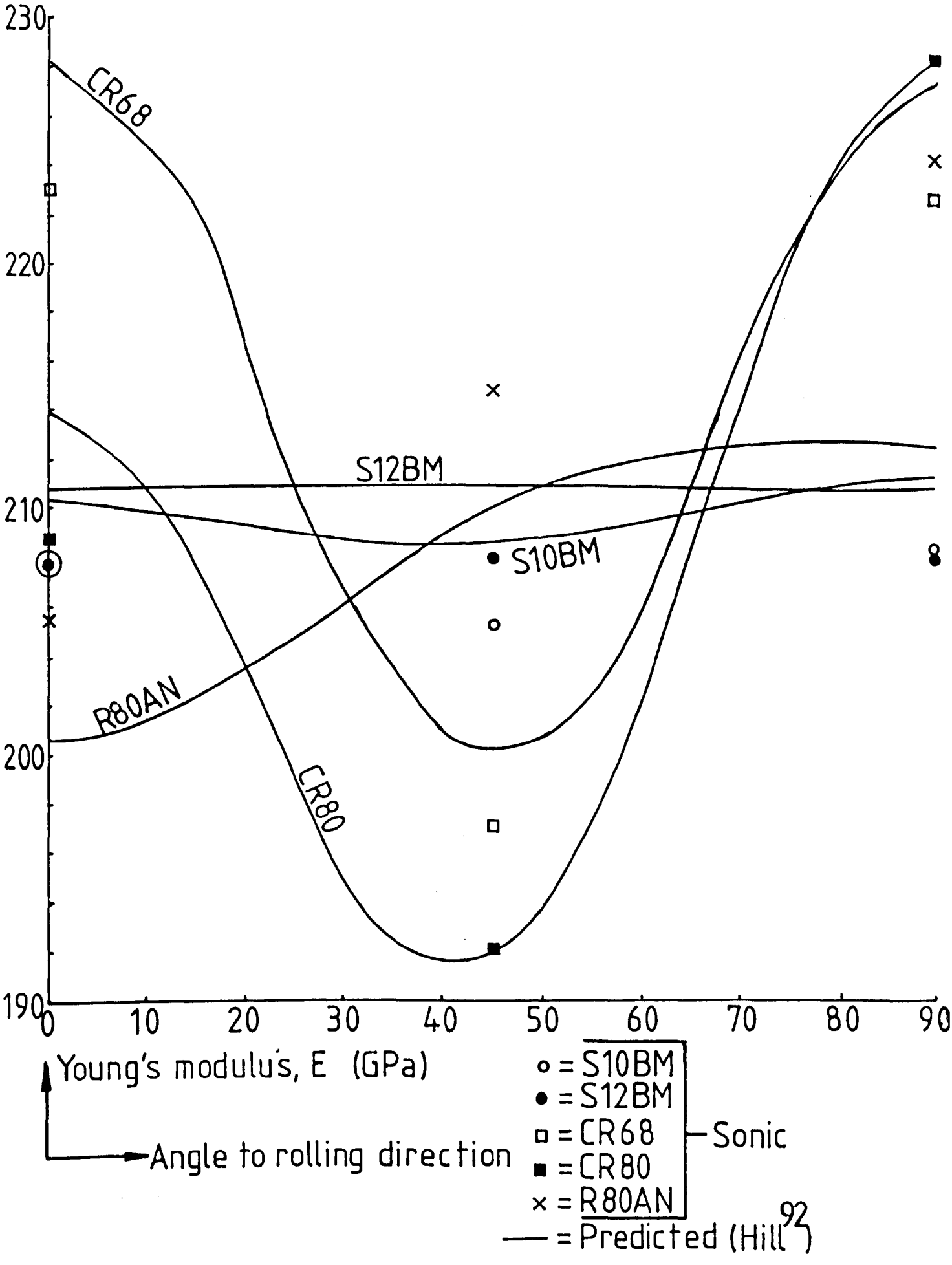

FIGURE 52: Predicted and experimental values of Young's modulus, E.

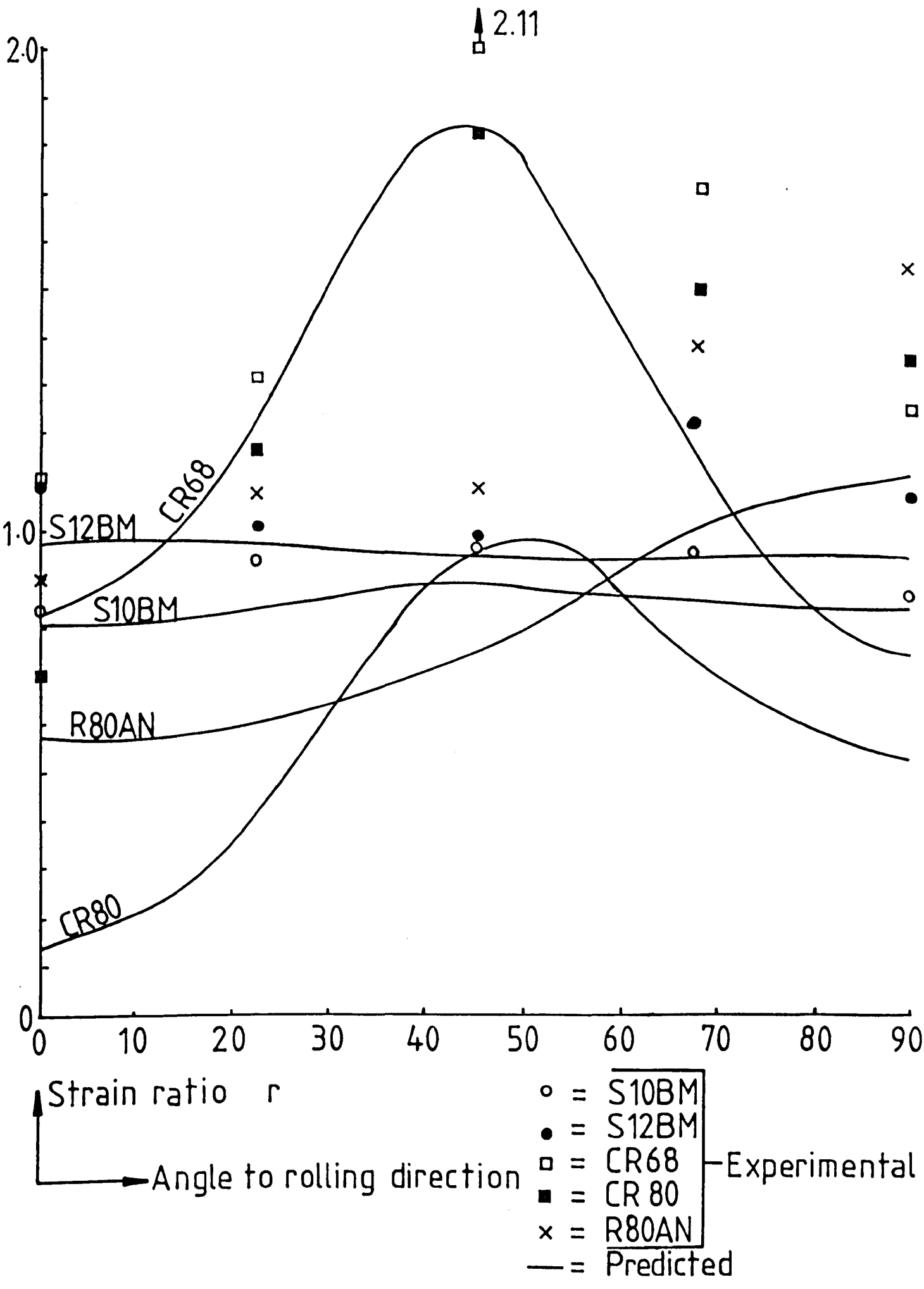

FIGURE 53: Predicted and experimental values of the strain ratio, r.

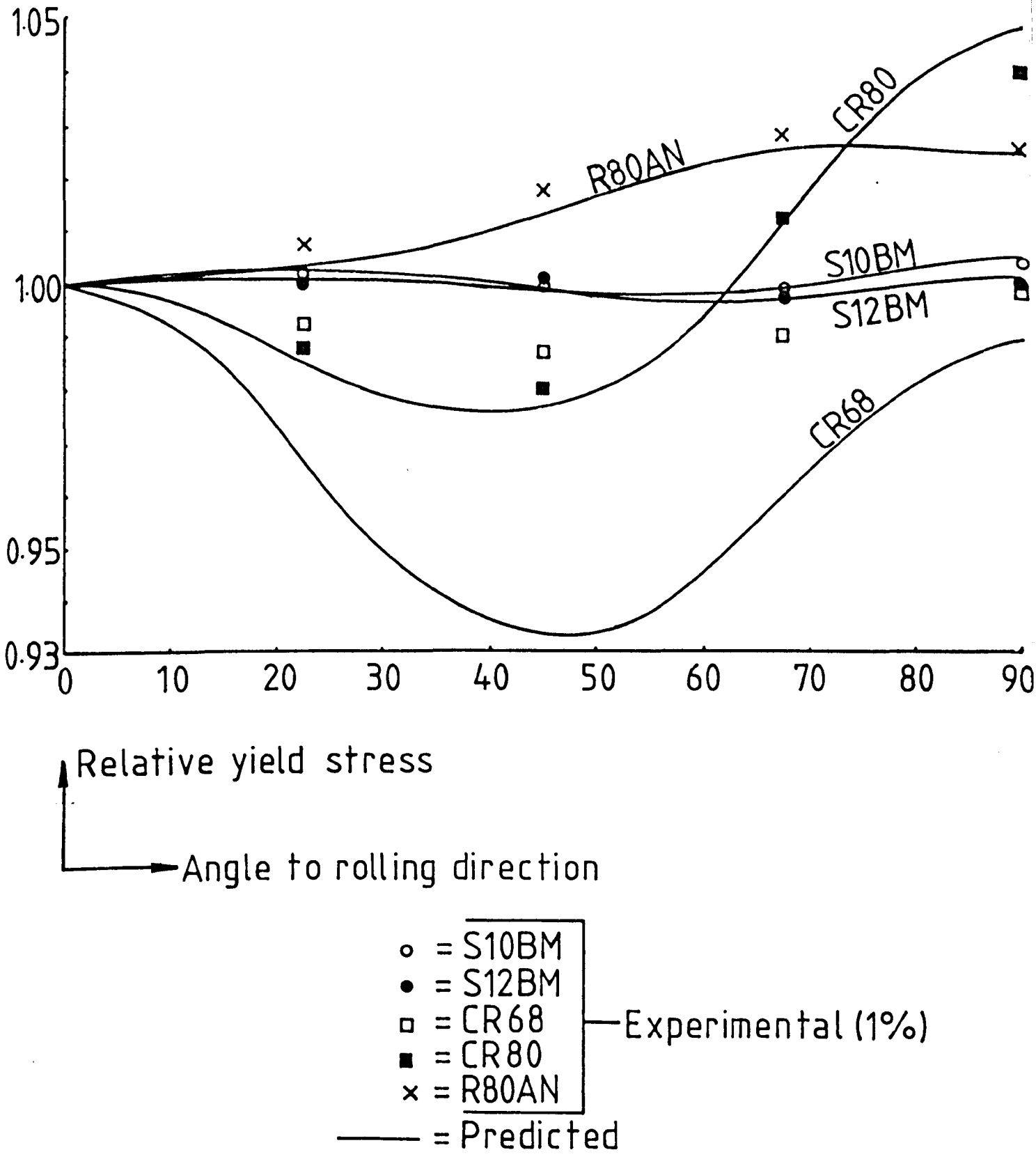

FIGURE 54: Predicted and experimental values of the relative yield stress.

FIGURE 55: The cyclic stress-strain curve of S10BM0

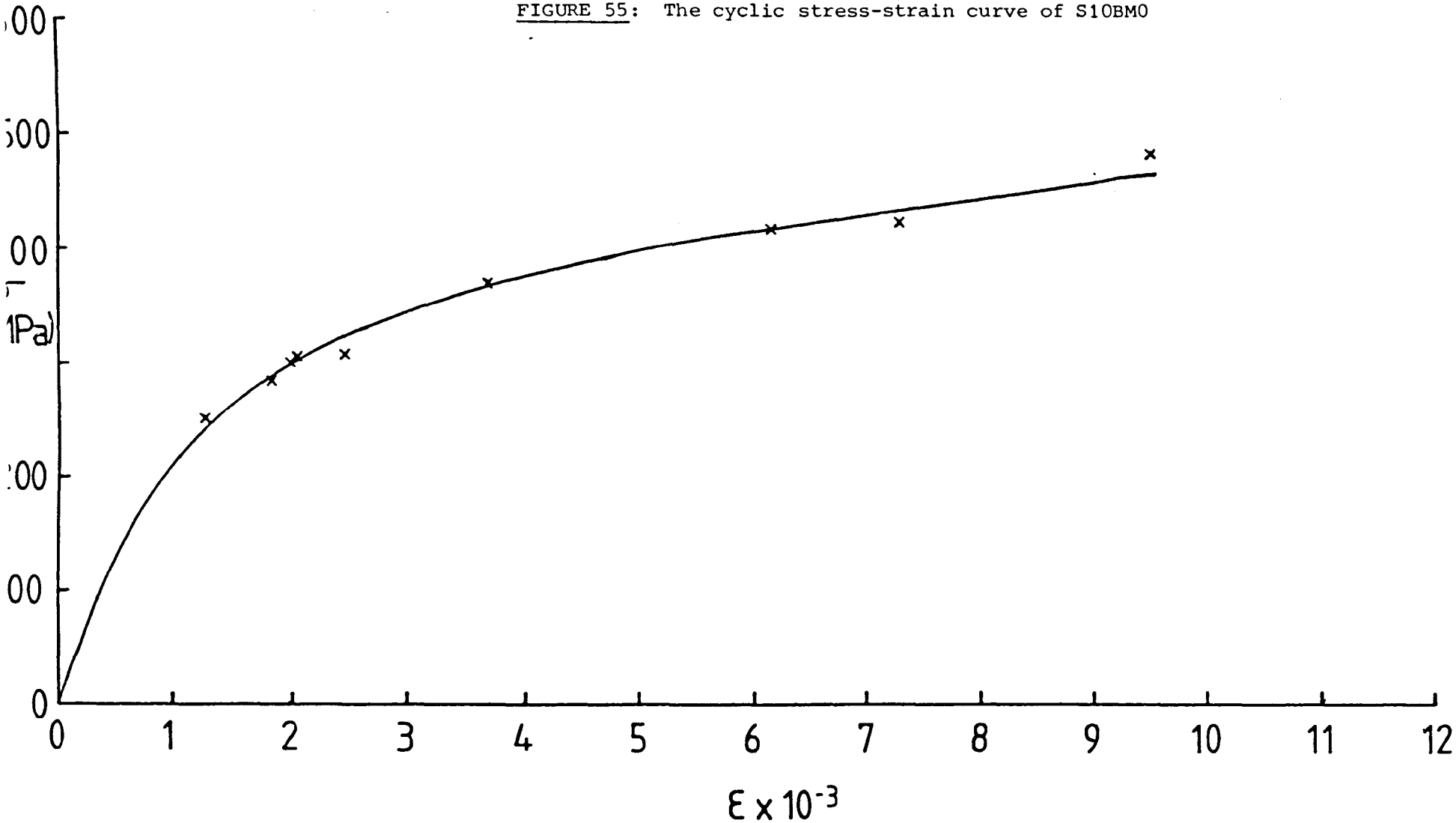

FIGURE 56: The cyclic stress-strain curve of S10BM45

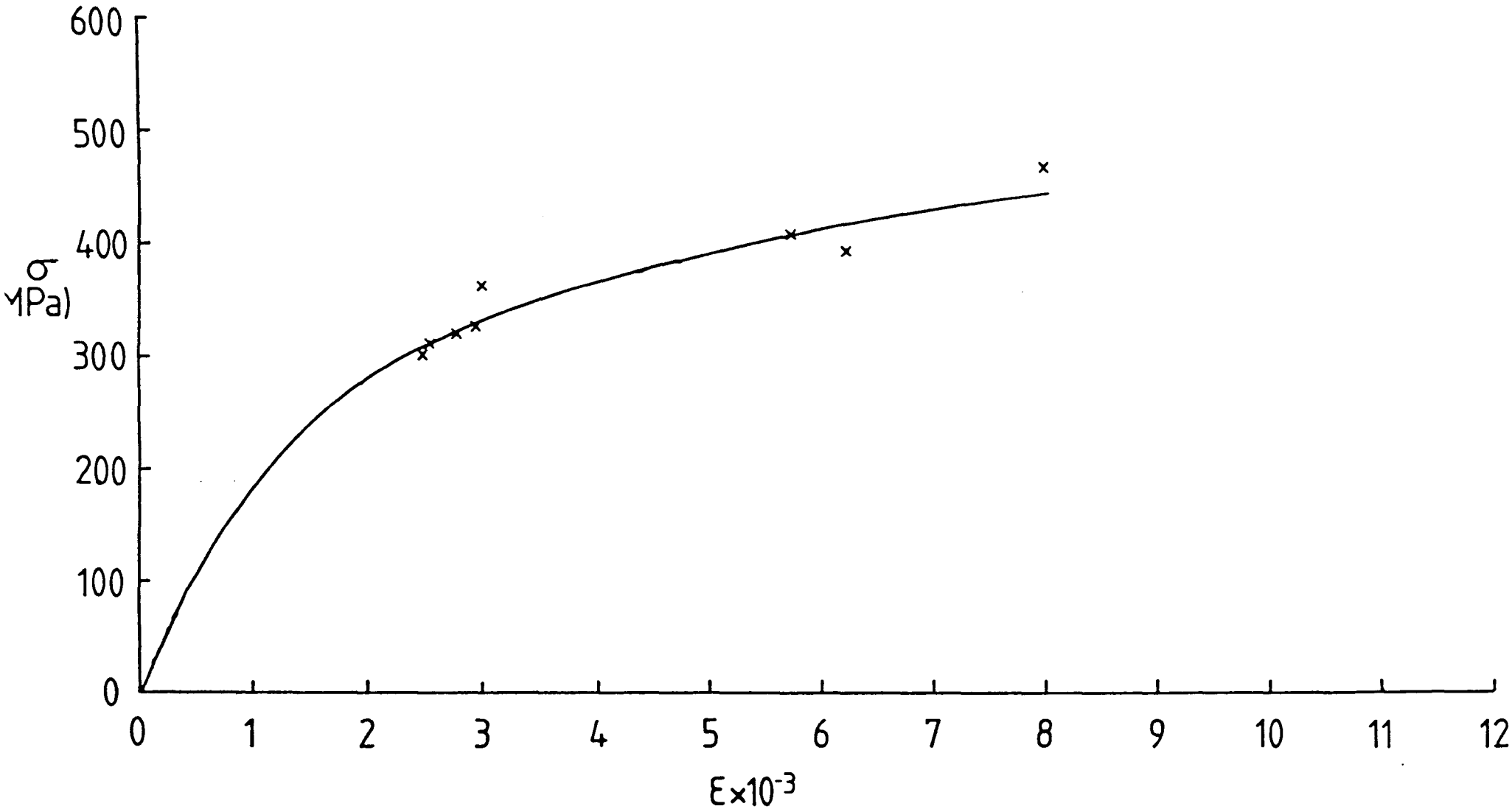

FIGURE 57: The cyclic stress-strain curve of S10BM90

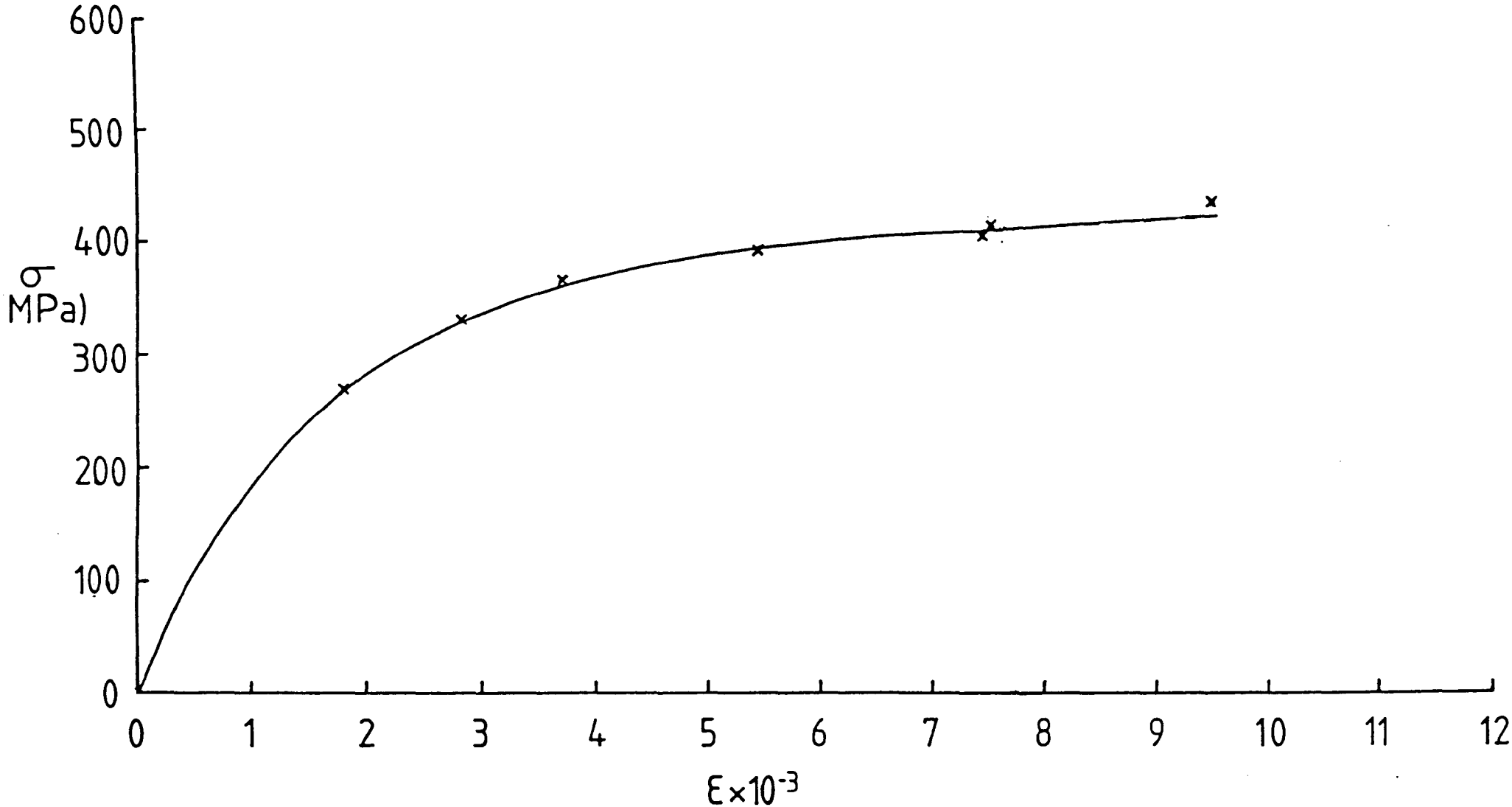

FIGURE 58: The cyclic stress-strain curve of S12BM0

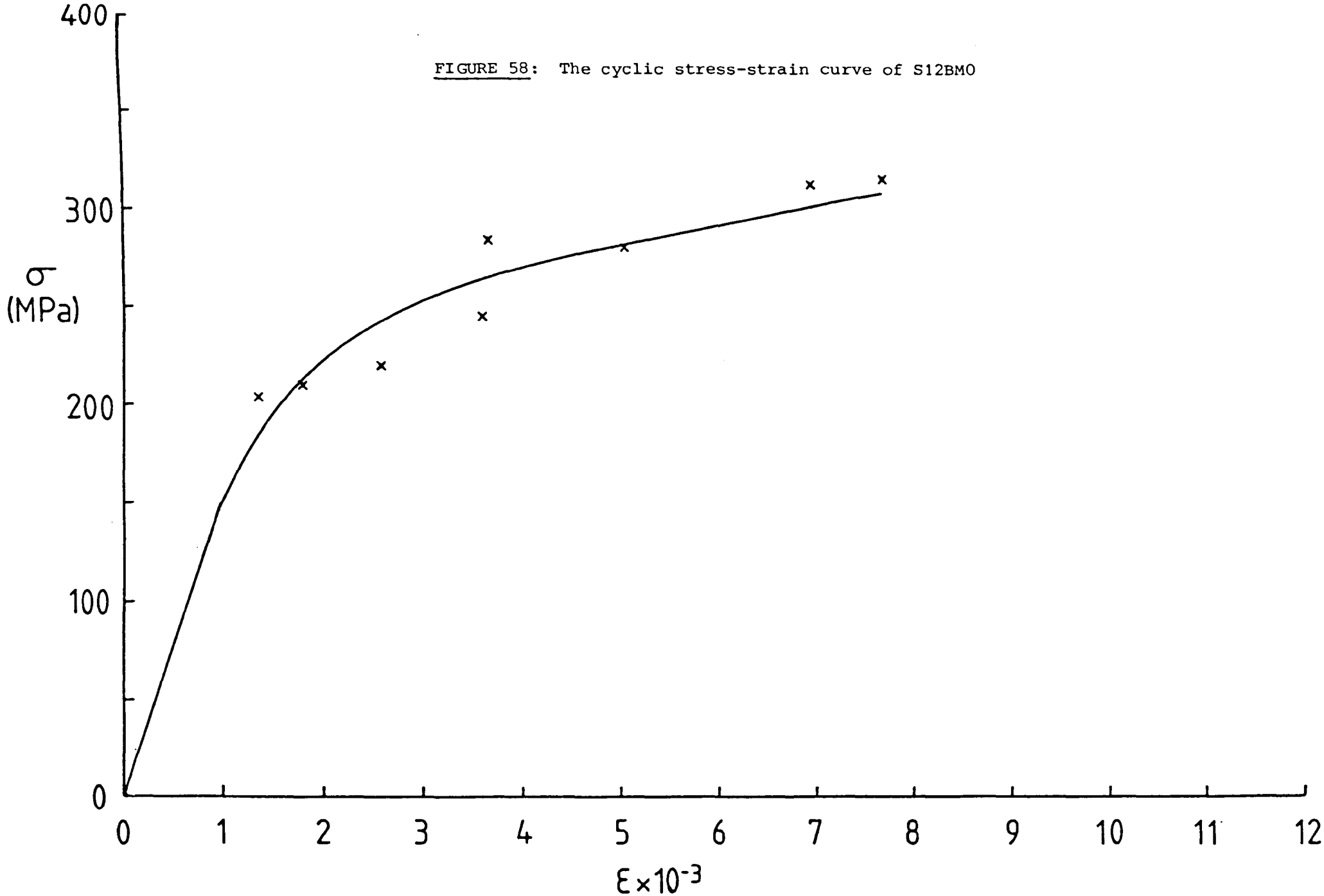

FIGURE 59: The cyclic stress-strain curve of S12BM45

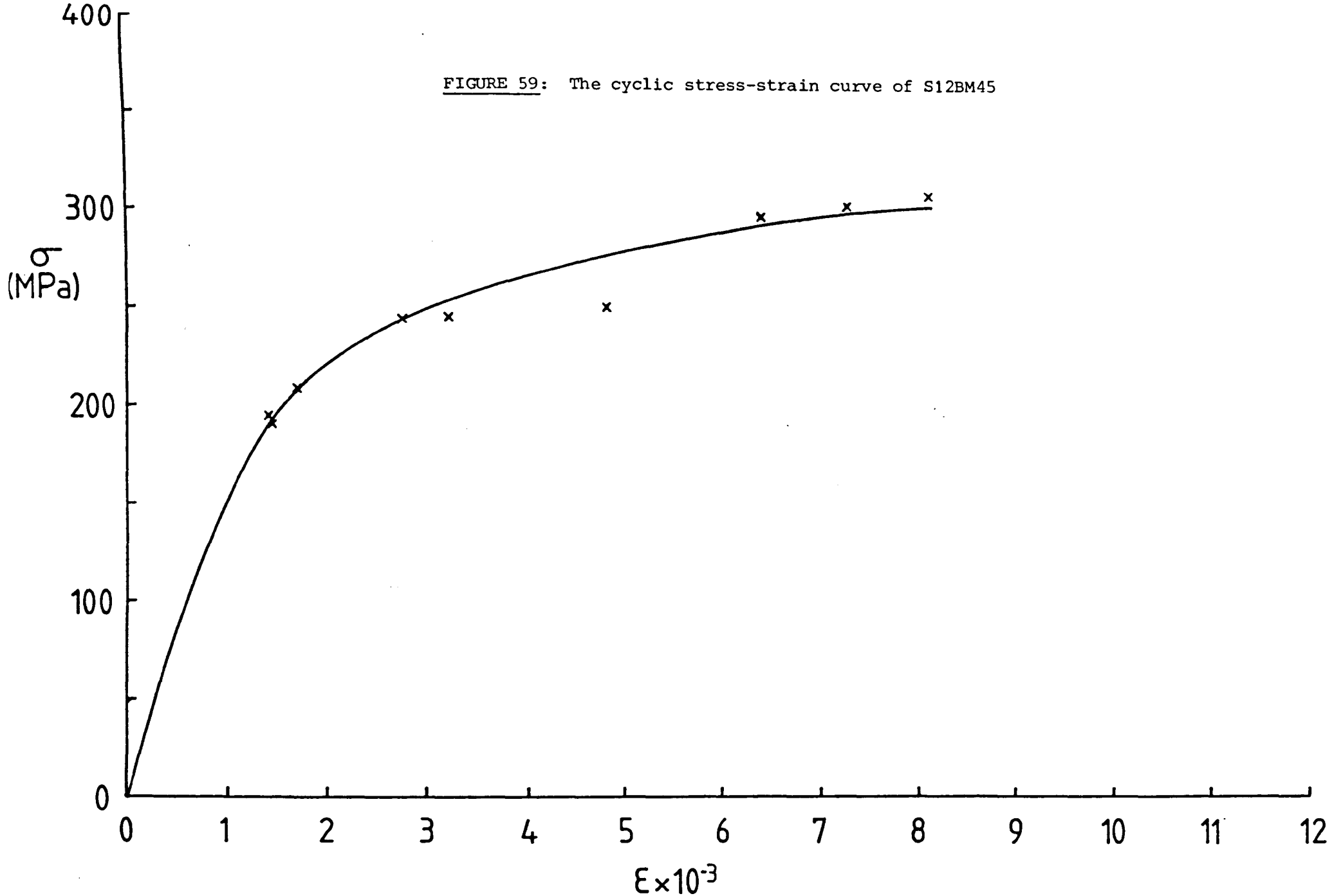

FIGURE 60: The cyclic stress-strain curve of S12BM90

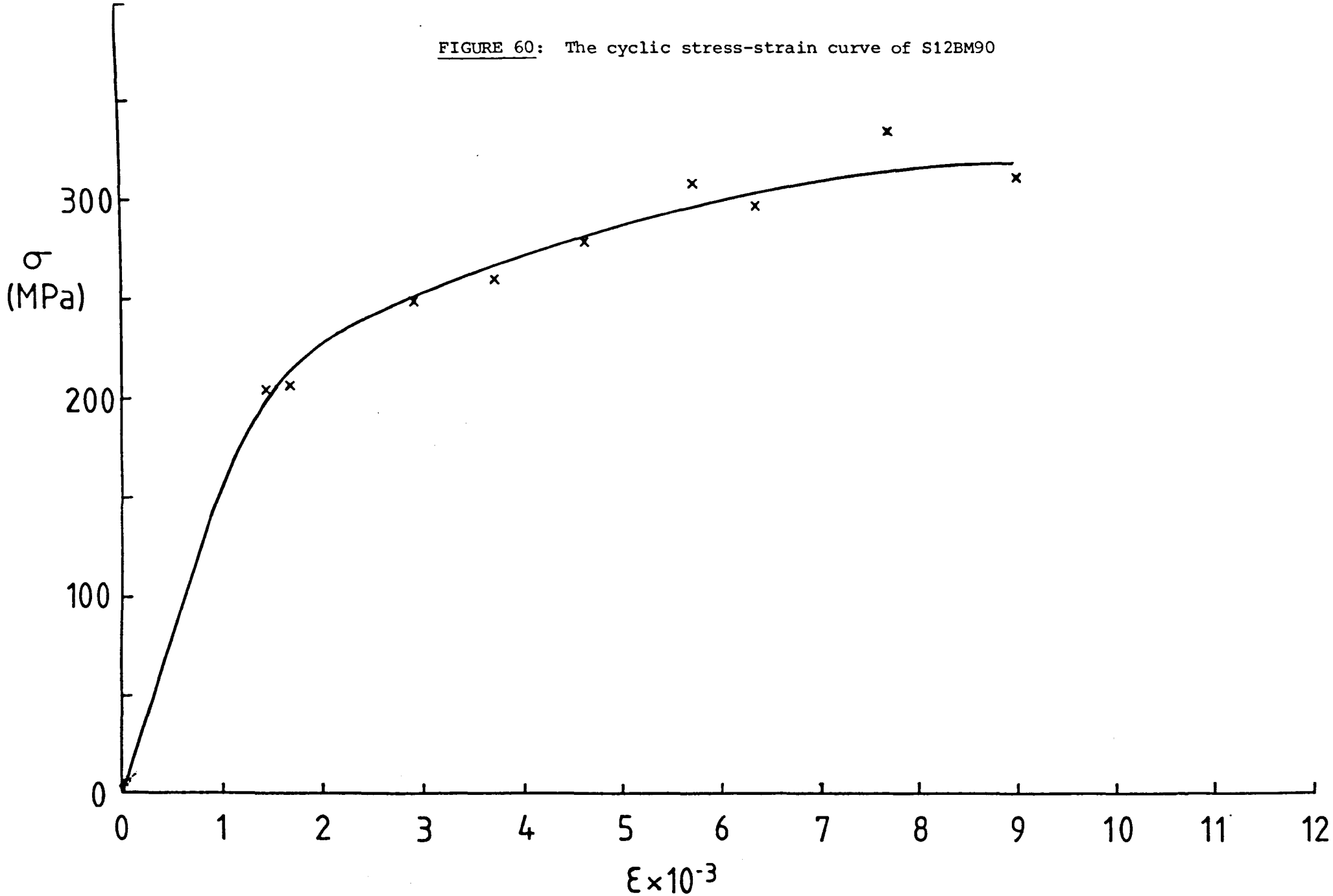

FIGURE 61: The cyclic stress-strain curve of CR680

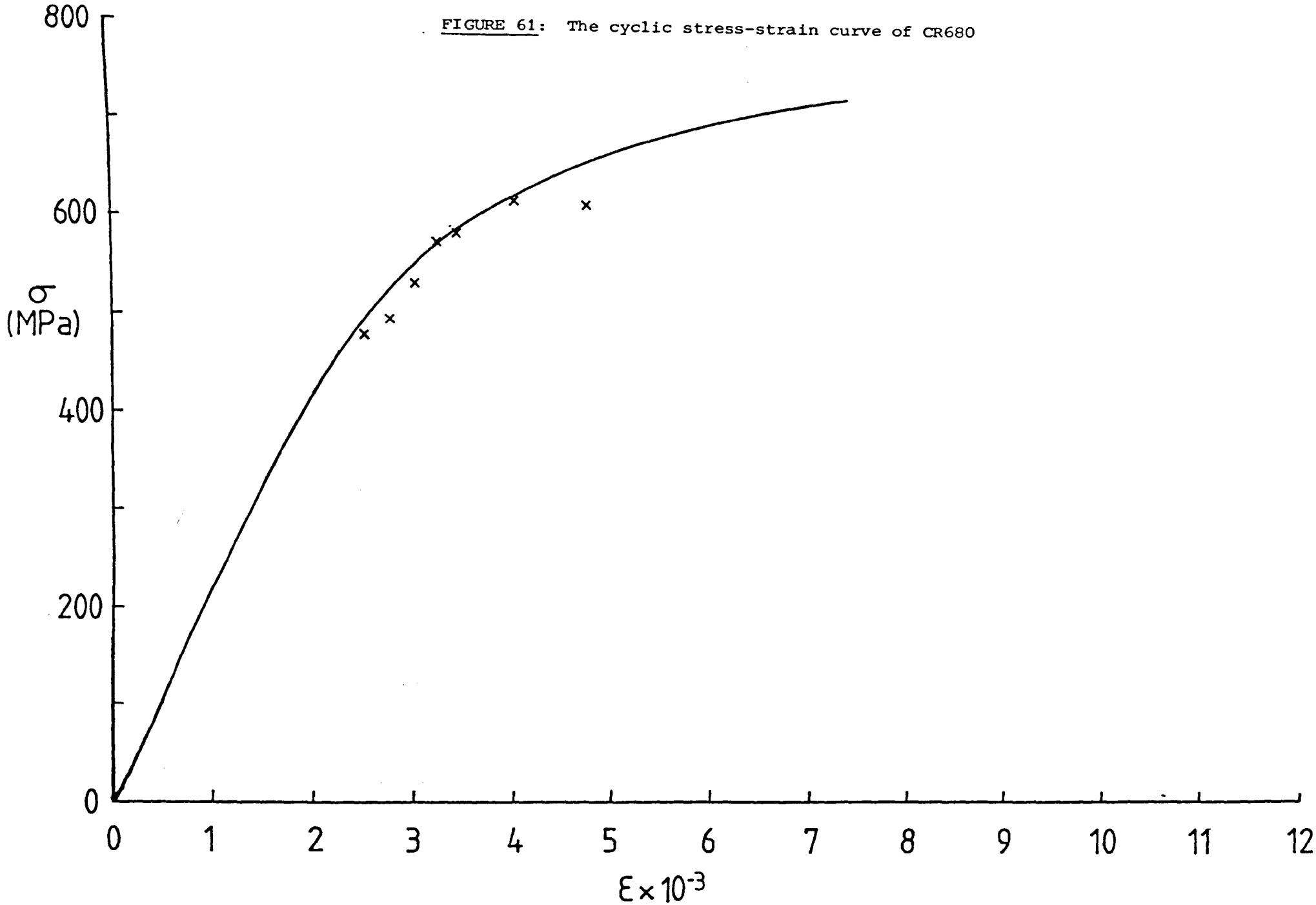

FIGURE 62: The cyclic stress-strain curve of CR6845

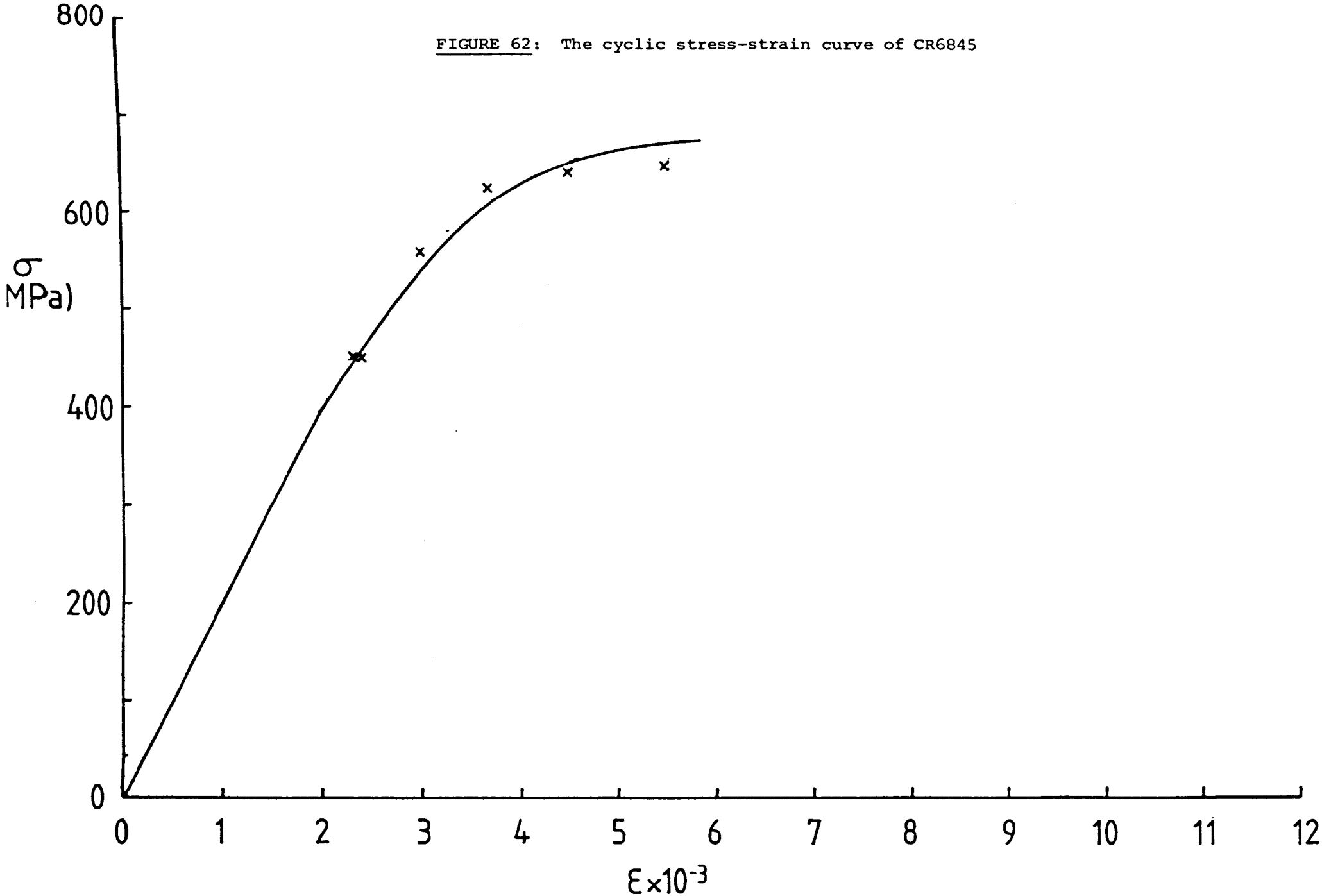

FIGURE 63: The cyclic stress-strain curve of CR6890

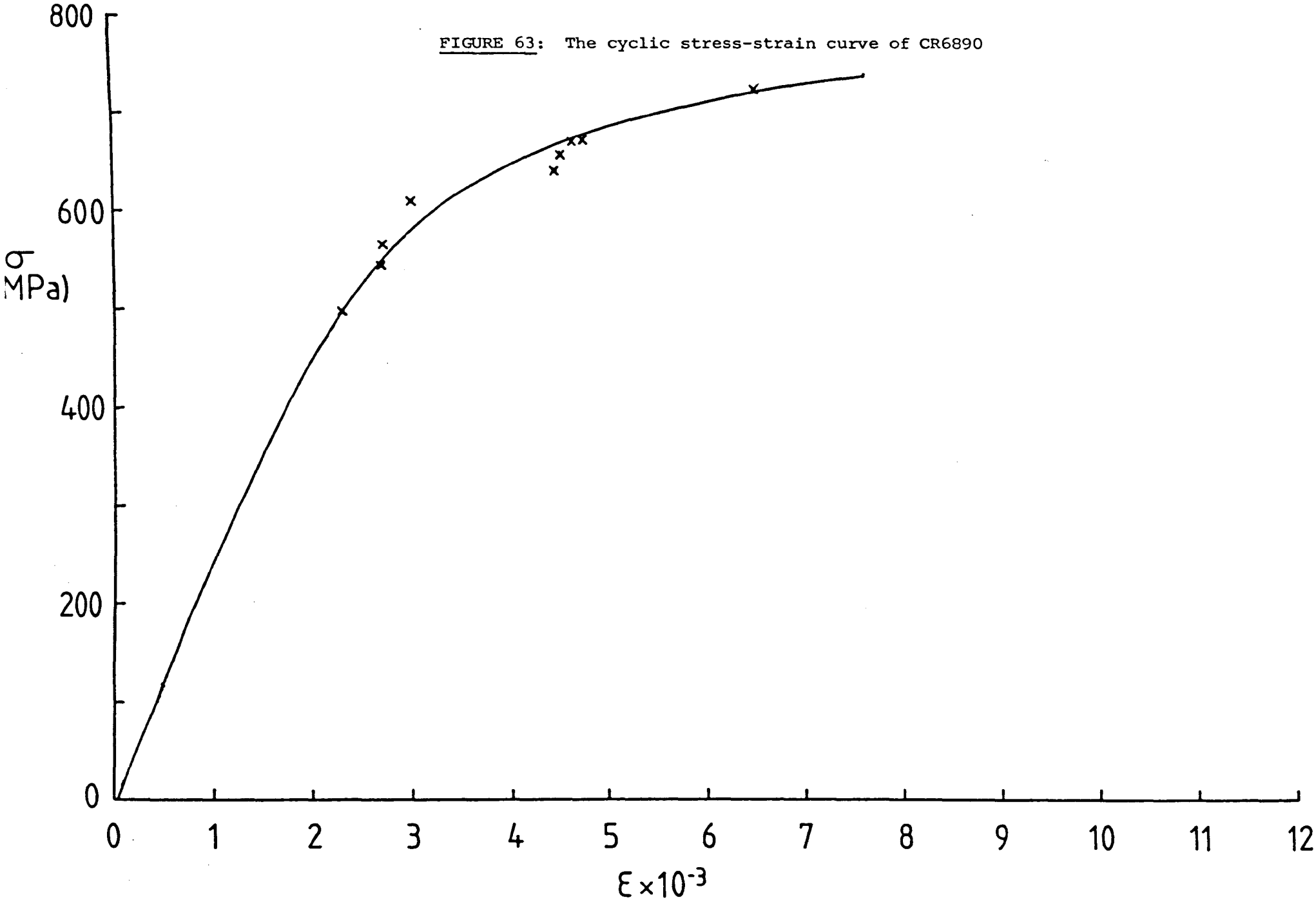

FIGURE 64: The cyclic stress-strain curve of CR800

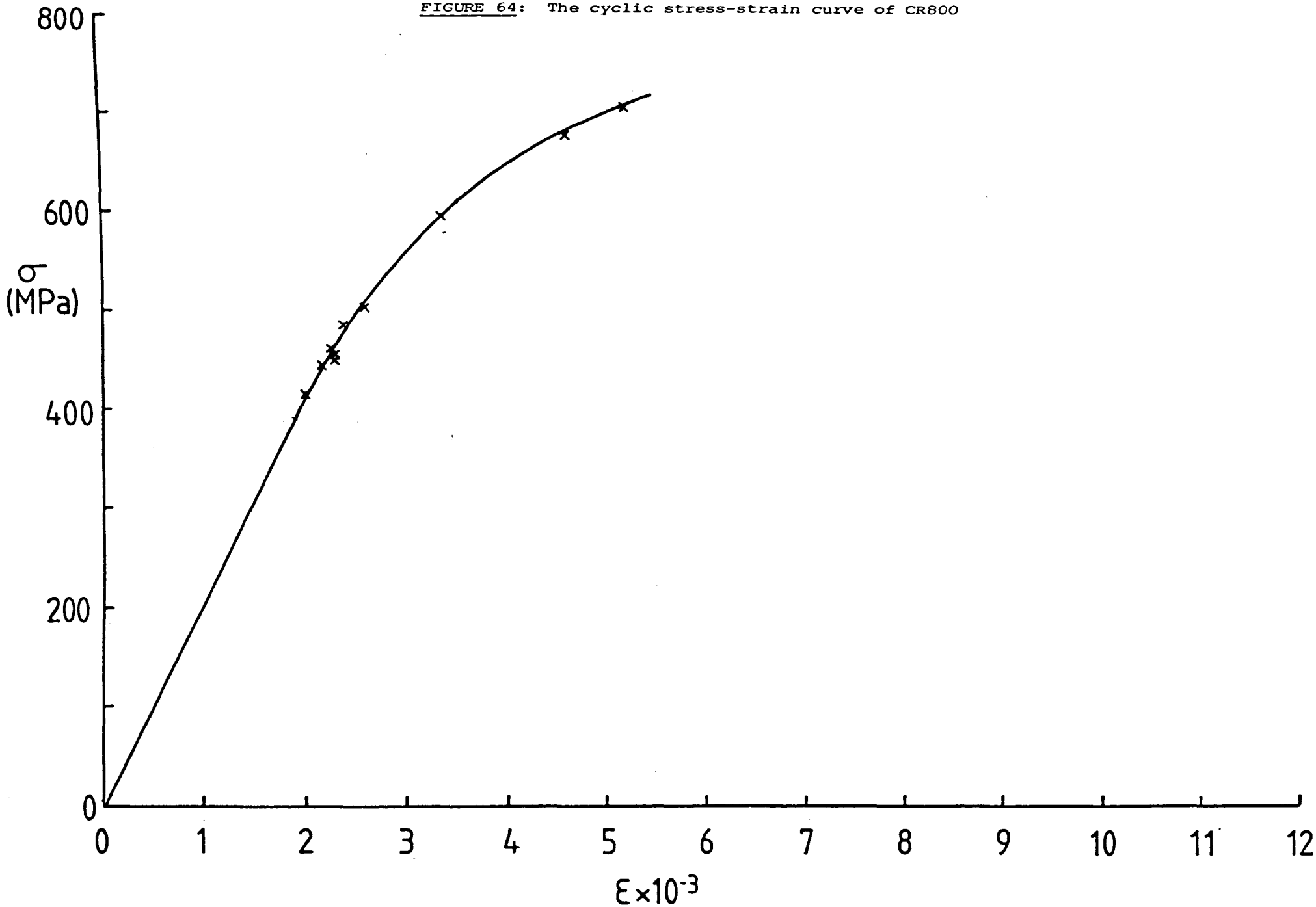

FIGURE 65: The cyclic stress-strain curve of CR8045

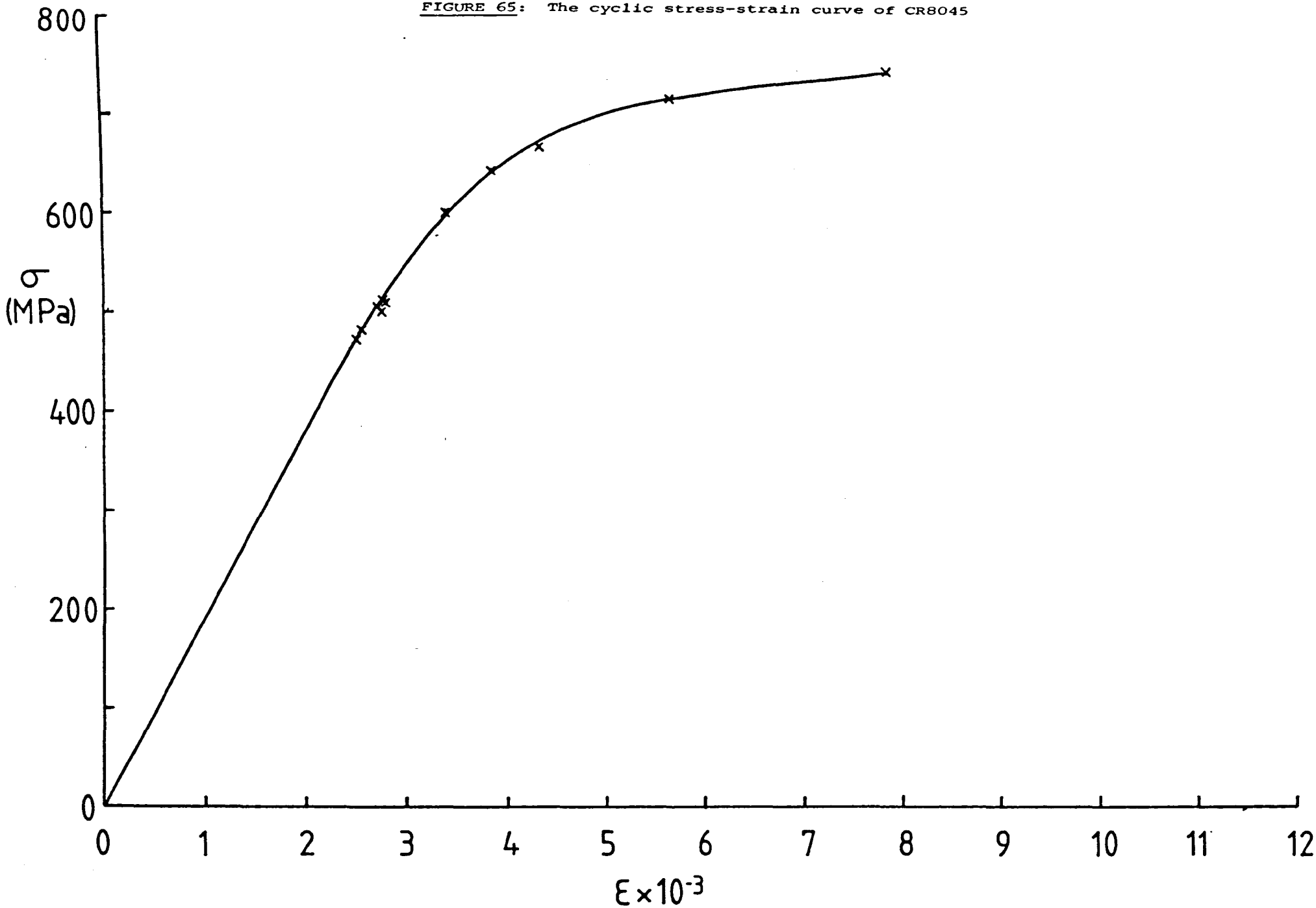

FIGURE 66: The cyclic stress-strain curve of CR8090

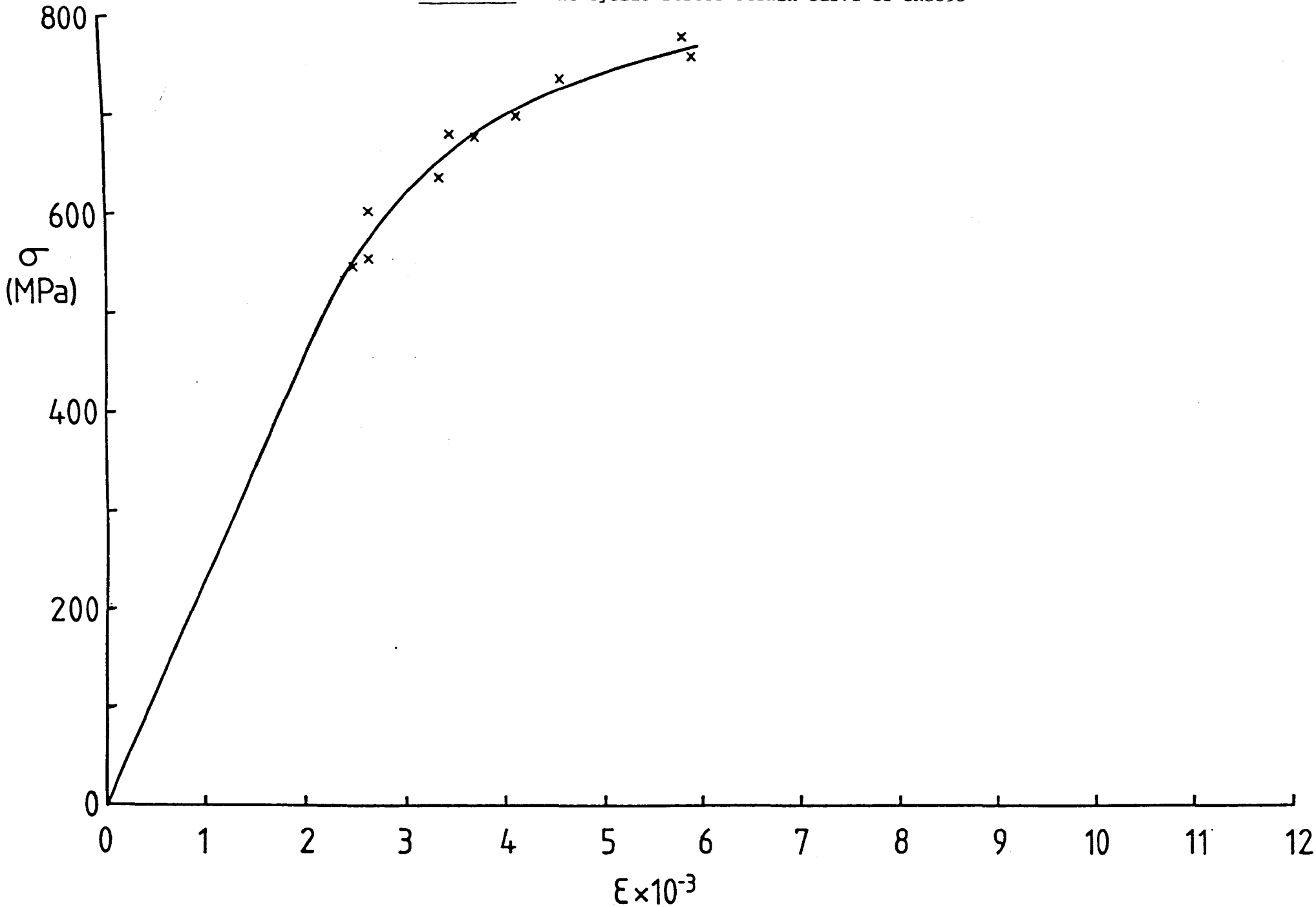

FIGURE 67: The cyclic stress-strain curve of R80AN0

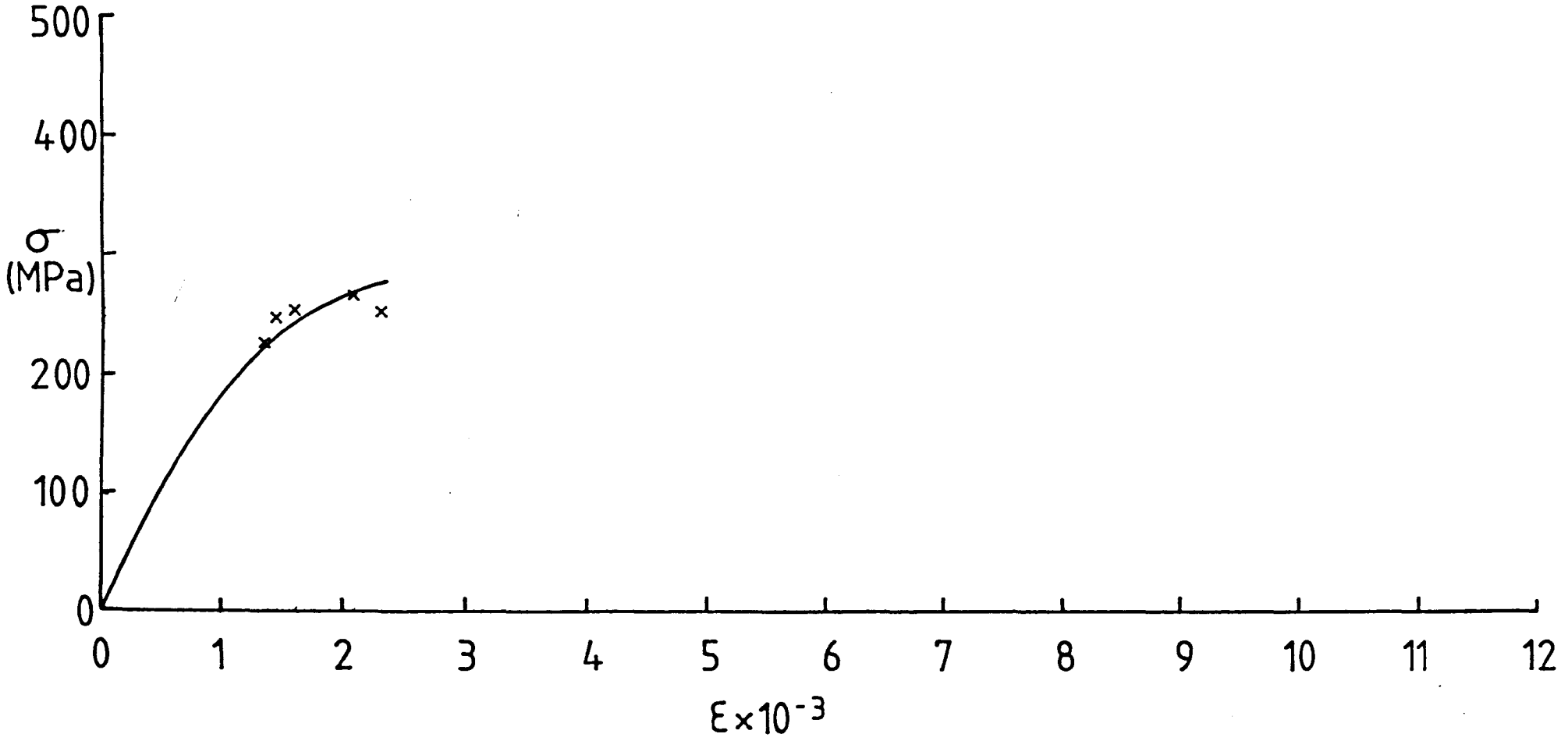

FIGURE 68: The cyclic stress-strain curve of R80AN45

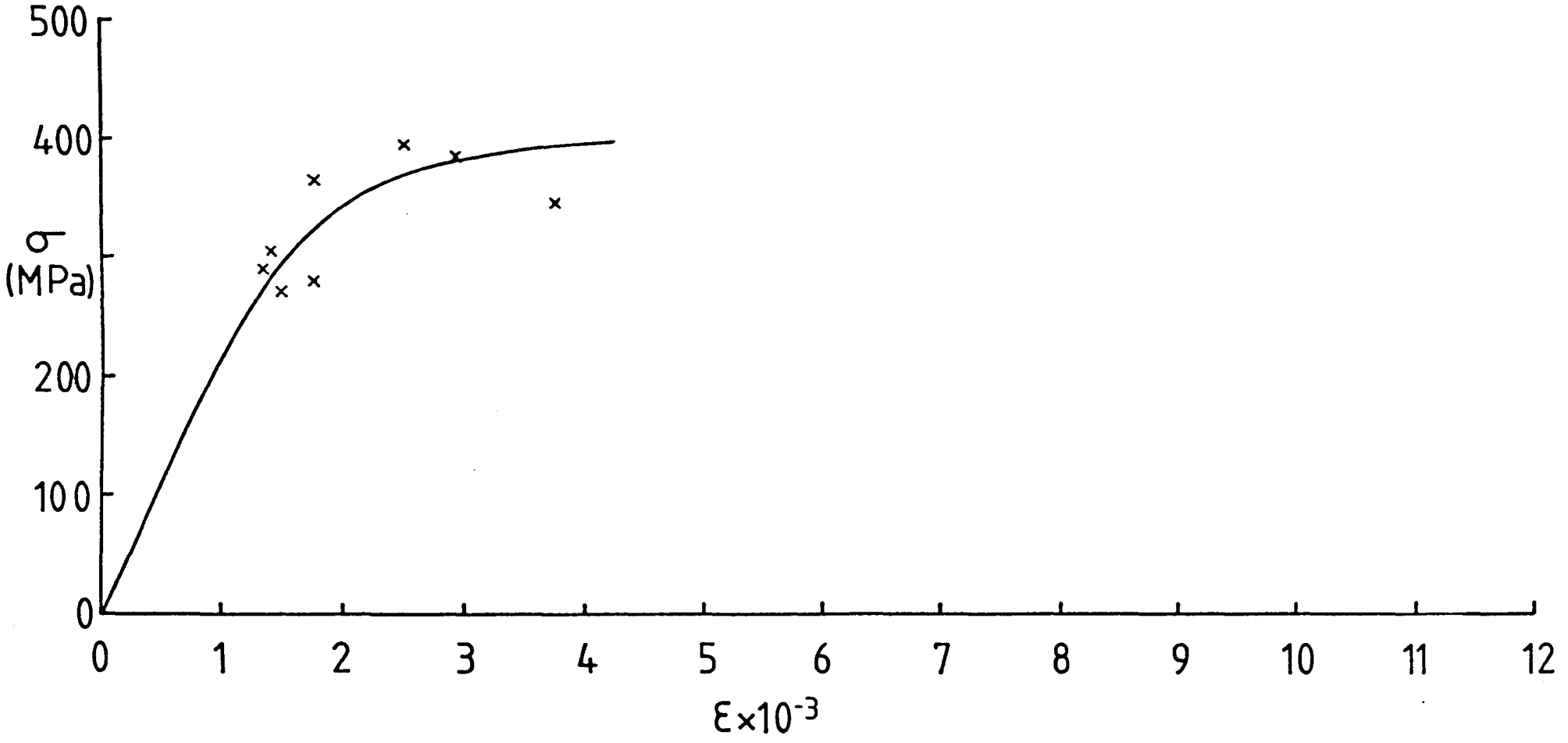

FIGURE 69: The cyclic stress-strain curve of R80AN90

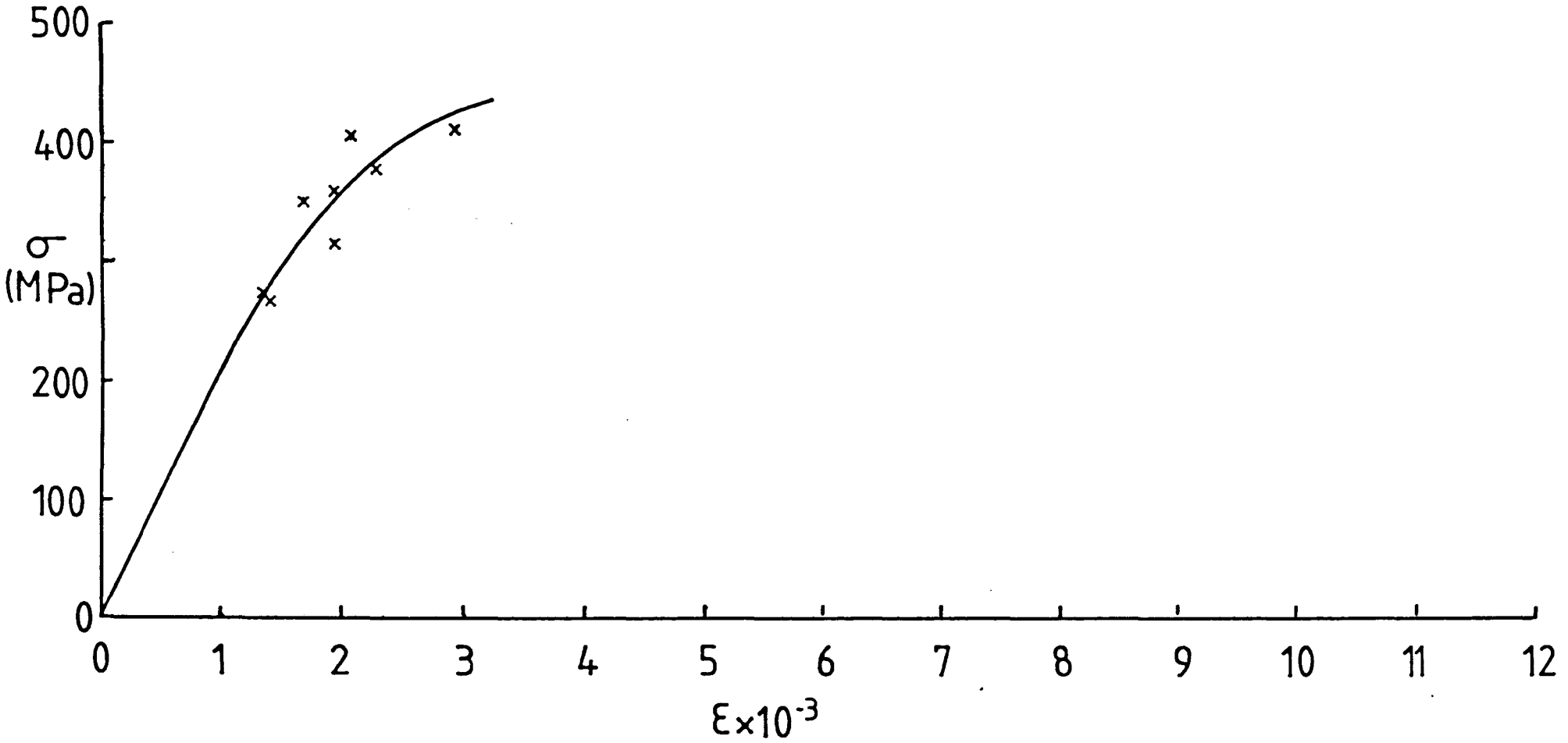

FIGURE 70: The strain-life curve of S10BM0

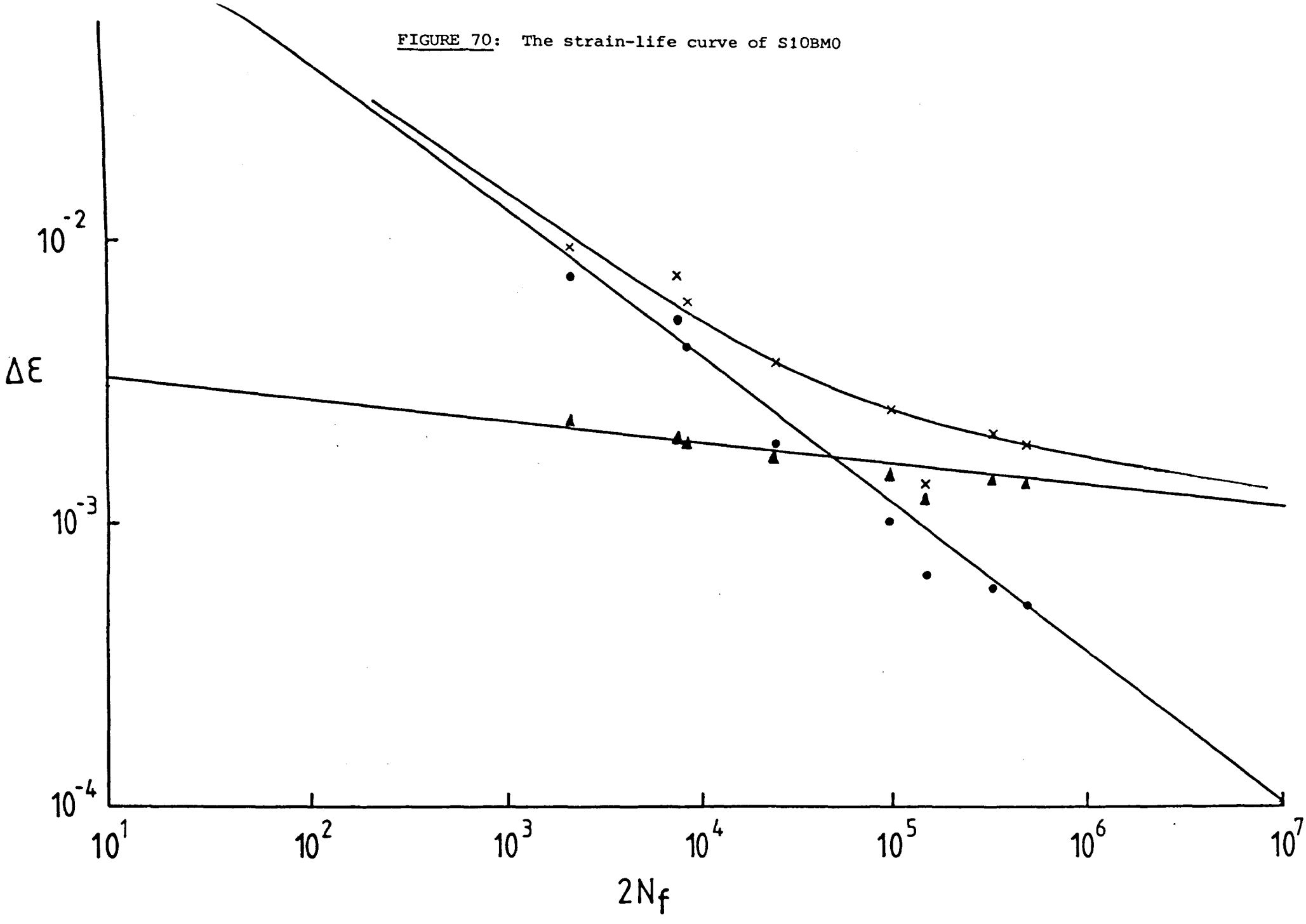

FIGURE 71: The strain-life curve of S10BM45

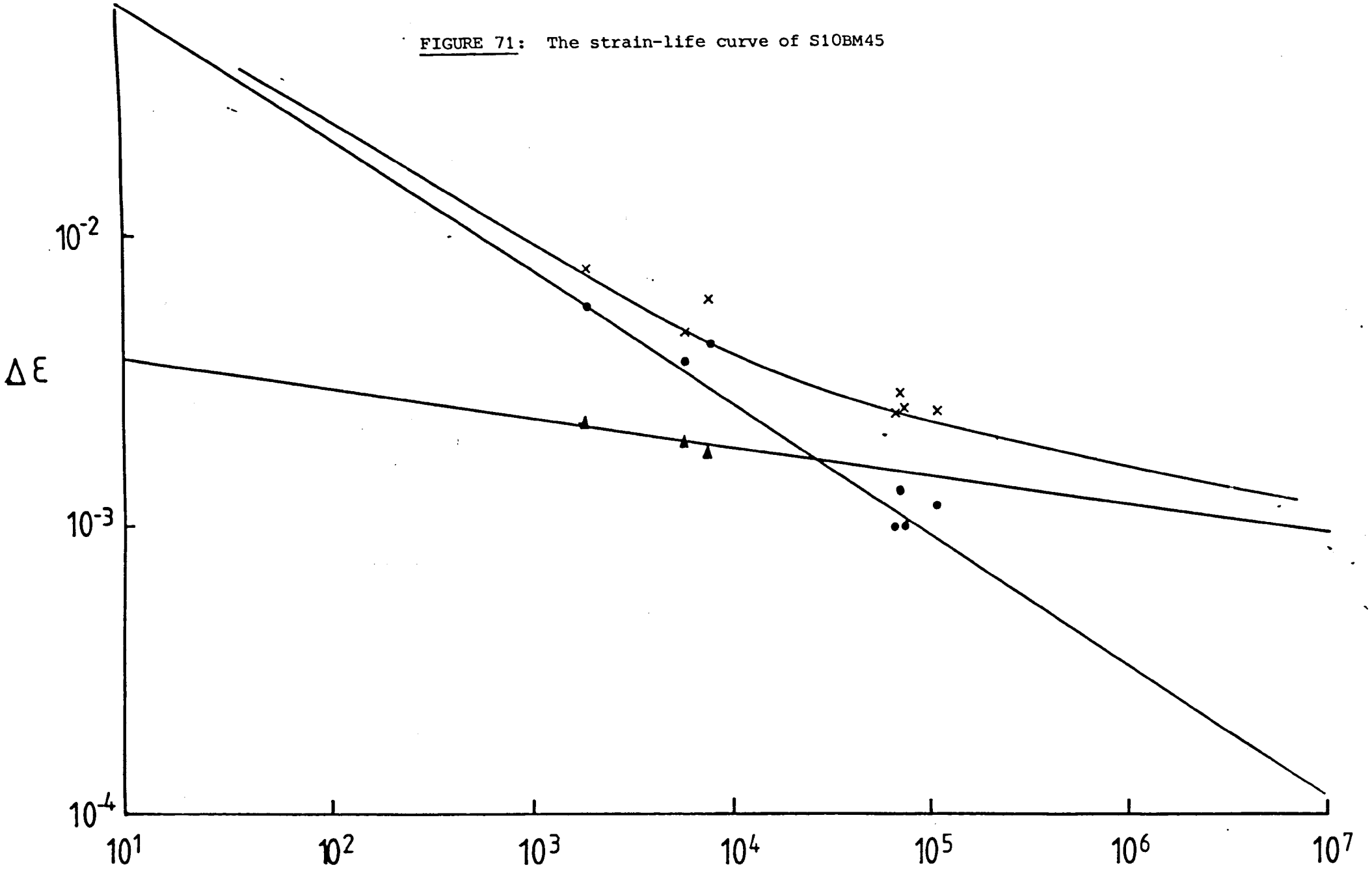

FIGURE 72: The strain-life curve of S10BM90

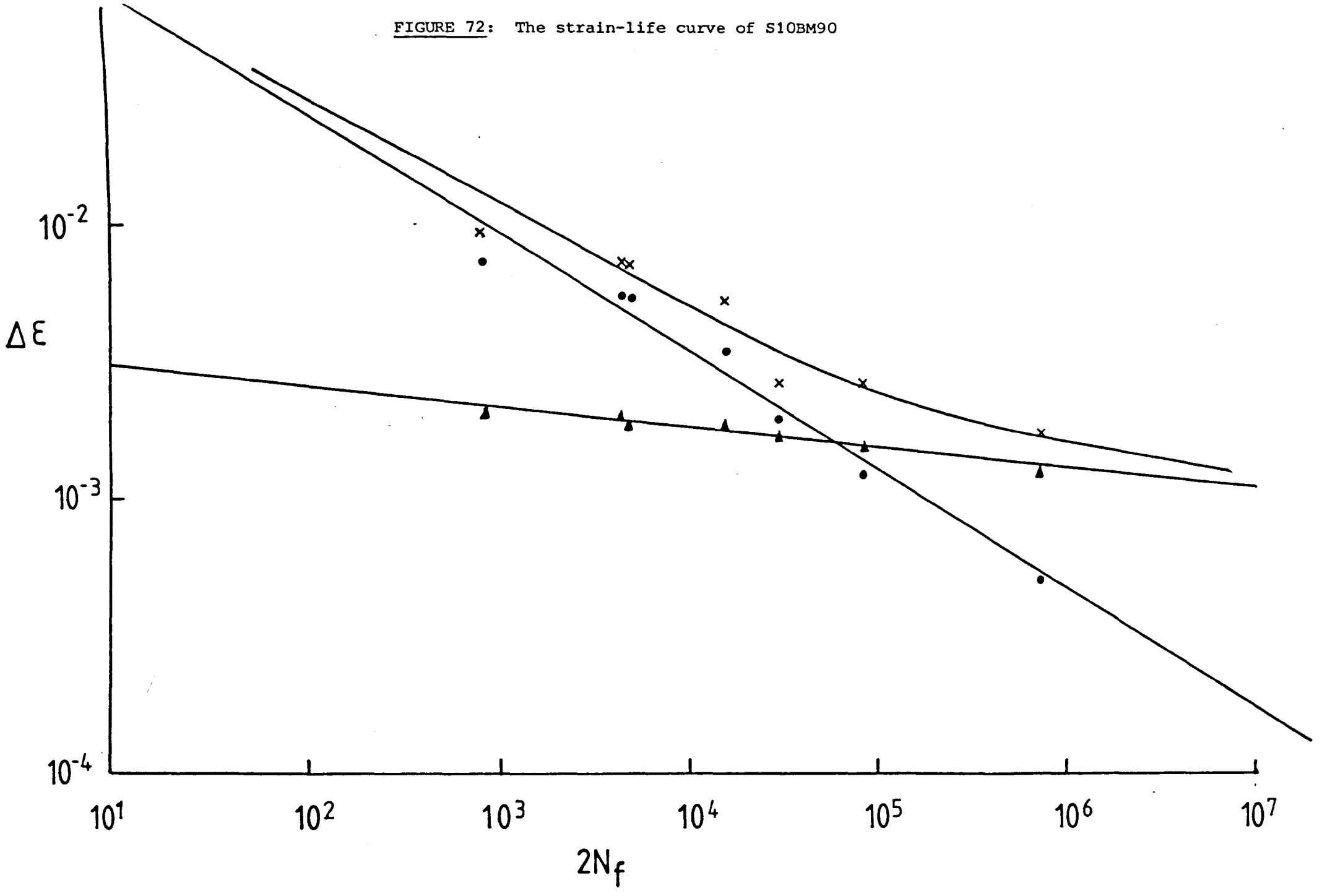

FIGURE 73: The strain-life curve of S12BM0

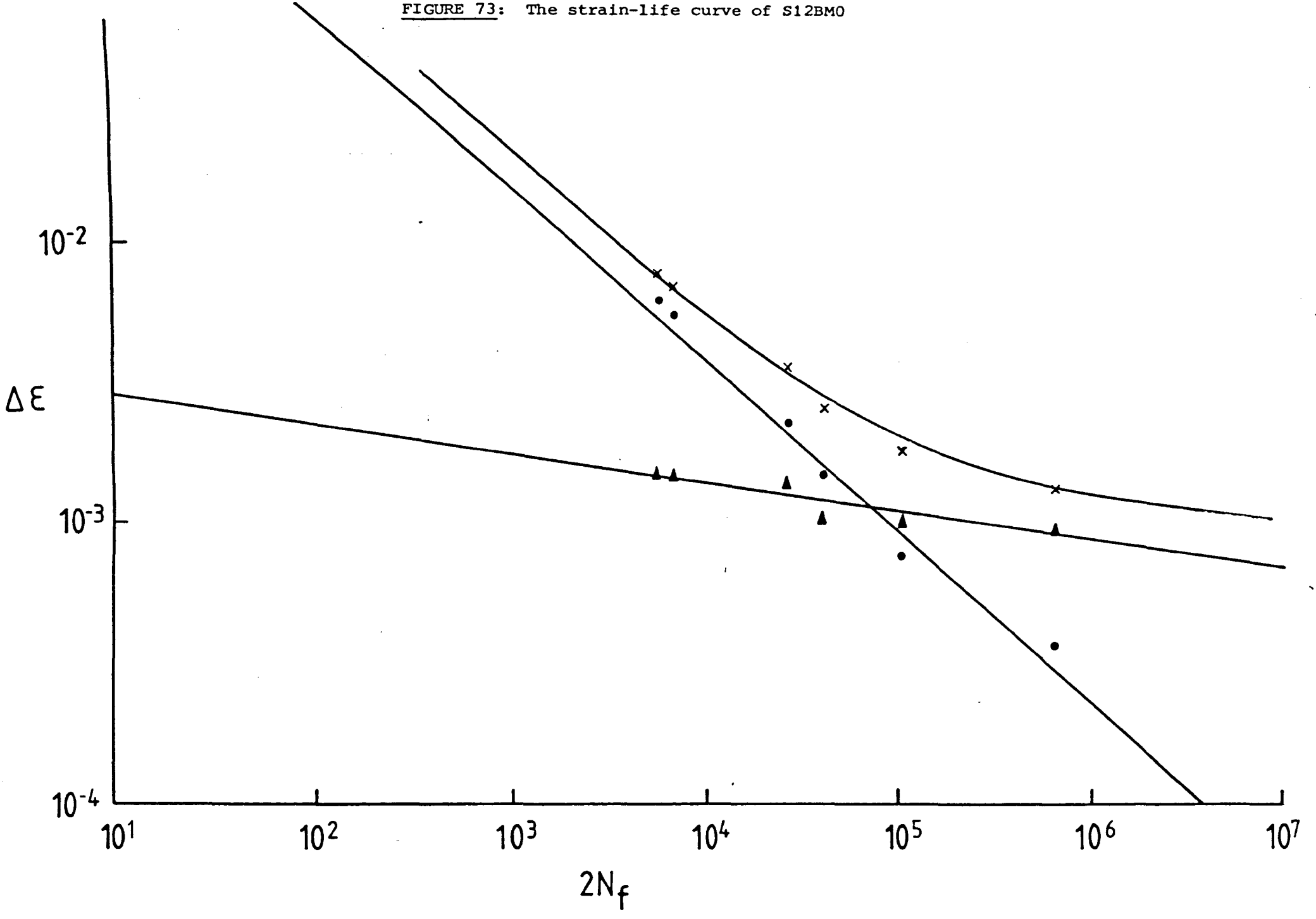

FIGURE 74: The strain-lfie curve of S12BM45

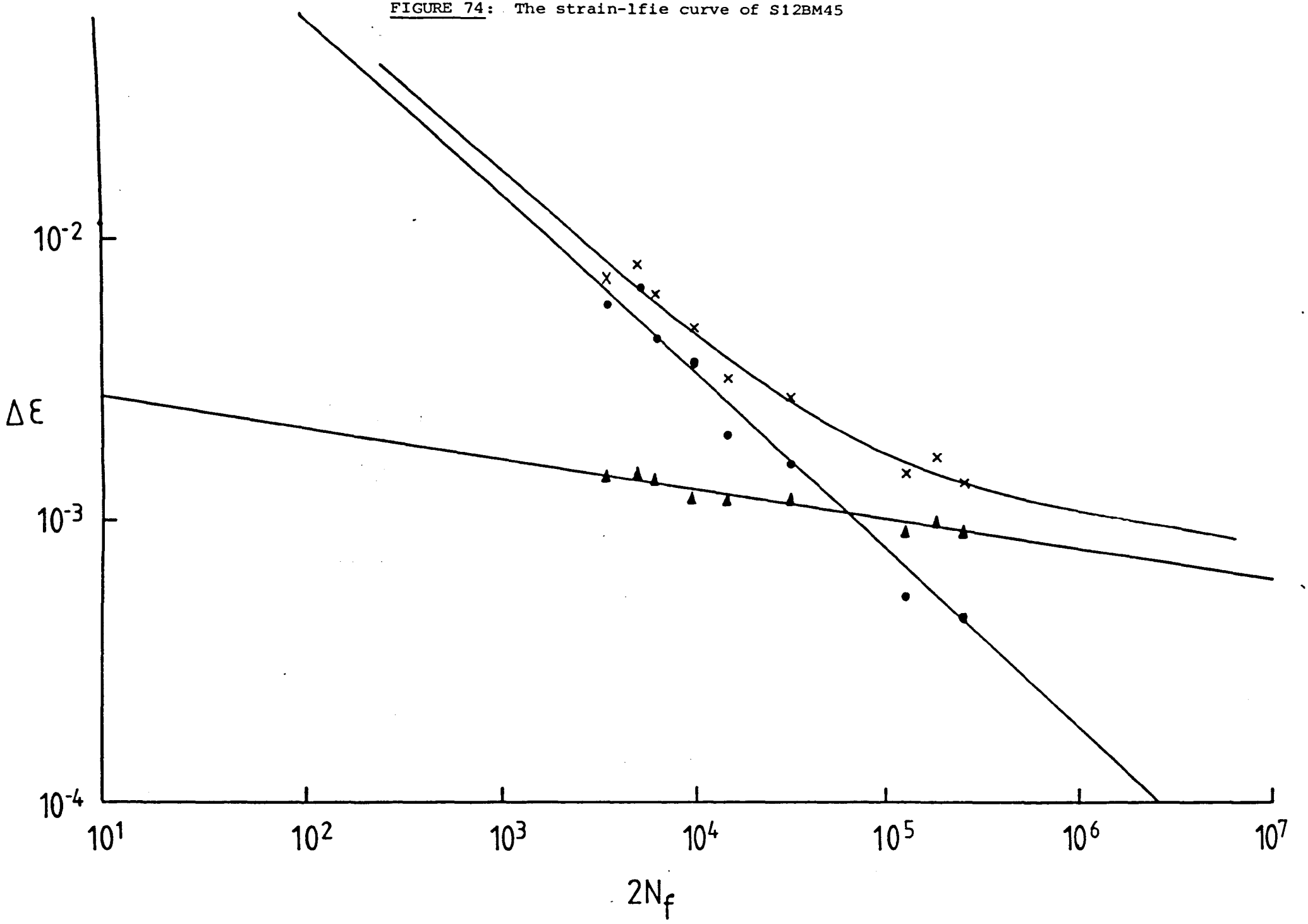

FIGURE 75: The strain-life curve of S12BM90

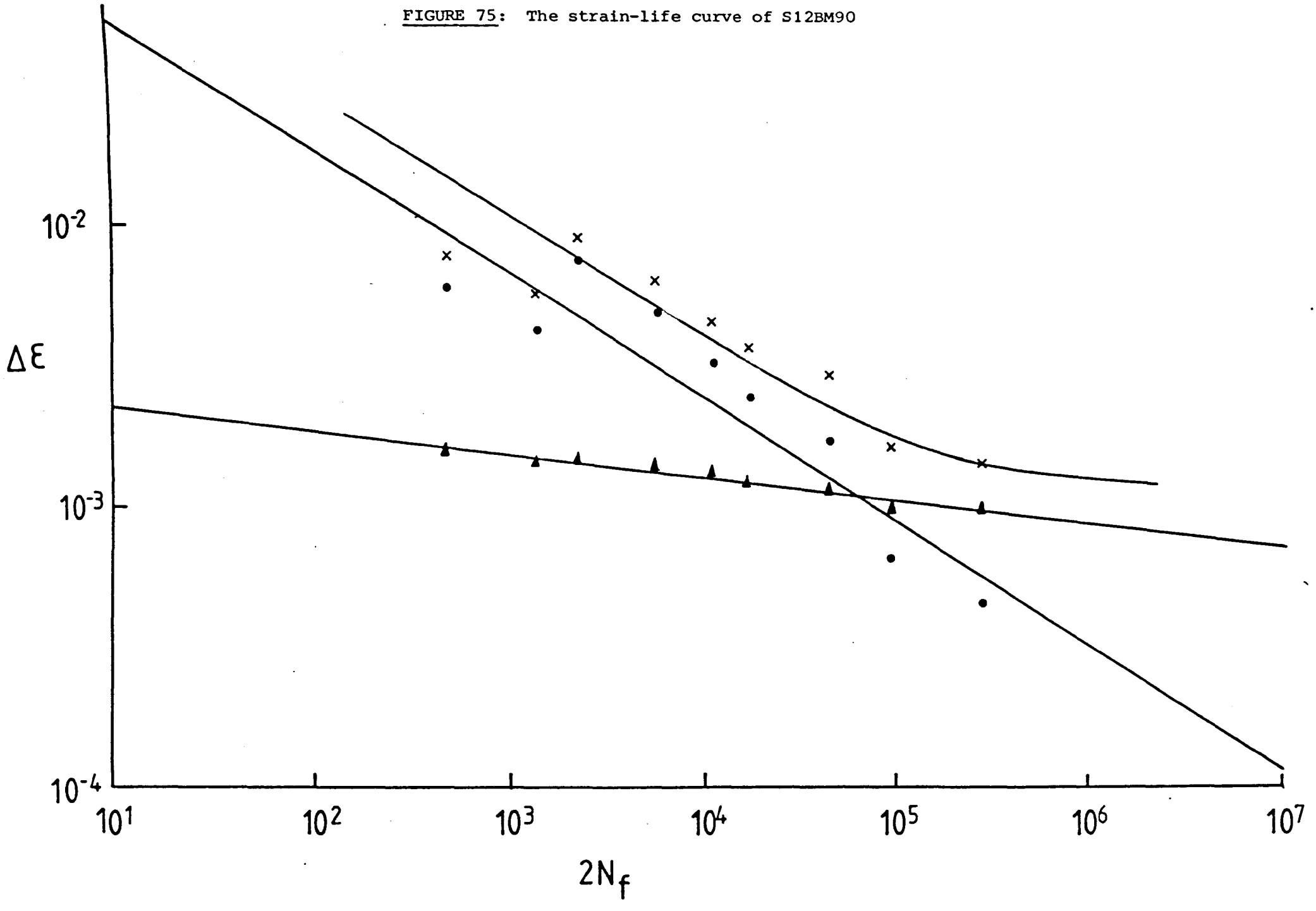

FIGURE 76: The strain-life curve of CR680

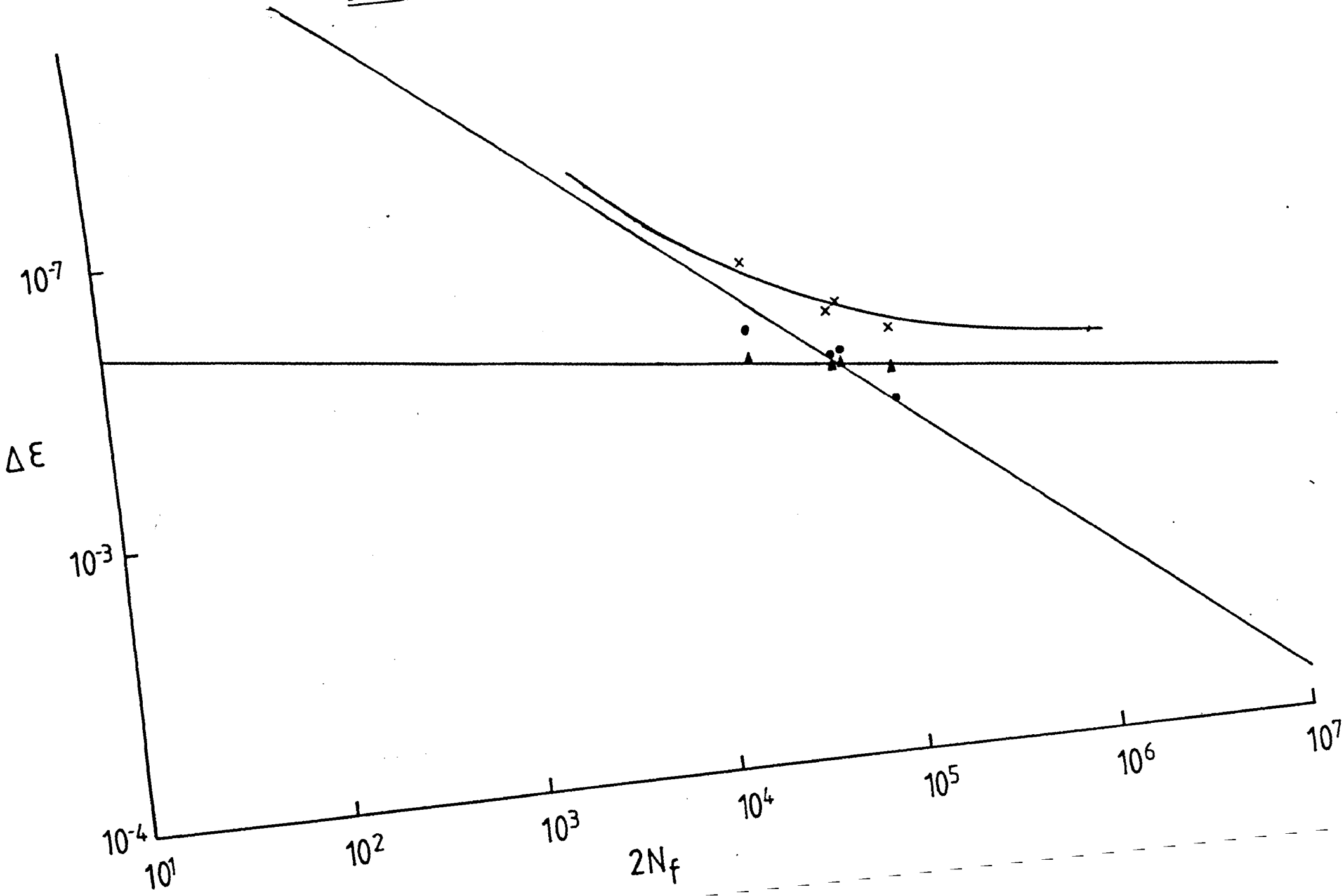

FIGURE 77: The strain-life curve of CR6845

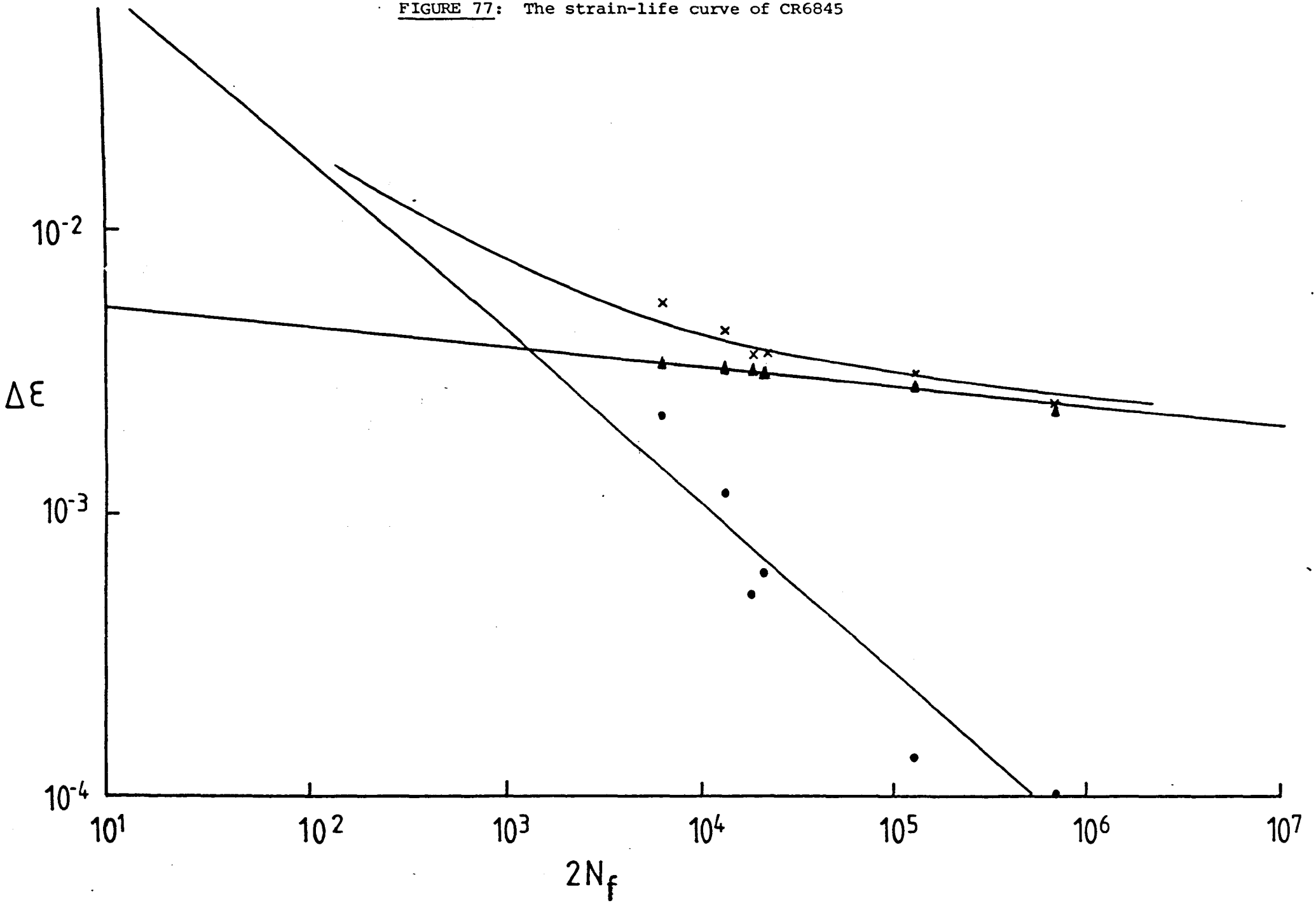

FIGURE 78: The strain-life curve of CR6890

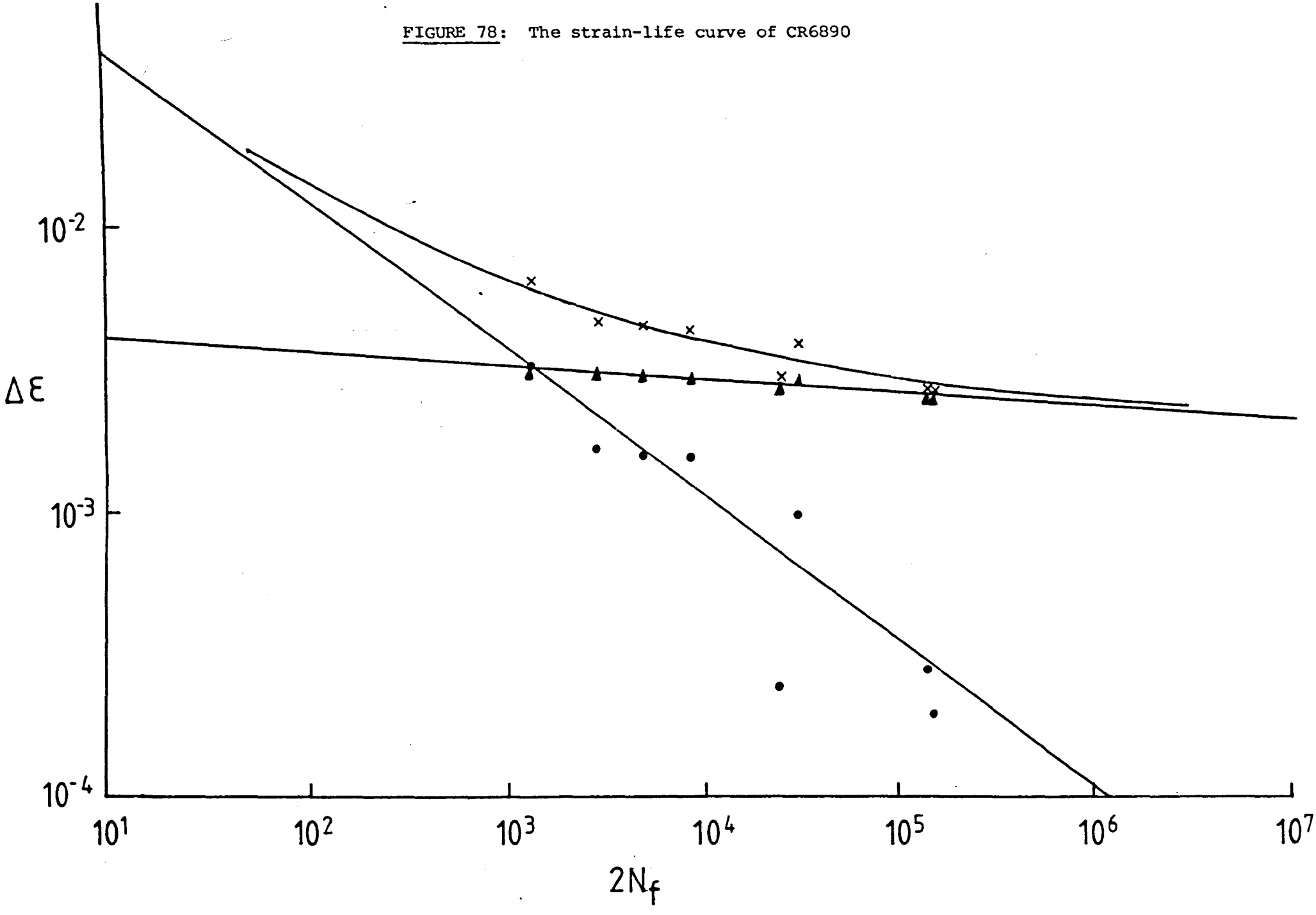

FIGURE 79: The Strain-life curve of CR800

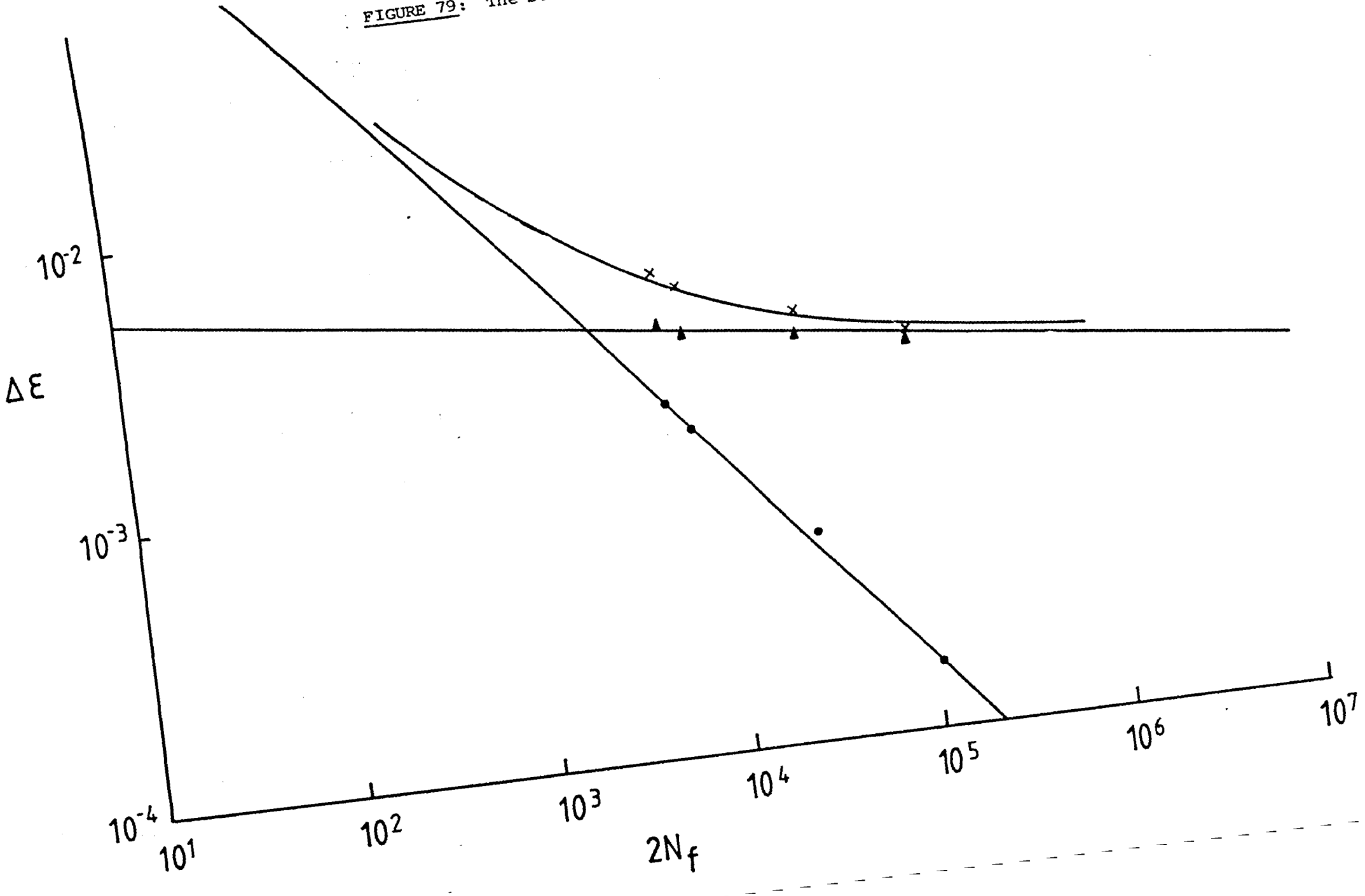

FIGURE 80: The strain-life curve of CR8045

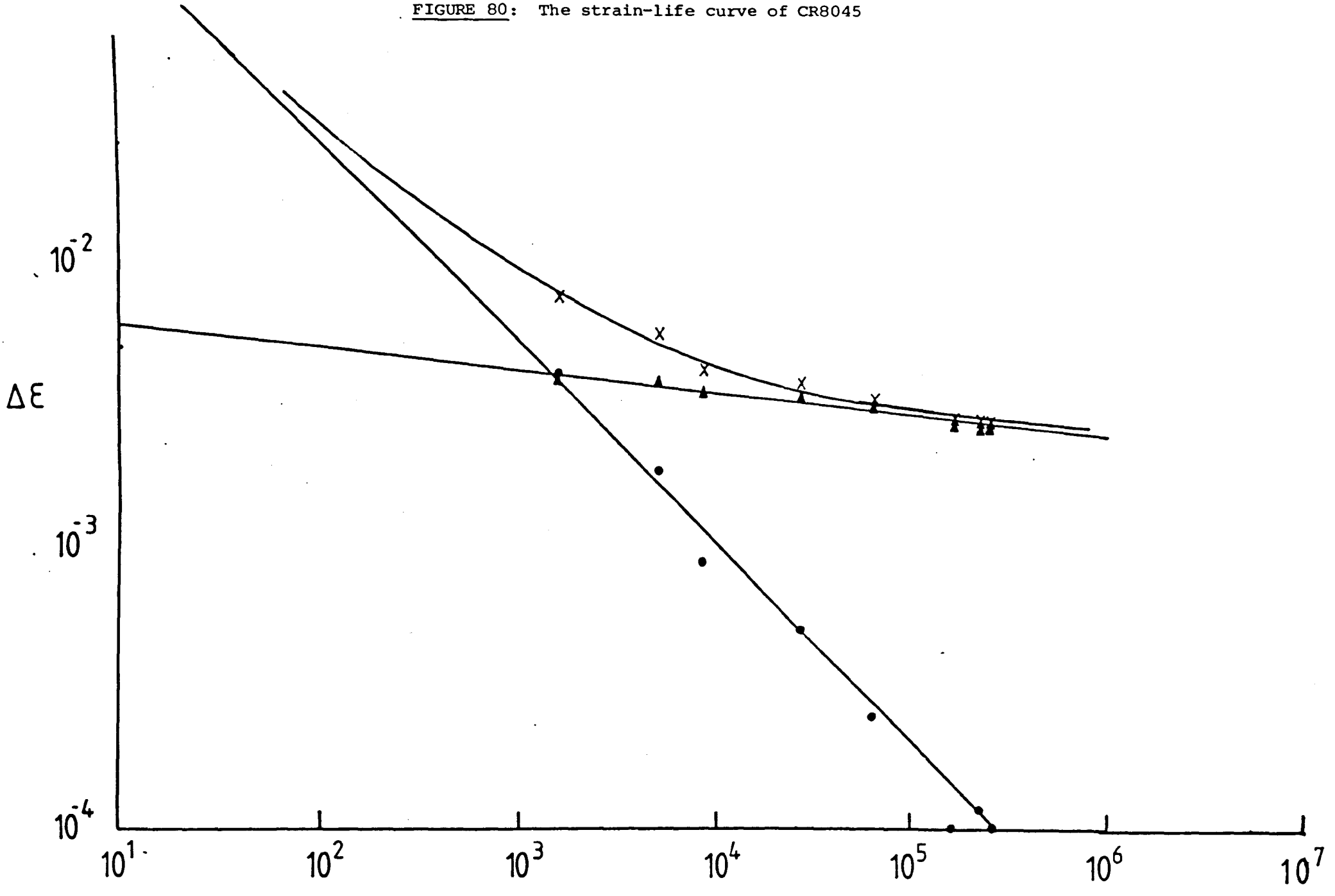

FIGURE 81: The strain-life curve of CR8090

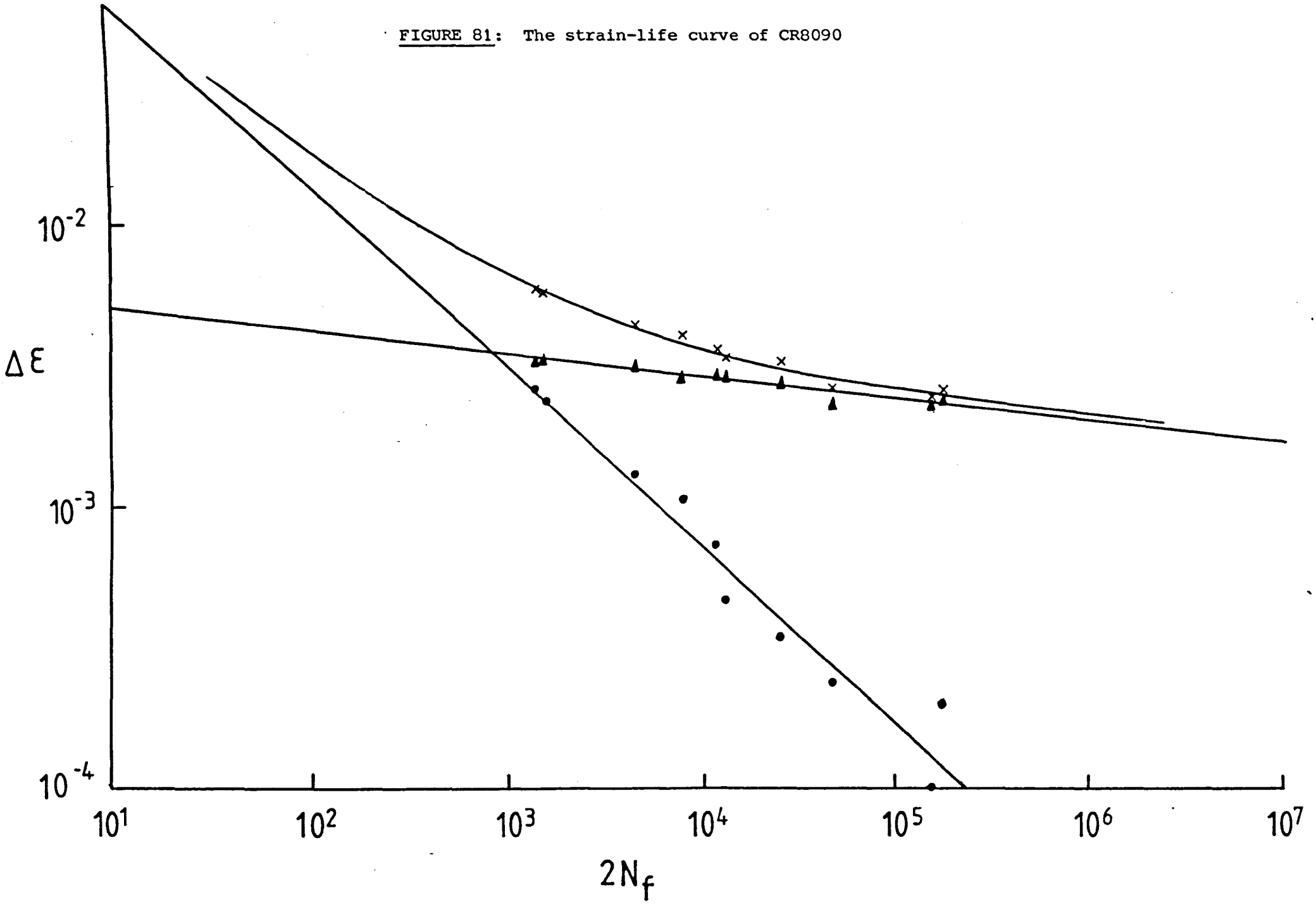

FIGURE 82: The strain-life curve of R80AN0

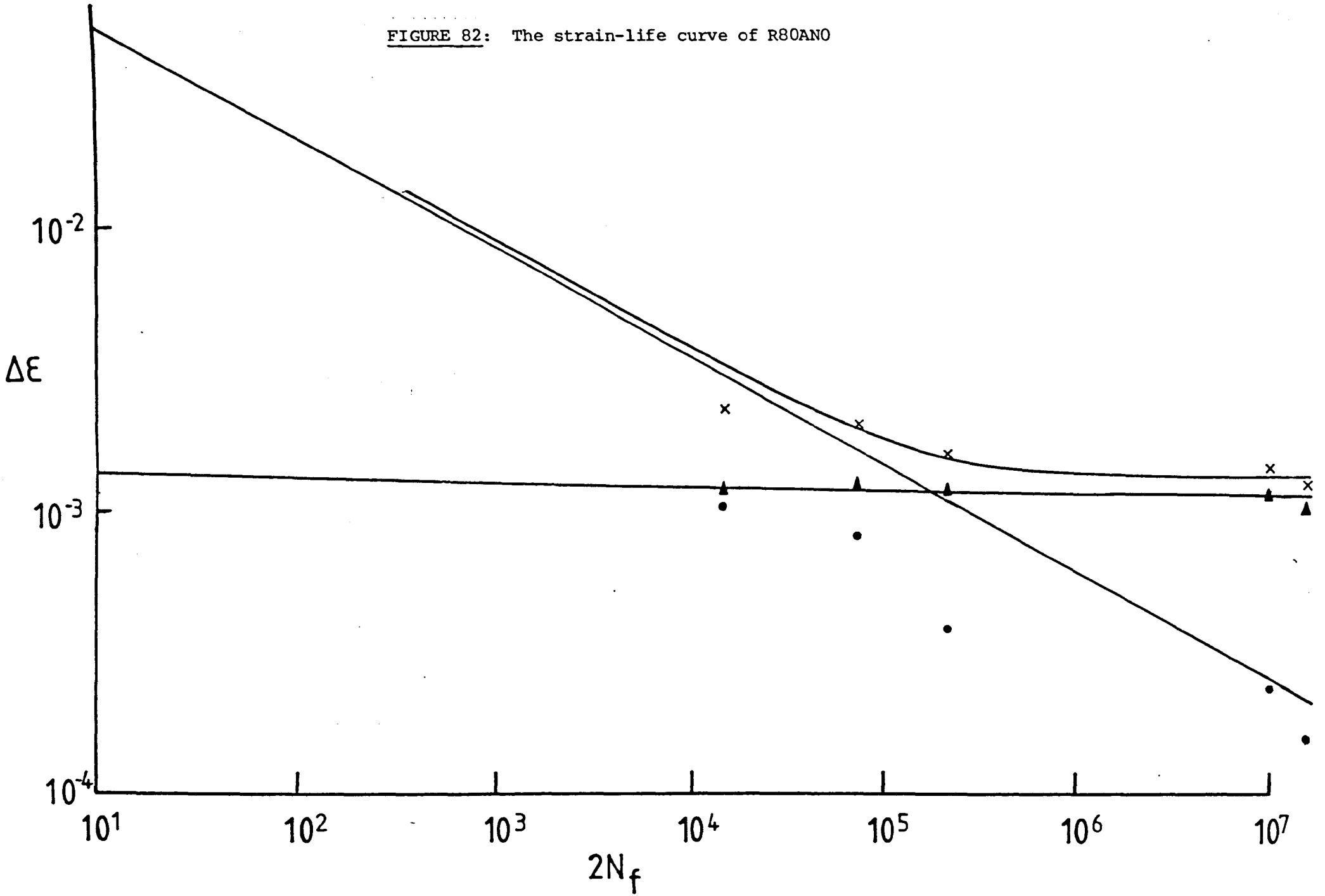

FIGURE 83: The strain-life curve of R80AN45

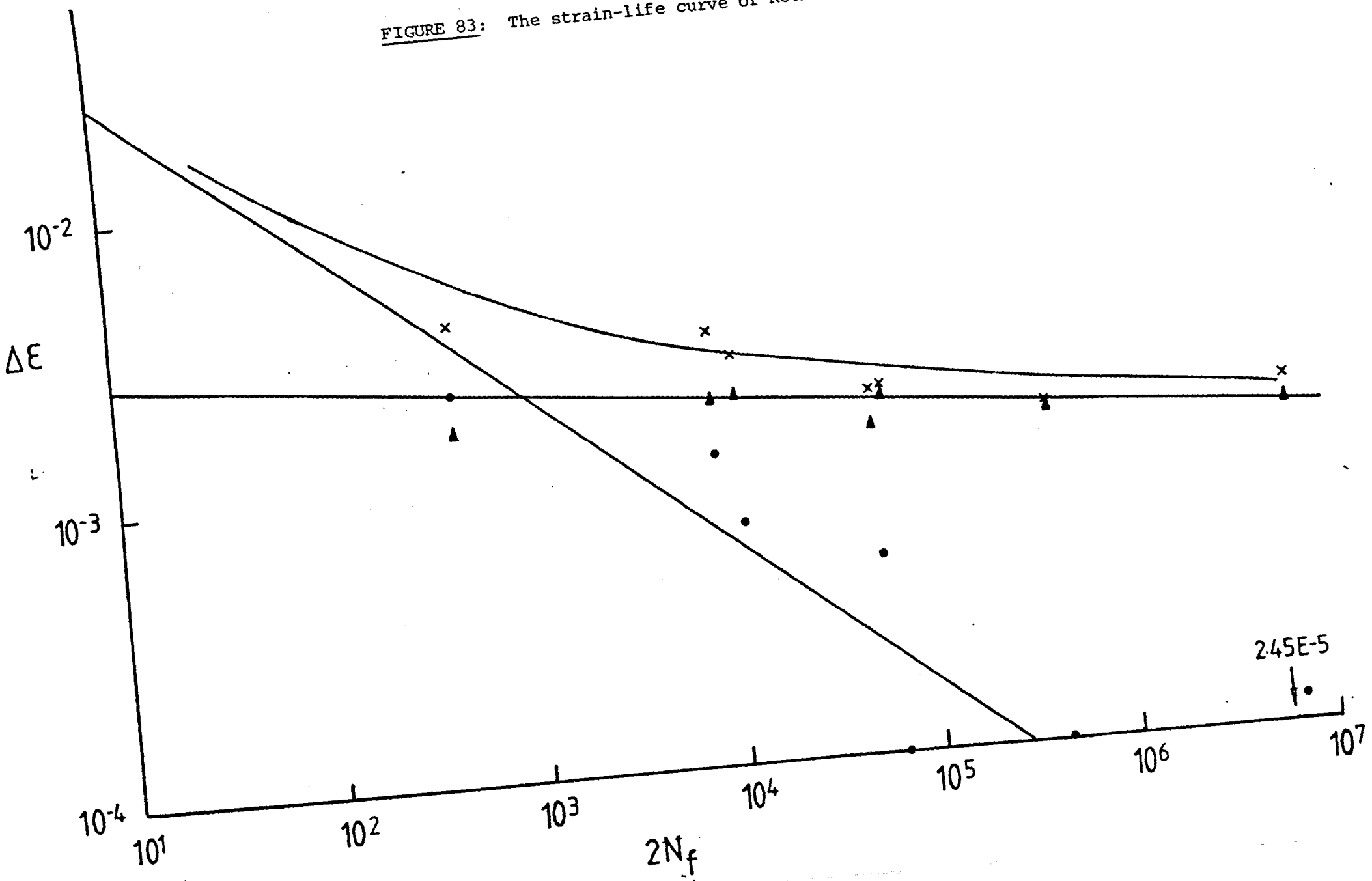

FIGURE 84: The strain-life curve of R80AN90

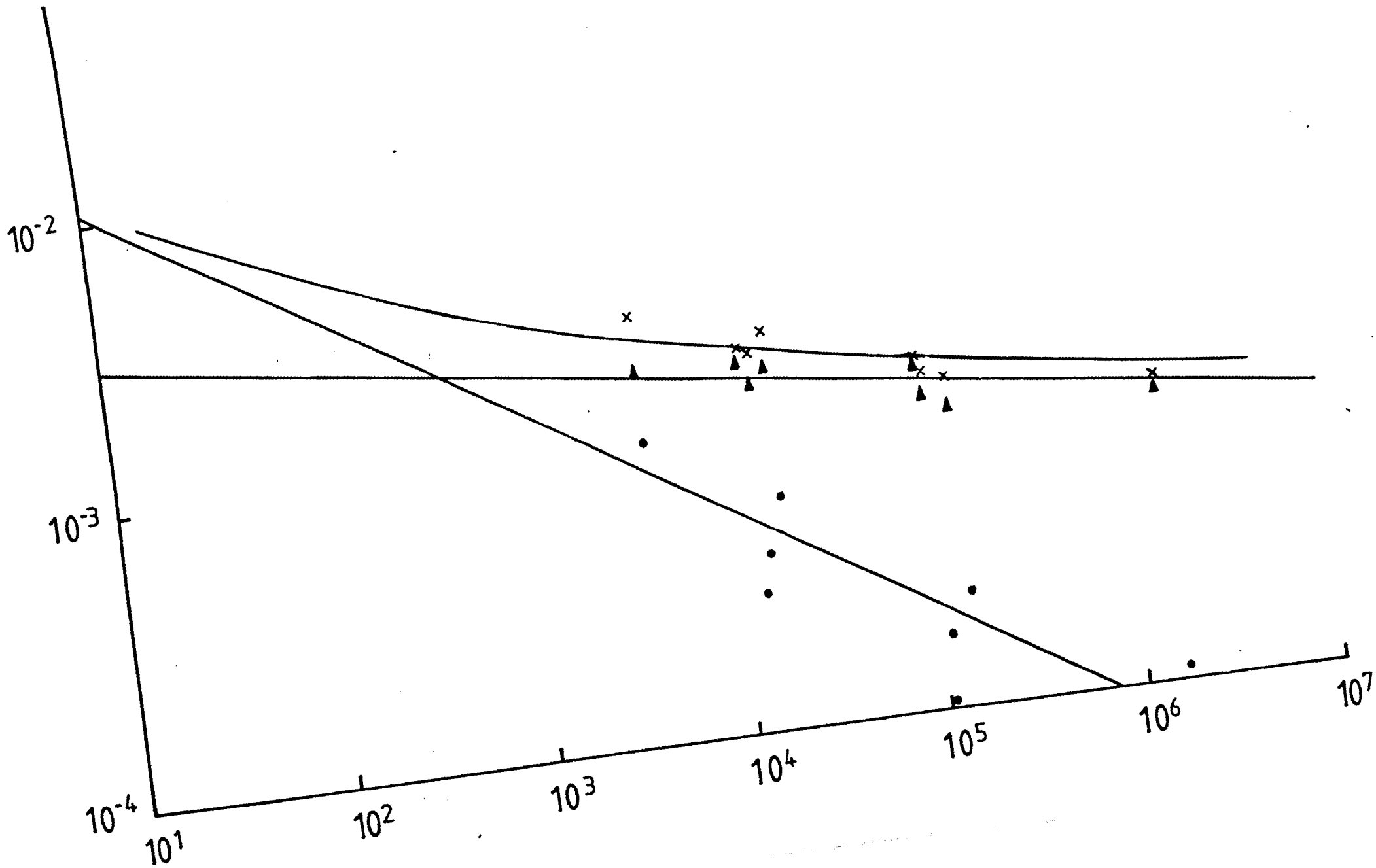

FIGURE 85: A summary of the elastic strain-life data generated in this investigation.

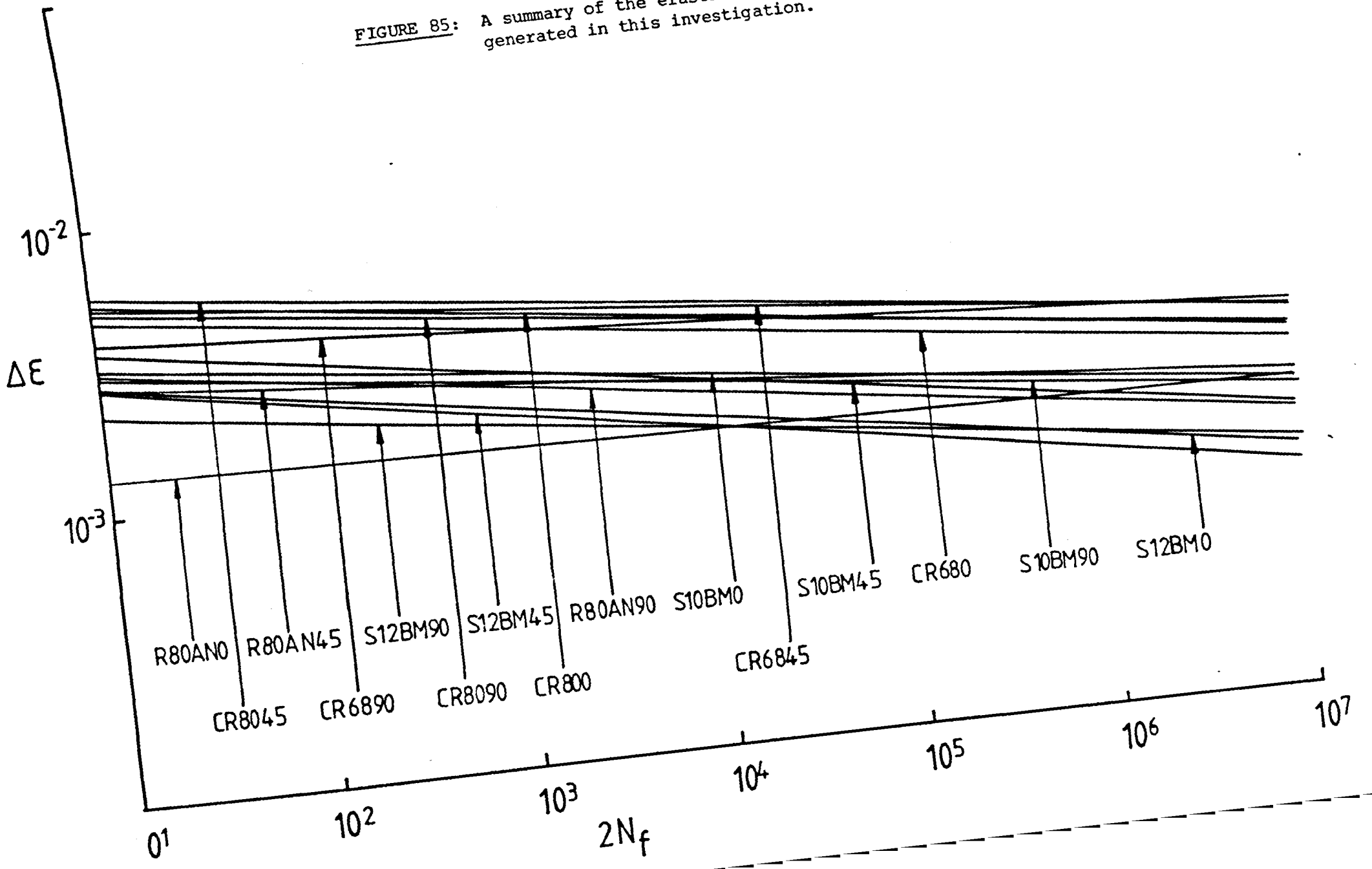

FIGURE 86: A summary of the plastic strain-life data generated in this investigation.

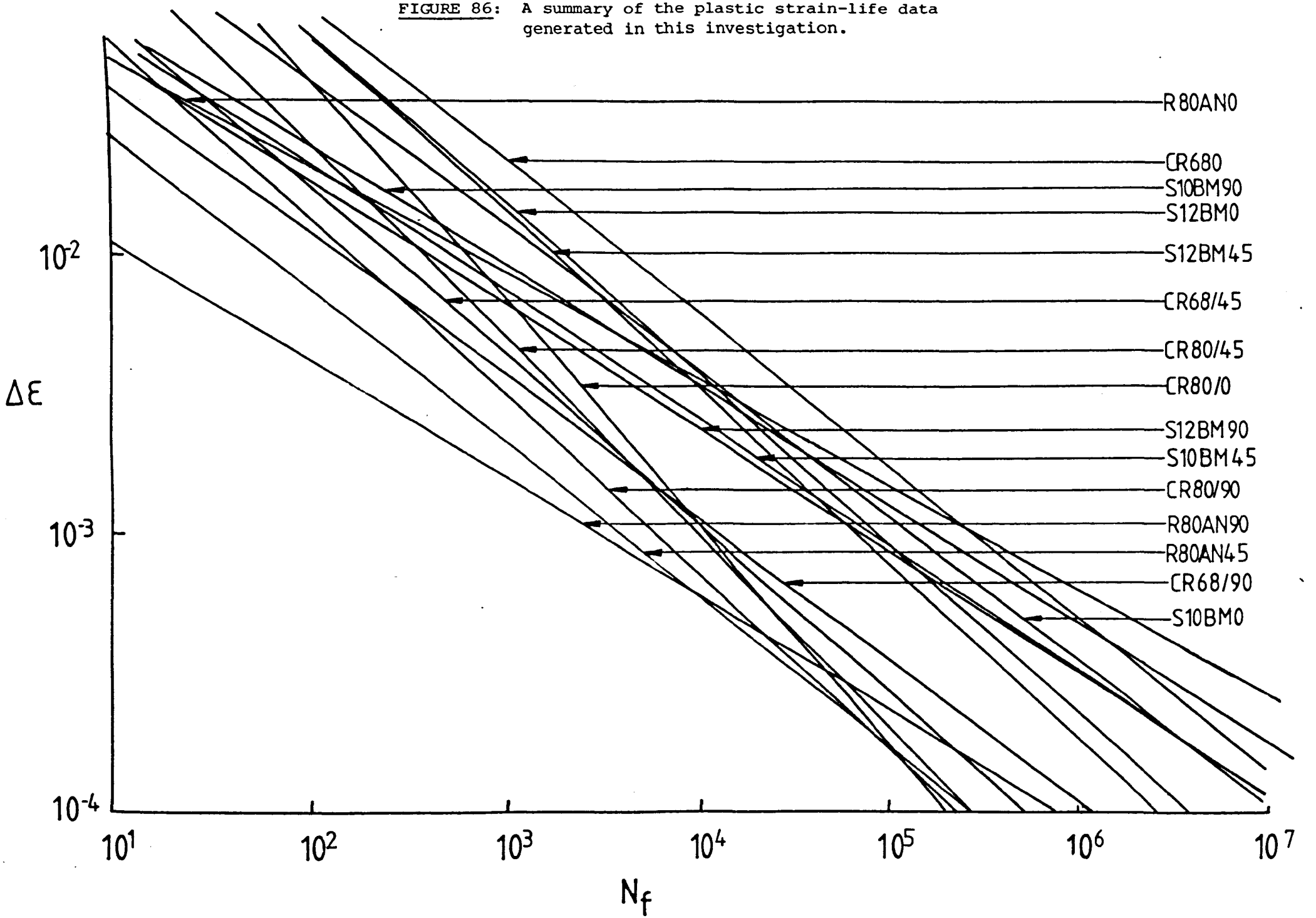

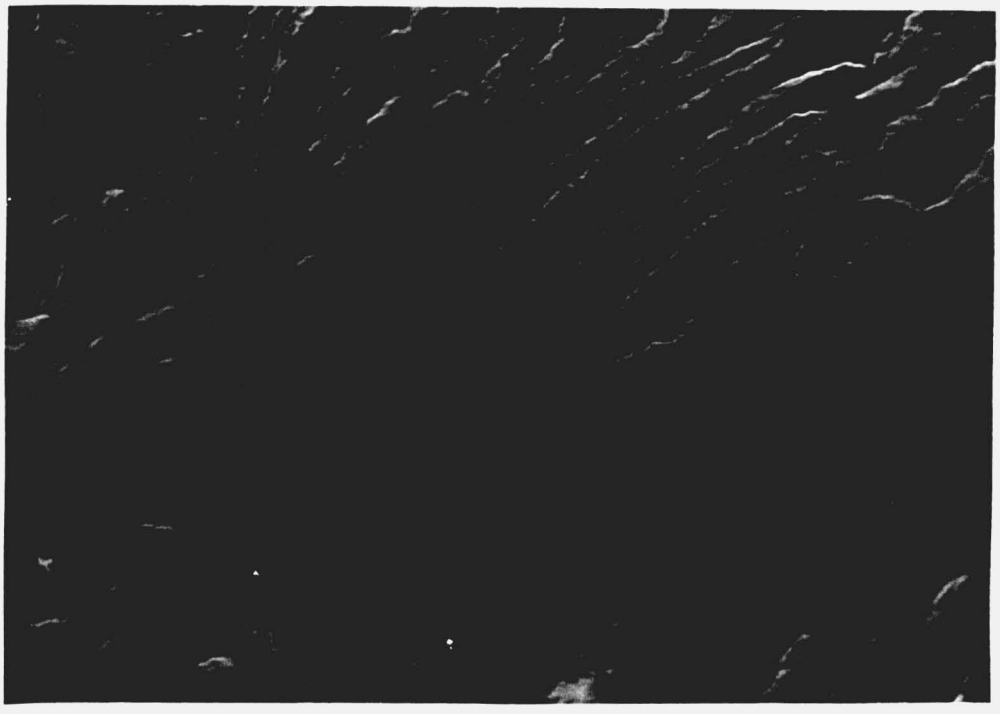

FIGURE 89 The initiation site of a fatigue crack in a specimen of S12BM45. x 80

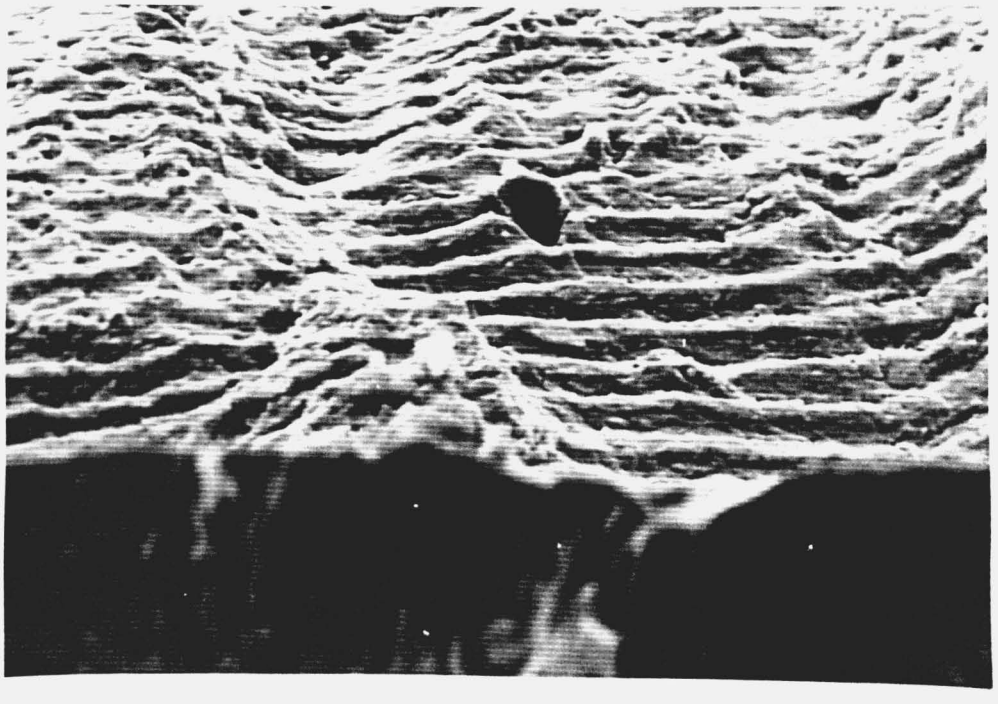

FIGURE 90 Fatigue striations and cleavage steps in S12BM0. x 320

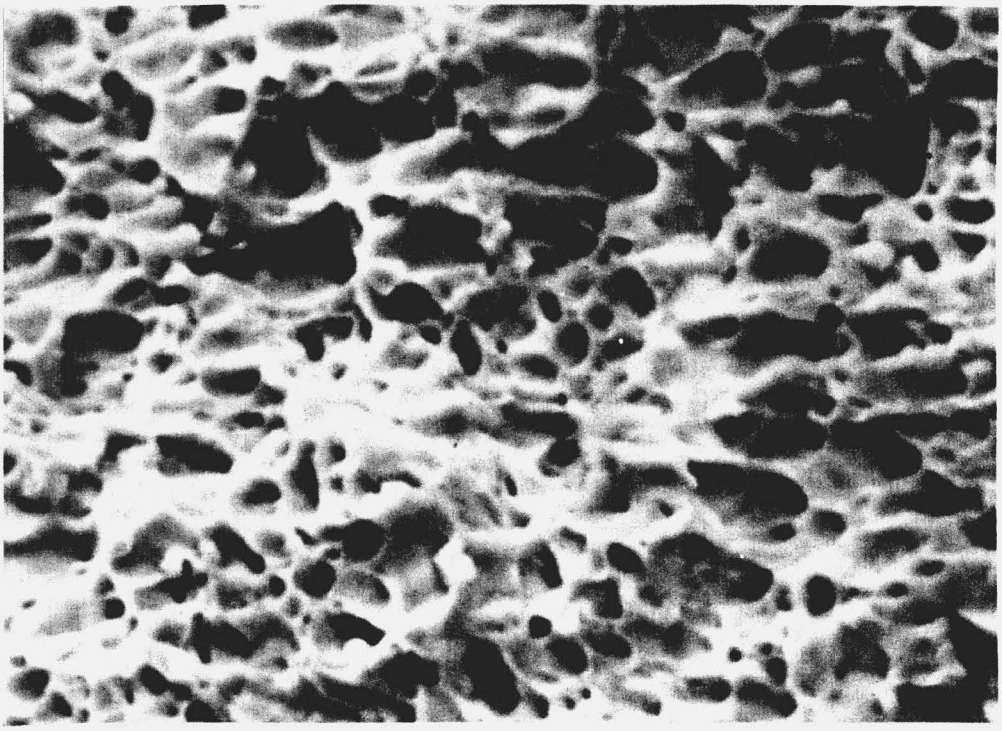

FIGURE 91 The ductile fracture surface of S10BM0.
The void-sheet mechanism is plainly exhibited. x 1250

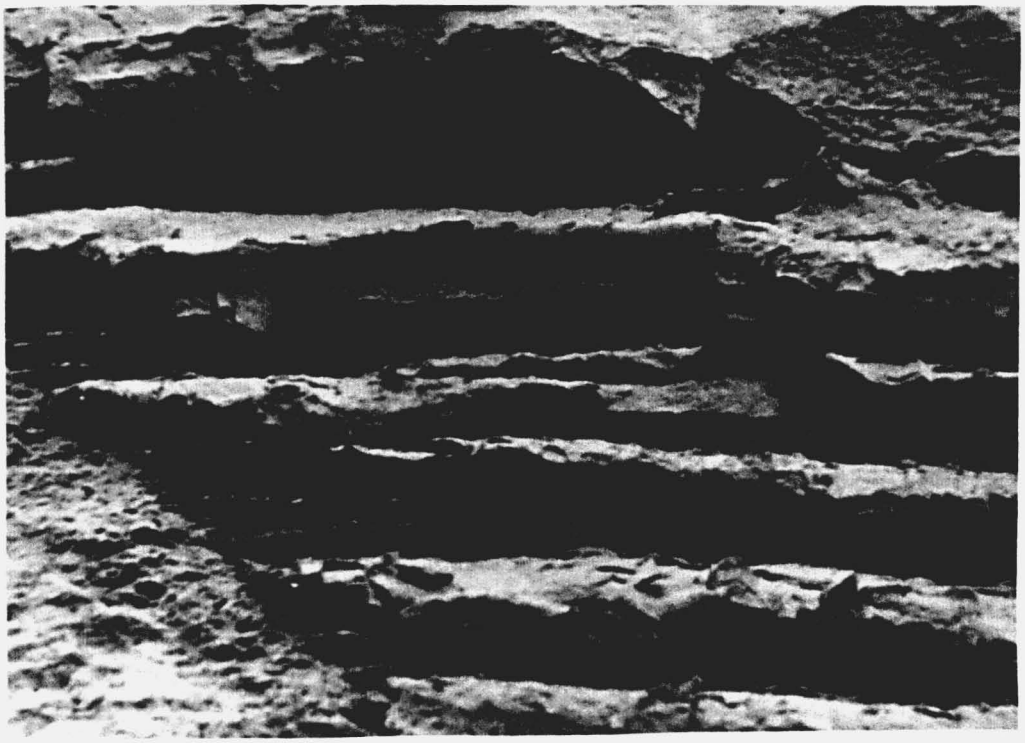

FIGURE 92a The faceted fracture surface of a specimen of CR6890 x 40

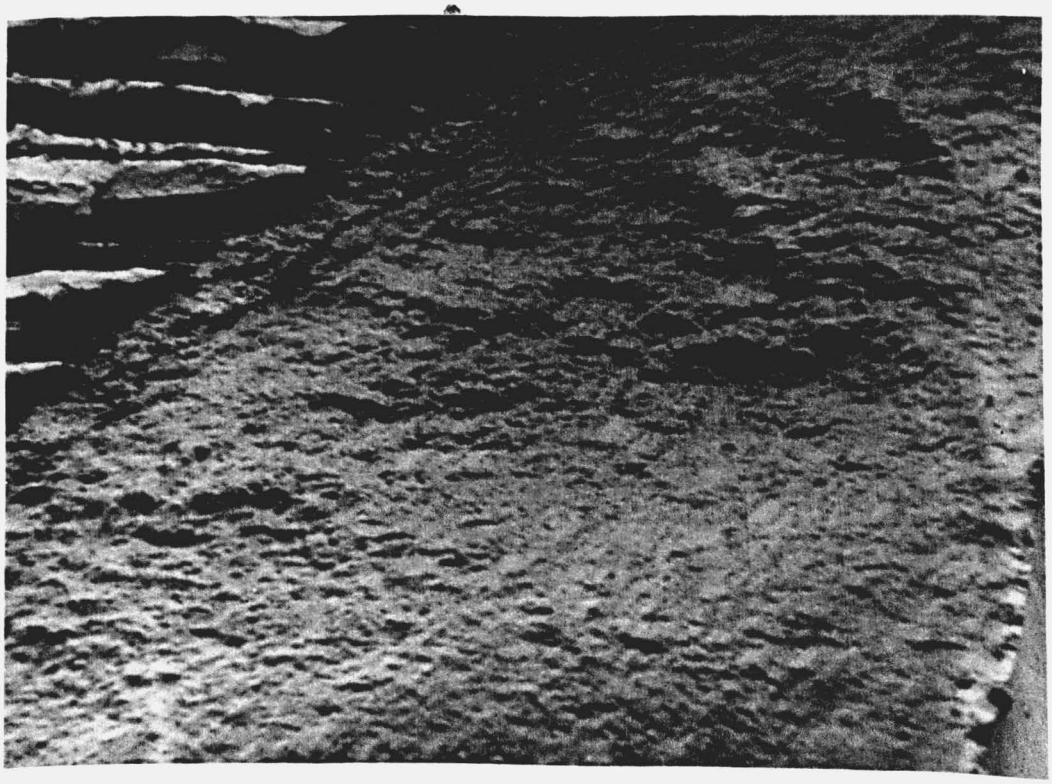

FIGURE 92b The area of crack growth in a specimen of CR6890. x20

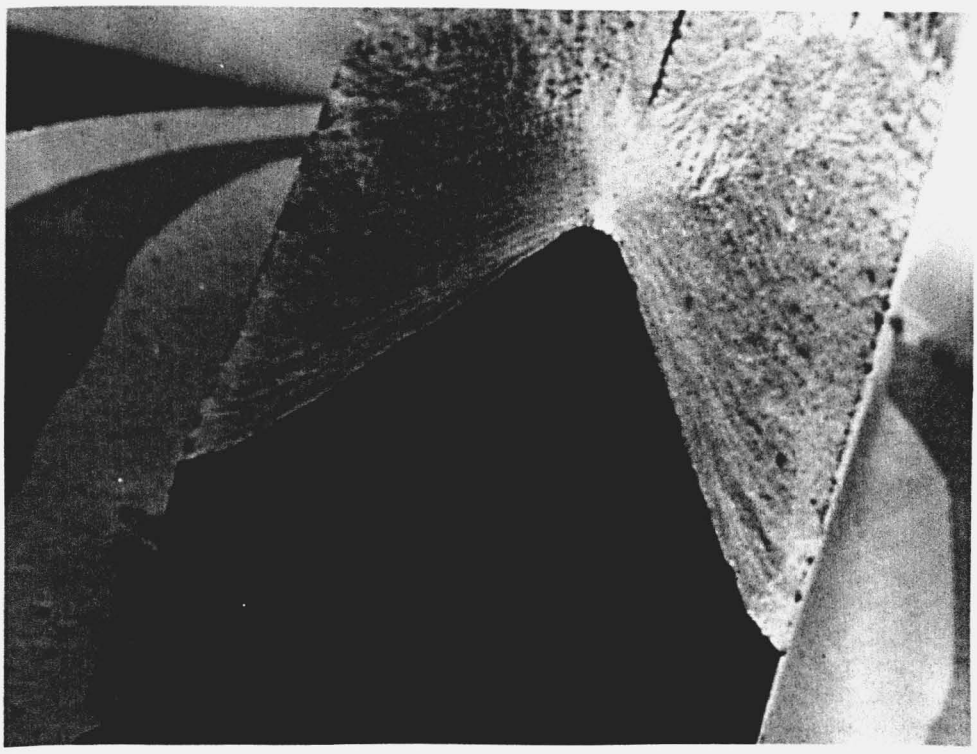

FIGURE 93 Two separate, inclined cracks have caused failure in this CR80/0 specimen. x 10

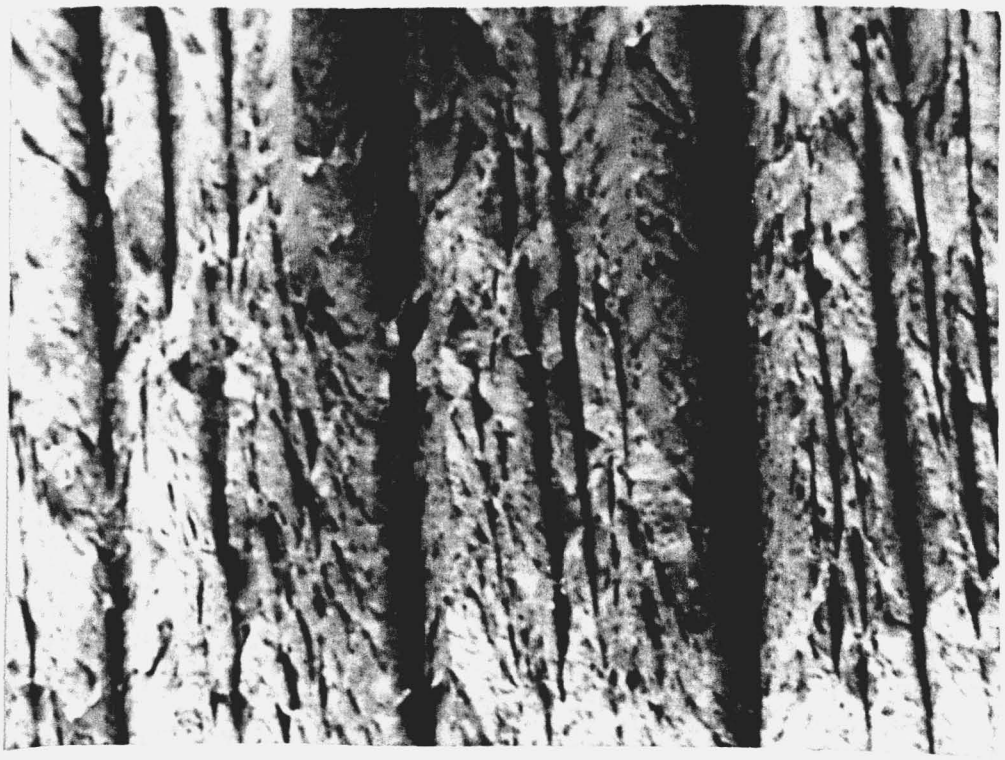

FIGURE 94 The delamination apparent in all fatigue specimens of the cold-rolled materials. x 20

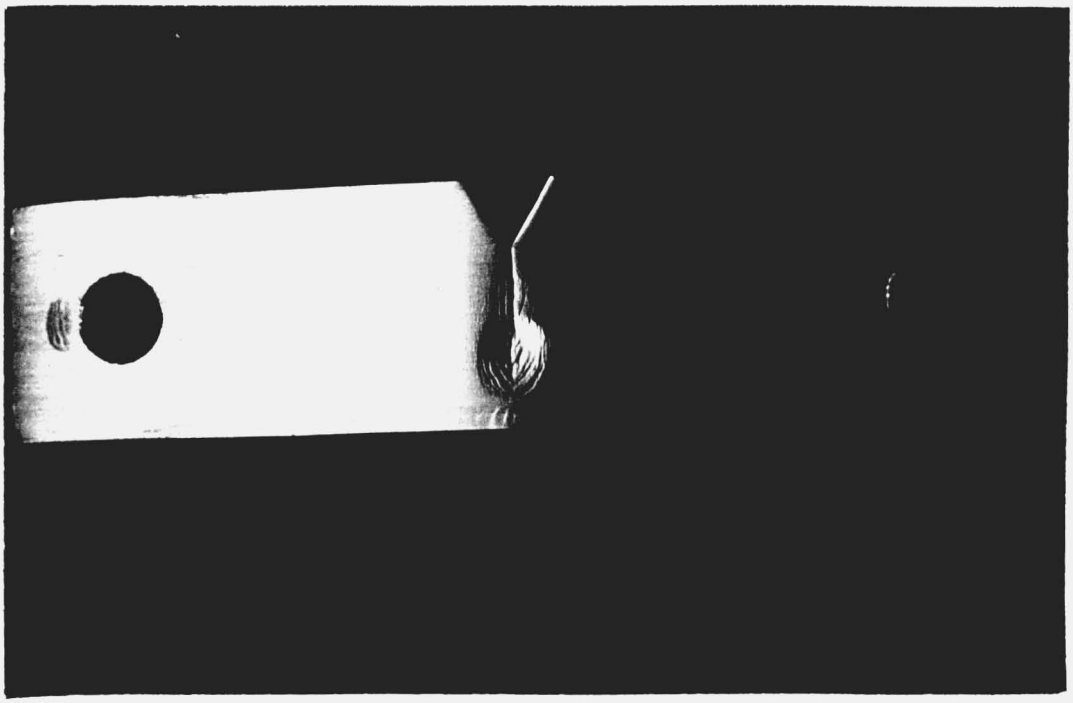

FIGURE 95 The large plastic zone, with slip bands, on the crack propagation specimens of R80AN. x 1·5

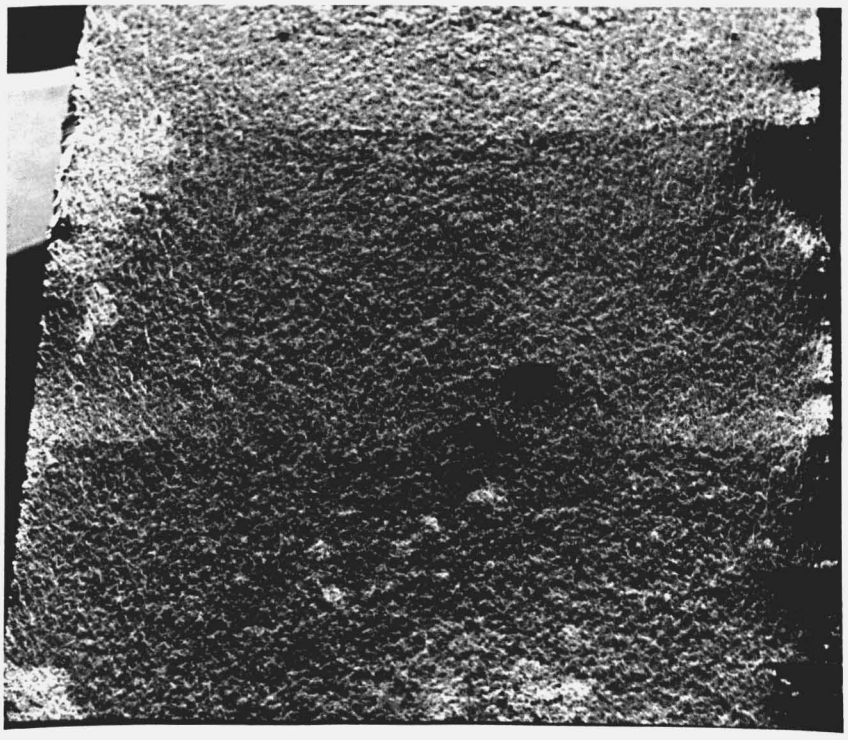

FIGURE 96 A typical crack propagation specimen fracture surface. (R80AN). x 2

FIGURE 97: The cyclic shear stress-shear strain for four of the materials employed in this investigation

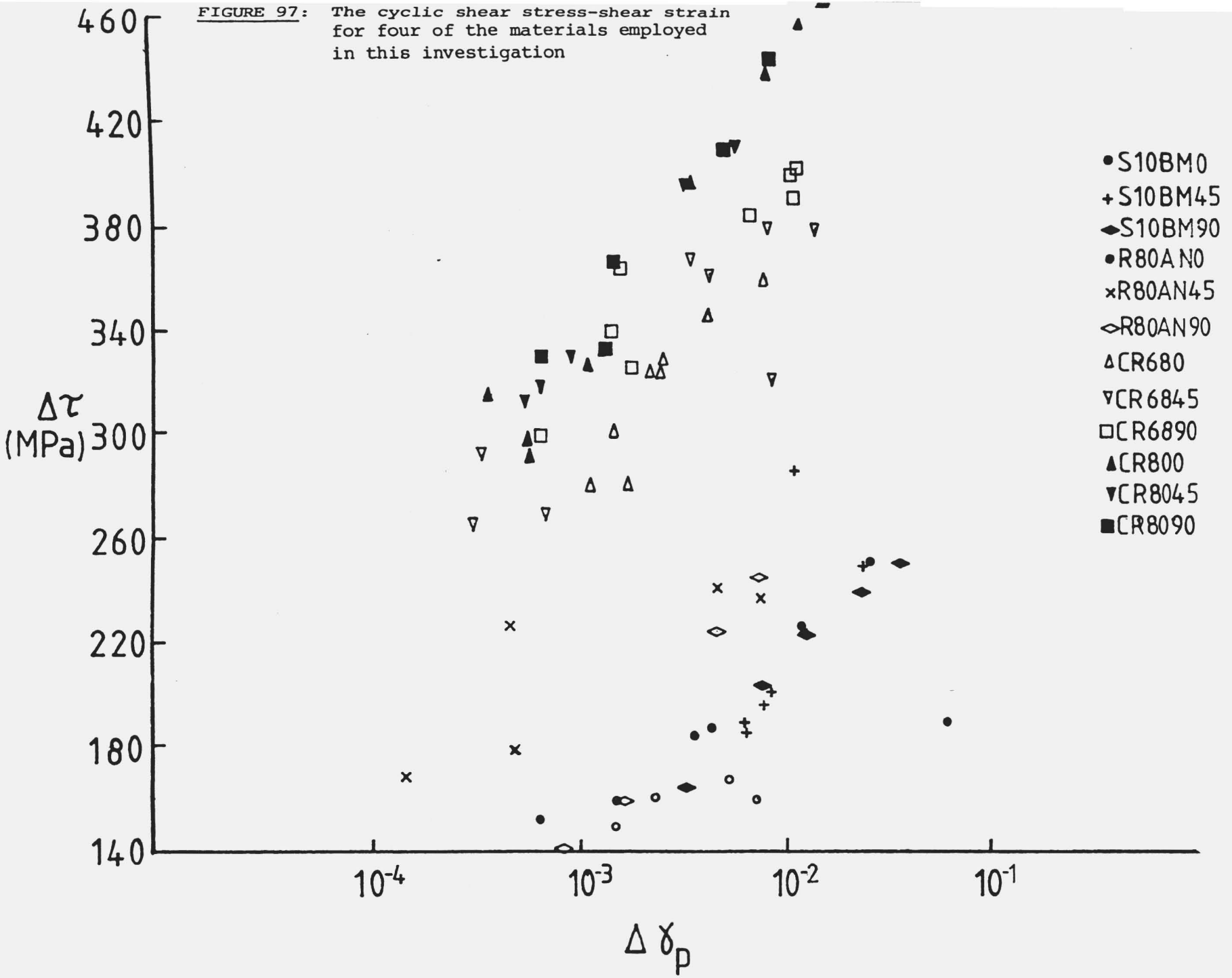

FIGURE 98: The analogy between a 'soft' grain in a polycrystal and a 'hard' grain in a continuum.

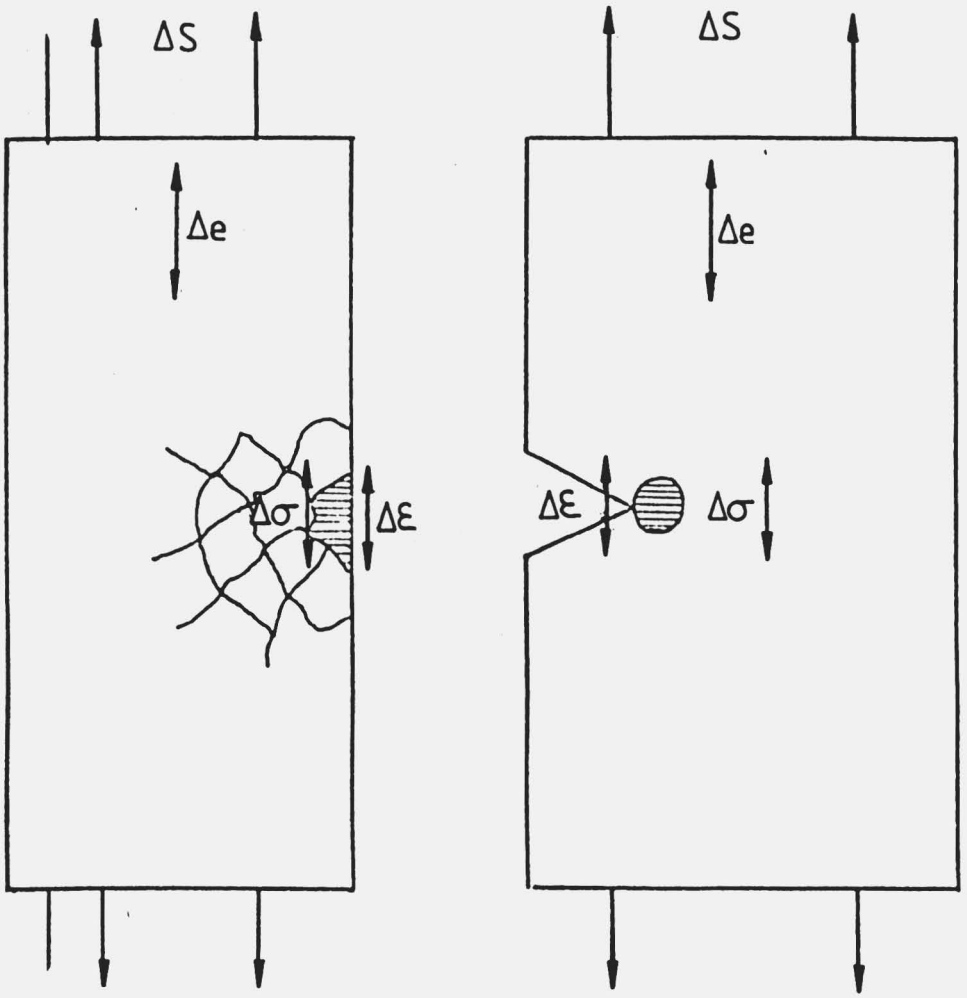

Polcrystalline crack nucleation in a soft grain

Fatigue crack nucleation in a notched body

FIGURE 99: Fatigue-life data for CR80 calculated from the parameters in Table 22.

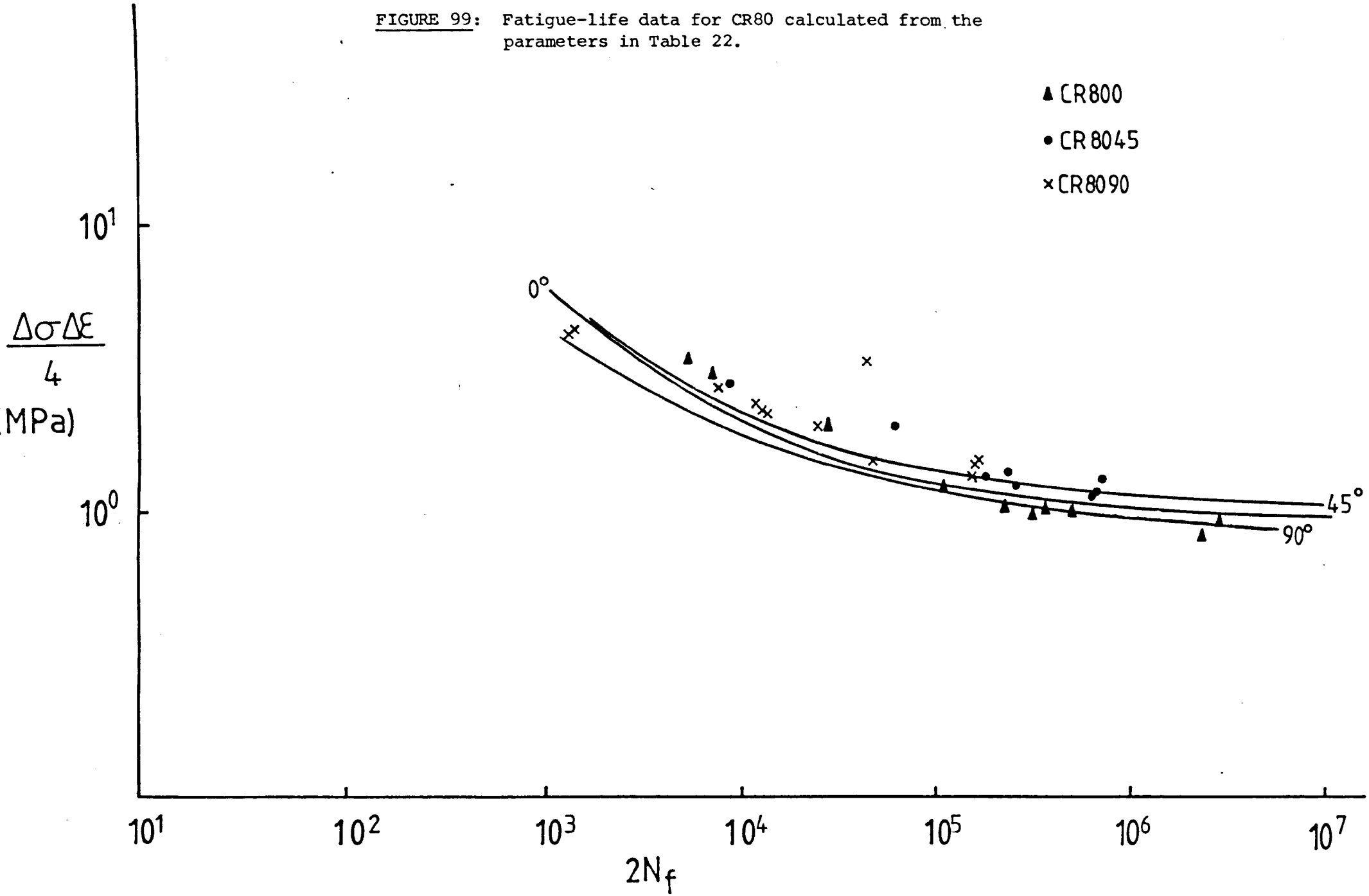

FIGURE 100: Fatigue-life data for R80AN calculated from the parameters in Table 22.

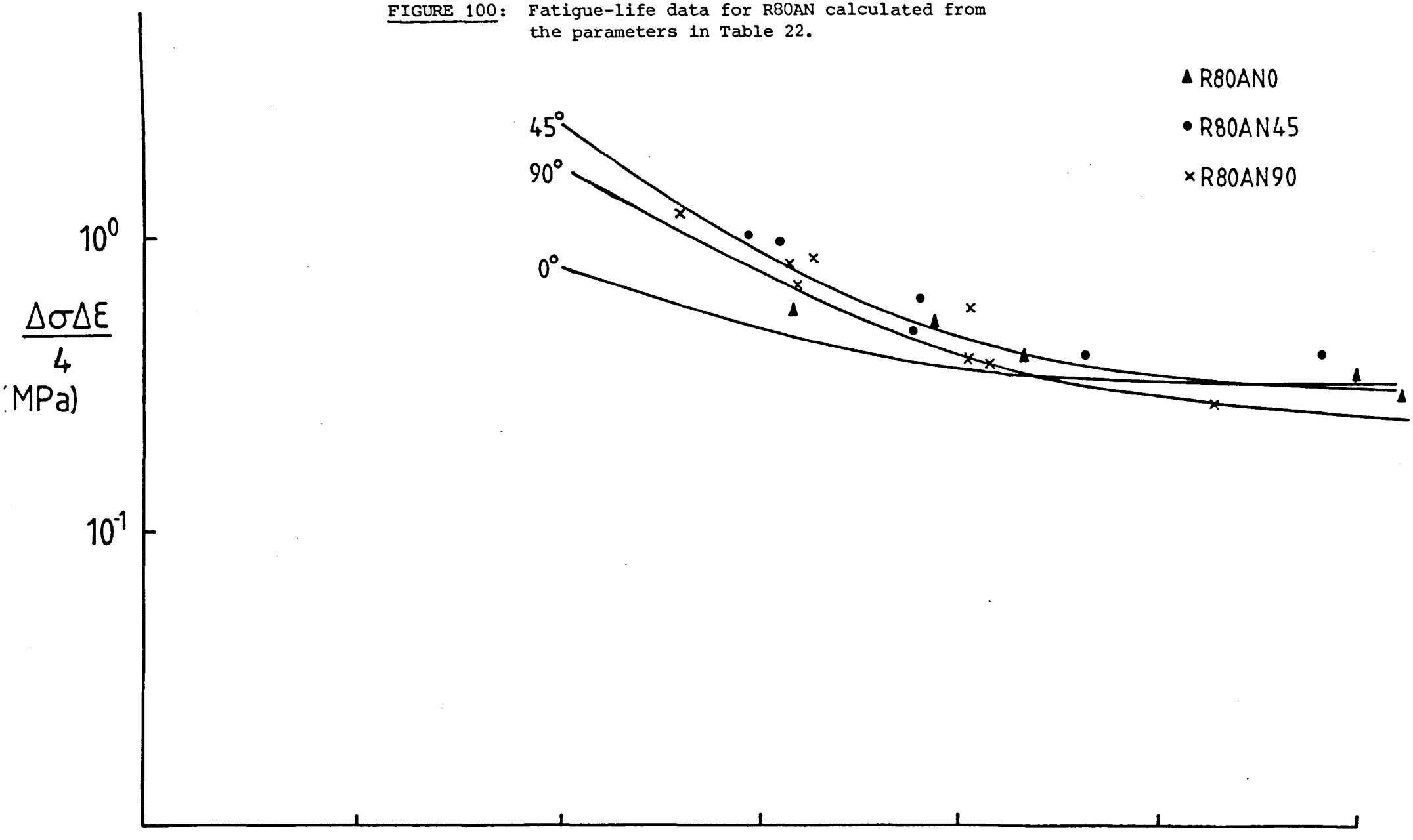

FIGURE 101: Fatigue-life data for CR68 calcu ted from the parameters in Table 22.

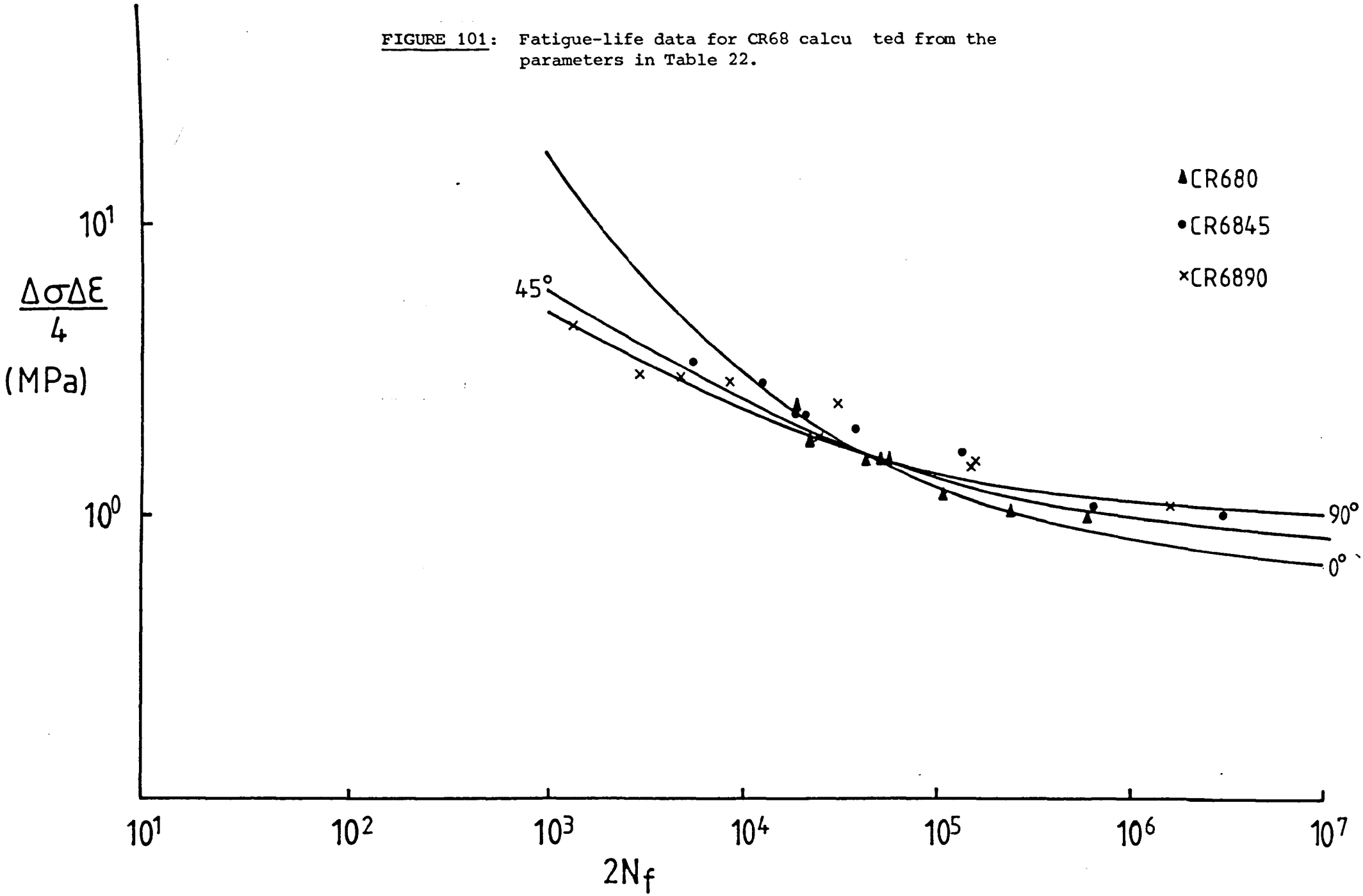

FIGURE 102: Representation of the ductile propagation of a fatigue crack by the formation of shear at the crack tip.